

**A Fugal Discourse on the Electromagnetic
Coupling of Electromagnetic Processes in the
Earth-Ionosphere and the Human Brain**

by

Kevin S. Saroka

**A thesis submitted in partial fulfillment
of the requirements for the degree of
Doctor of Philosophy (PhD) in Human Studies**

**The Faculty of Graduate Studies
Laurentian University
Sudbury, Ontario**

© Kevin S. Saroka, 2016

THESIS DEFENCE COMMITTEE/COMITÉ DE SOUTENANCE DE THÈSE
Laurentian Université/Université Laurentienne
Faculty of Graduate Studies/Faculté des études supérieures

Title of Thesis Titre de la thèse	A Fugal Discourse on the Electromagnetic Coupling of Electromagnetic Processes in the Earth-Ionosphere and the Human Brain	
Name of Candidate Nom du candidat	Saroka, Kevin	
Degree Diplôme	Doctor of Philosophy	
Department/Program Département/Programme	Human Studies	Date of Defence Date de la soutenance November 26, 2015

APPROVED/APPROUVÉ

Thesis Examiners/Examineurs de thèse:

Dr. Michael Persinger
(Supervisor/Directeur(trice) de thèse)

Dr. Cynthia Whissell
(Committee member/Membre du comité)

Dr. John Lewko
(Committee member/Membre du comité)

Dr. Thilo Hinterberger
(External Examiner/Examineur externe)

Dr. Robert Lafrenie
(Internal Examiner/Examineur interne)

Approved for the Faculty of Graduate Studies
Approuvé pour la Faculté des études supérieures
Dr. David Lesbarrères
Monsieur David Lesbarrères
Dean, Faculty of Graduate Studies
Doyen, Faculté des études supérieures

ACCESSIBILITY CLAUSE AND PERMISSION TO USE

I, **Kevin Saroka**, hereby grant to Laurentian University and/or its agents the non-exclusive license to archive and make accessible my thesis, dissertation, or project report in whole or in part in all forms of media, now or for the duration of my copyright ownership. I retain all other ownership rights to the copyright of the thesis, dissertation or project report. I also reserve the right to use in future works (such as articles or books) all or part of this thesis, dissertation, or project report. I further agree that permission for copying of this thesis in any manner, in whole or in part, for scholarly purposes may be granted by the professor or professors who supervised my thesis work or, in their absence, by the Head of the Department in which my thesis work was done. It is understood that any copying or publication or use of this thesis or parts thereof for financial gain shall not be allowed without my written permission. It is also understood that this copy is being made available in this form by the authority of the copyright owner solely for the purpose of private study and research and may not be copied or reproduced except as permitted by the copyright laws without written authority from the copyright owner.

Abstract

There exists a space between the ionosphere and the surface of the earth within which electromagnetic standing waves, generated by lightning strikes, can resonate around the earth; these standing waves are known collectively as the Schumann resonances. In the late 1960s König and Anker-muller already reported striking similarities between these electromagnetic signals and those recorded from the electroencephalograms (EEG) of the human brain; both signals exhibit similar characteristics in terms of frequency and electric and magnetic field intensity. The analyses reported here demonstrate that 1) microscopic (brain) and macroscopic (earth) representations of natural electromagnetic fields are conserved spatially, 2) that electric fields recorded from human brains exhibit strong correlation with the strength of these parameters and 3) that the human brain periodically synchronizes with signals generated within the earth-ionosphere waveguide at frequencies characteristic of the Schumann resonance for periods of about 300 msec. These findings recapitulate 17th century ideas of harmony amongst the cerebral and planetary spheres and may provide the means necessary to quantitatively investigate concepts of early 20th century psychology.

Acknowledgements

First I would like to thank the committee members Dr. Cynthia Whissell and Dr. John Lewko as well as internal examiner Dr. Robert Lafrenie whose questions, comments, and close reading of this manuscript were appreciated. I would also like to extend thanks to the Neuroscience Research Group for their endless supply of ideas during the development of many of the analyses employed in the following pages. Acknowledgements are also credited to Sam, Helen, Matthew and Stephany Saroka who all played a bigger role in the overall completion of this project than they will ever know. Finally thanks are directed to my supervisor and mentor Dr. Michael Persinger without whom the passion and curiosity to pursue many of the ideas explored in this dissertation would be absent—his patience and expertise were critical to the composition of this manuscript.

Table of Contents

Abstract	iii
Acknowledgements	iv
Table of Contents	v
List of Figures	viii
List of Tables	xvii
Chapter 1-Introduction	1
1.0 General Introduction	1
2.0 Basic Concepts.....	6
2.1 Natural Magnetic Fields	6
2.2 Quantitative Electroencephalography (QEEG)	17
2.3 Biological Effects of Natural and Experimental Electromagnetic Fields.	28
3.0 Apparent Earth-Ionosphere-Brain Connection	32
3.1 Experimental Motivations for Investigation	32
3.2 Quantitative Motivations for Investigation	34
4.0 Interdisciplinary Approach	36
5.0 Proposed Research and Methods	50
5.1 Relationships between brain activity and measures of the static geomagnetic field	50
5.2 Explorative Application of QEEG-related Methods to Investigate the Static Geomagnetic Field	51
5.3 Relationships between brain activity and measures of background AC magnetic fields	52
5.4 Schumann Resonance Signatures in the Human Brain.....	53
5.5 Relationships Between Extremely-Low Frequency Spectral Density and Human Brain Activity and Construction and Characterization of an Induction Coil Magnetometer For Measuring Extremely-Low Frequency Earth-Ionospheric Perturbations	55
5.6 Construction and Characterization of an Induction Coil Magnetometer For Measuring Extremely-Low Frequency Earth-Ionospheric Perturbations.....	56
5.7 Simultaneous Measurements of the Schumann Resonance and Brain Activity.....	57
6.0 References	58
Chapter 2- Greater electroencephalographic coherence between left and right temporal lobe structures during increased geomagnetic activity	71
2.1 Abstract	71
2.2 Introduction.....	72
2.3 Methods and Materials	74
2.4 Results.....	77
3.5 Discussion and Conclusion	80
3.6 References	84

Chapter 3- Assessment of Geomagnetic Coherence and Topographic Landscapes of the Static Geomagnetic Field in Relation to the Human Brain Employing Electroencephalographic Methodology	88
3.1 Introduction.....	88
3.2 Materials and Methods	91
3.3 Results.....	93
3.4 Discussion and Conclusion	98
3.5 References	100
Chapter 4- The Proximal AC Electromagnetic Environment and Human Brain Activity	104
4.1 Introduction.....	104
4.2 Methods and Materials	106
4.3 Results.....	109
4.4 Discussion and Conclusion	112
4.5 References	115
Chapter 5-Quantitative Convergence of Major-Minor Axes Cerebral Electric Field Potentials and Spectral Densities: Consideration of Similarities to the Schumann Resonance and Practical Implications	119
4.1 Introduction.....	119
4.2 Materials and Methods	120
5.3 Results.....	125
5.4 Discussion	133
5.5 References	140
Chapter 6-Quantitative Evidence for Direct Effects Between Earth-Ionosphere Schumann Resonances and Human Cerebral Cortical Activity	146
6.1 Introduction.....	146
6.2 Construction and Characterization of an Induction Coil Magnetometer ..	156
6.3 Potential Fugal Patterns in the Schumann Resonance Signal	161
6.4 Correlation between Real Schumann and Cerebral Coherence Values..	168
6.5 The Parahippocampal Region as a Locus of Interaction	174
6.6 Extended Correlations	179
6.7 Implications of Schumann Amplitude Facilitation of Interhemispheric Coherence in the Human Brain	183
6.8 Real-time Coherence Between Brain Activity and Schumann Frequencies	185
6.7 The Importance of Human Density For Potential Convergence Between Global Schumann Frequencies and Aggregates of Human Brains	190
6.8 Conclusions	193
6.9 References	193

Chapter 7-Occurrence of Harmonic Synchrony Between Human Brain Activity and the Earth-Ionosphere Schumann Resonance Measured Locally and Non-locally	199
7.1 Introduction.....	199
7.2 Materials and Methods	202
7.3 Results.....	207
7.4 Discussion	212
7.5 Conclusion.....	217
7.6 References	217
Chapter 8-Synthesis, Implications, and Conclusion	220

List of Figures

Figure 1.1 Fugue in D Major from “The Well-Tempered Clavier, Book 2”. In this fugal passage, the subject melody (red) is repeated verbatim in 3 other voices.....	3
Figure 1.2 Fugue in C-Minor from “The Well-Tempered Clavier, Book 2”. The subject in this passage is stated along two different speeds (green=fast, blue=slow) in a way that can be likened to celestial bodies rotating around the sun with different temporal periods.....	4
Figure 1.3 Classical example of electric fields generated by a positively-charged (proton) and negatively-charged (electron) particles.....	7
Figure 1.4 The magnetosphere and associated boundaries. Picture from (Russell, 1972).....	8
Figure 1.5 Example of a geomagnetic storm. The y-axis refers to gammas (each gamma represents one nanoTesla) and x-axis is time. Picture in (Bleil, 1964).....	10
Figure 1.6 Schematic diagram of the cavity bounded by the earth and the ionosphere.	11
Figure 1.7 (A) Spectral density profile of the Schumann resonance (B) Exemplary time-series from which Schumann resonance spectra are obtained.....	13
Figure 1.8 (Above) Time-series and (Below) sonogram of a Pc1 micropulsation event showing ‘rising-tones’ in the range of 0.4 to 0.5Hz. Picture in Volume 2 of Matsushita and Campbell (1967).....	16

Figure 1.10 Schematic of a typical spectral analysis performed on quantitative EEG data.
The original signal (top) is modeled after a series of sine waves (middle) and the area under the curve of each signal is then calculated and graphed (bottom). 20

Figure 1.11 The 4 classes of normative microstates as originally discovered by Koenig and Lehmann (2002). 23

Figure 1.12 (Top) Two signals derived from P3 and P4 sensors on the scalp show evident synchronicity (Bottom) Coherence analysis indicating that both sensors are periodically coherent within the 9-10Hz range. 26

Figure 1.13 Original comparison between electromagnetic signals (Left) and signals derived from human electroencephalograms (right) made by Konig. Picture found in Persinger (1974). 32

Figure 1.14 Schamatic diagram of a section of neocortex that can be modeled as two parallel plates with the positive plate closer to cortex/white matter interface and the negative plate closer to the surface of the cortex. 35

Figure 1.15 The ‘holographic’, or fractal relationships explored in a mathematical set (A), a musical fugue (B), and the proposed connection between electromagnetic processes of the human brain and the earth-ionosphere (C). (A) Example of a fractal mathematical set known as the Sierpinski Triangle. The process shows how the information within one component of the object can be broken down into constituent parts, each possessing the same informational content. (Image Source: <http://math.bu.edu/DYSYS/chaos-game/node2.html>) (B) Fugue in C-Minor from “The Well-Tempered Clavier, Book 2 ”. The subject in this passage is stated along two

different speeds (green=fast, blue=slow) in a way that can be likened to celestial bodies rotating around the sun with different temporal periods. (C) Relationship between standing waves formed within the earth-ionosphere cavity and the human brain. (Image Source: Nunez (1995), p.83) 47

Figure 1.16 Temporal courses of amplitude frequency spectra averaged over five minutes (from Kloppel in Popp, 1979). 54

Figure 2.1 Mean coherence score between the left (T5) and right (T6) temporal lobes as a function of the global geomagnetic (K_p) during the 3 h period of the measurements. The numbers of subjects (parentheses) per group intensity were: 0 (47), 1 (105), 2 (51), 3(23) and >4 (7); they were tested over a 3.5 years period. Vertical bars indicate SEM..... 77

Figure 2.2 Effect sizes for the correlation between the K indices at the time of the measurements and the net differences in power between the left and right parahippocampal regions for each 1 Hz increment. 78

Figure 2.3 Mean standardized residuals for the difference between the two parahippocampal regions extracted by sLORETA after removal of variance associated with cortical activity as a function of geomagnetic activity. Vertical bars are SEM..... 79

Figure 2.4 Effect sizes for the correlations between standardized residuals from Figure 3 with the coherence measures between T5 and T6 across all frequencies. The first two peaks are ~7.6 Hz and ~19.6 Hz. 80

Figure 3.1 (A) Geographical regions from which samples of the geomagnetic field were sampled (B) Montage for the 8 ‘sensors’ of the world fitted to their approximate locations if they were modeled on the classic 10-20 system used regularly within electroencephalography. 93

Figure 3.2 Time-series of 50 days of the geomagnetic field fluctuations sampled at the respective stations with the planetary k-index plotted at the bottom. 94

Figure 3.3 Mean global coherence plotted as a function of the planetary k-index showing that mean global geomagnetic coherence is strongest during days when the k-index is greater than or equal to 4. 95

Figure 3.4 Effect sizes for the 28 bivariate combinations coherence. The strongest effect size was observed between the PPT and KDU sites..... 96

Figure 3.5 Sequence of microstates of the geomagnetic field for 350-days during year 2014..... 97

Figure 3.6 Topographies of the static geomagnetic field inferred from microstate analysis for the years 2013 and 2014 separately. The results suggest a high congruency between ‘field maps’ of the static geomagnetic field from year-to-year. 97

Figure 4.1 (Top) Scattergram depicting the correlation between left (T5) and right (T6) posterior temporal lobe coherence with regression score comprising (Below) predicted power meter spectral densities for frequencies comparable to harmonics of the Schumann resonance..... 110

Figure 4.2 (Top) Scattergram depicting the correlation between left parahippocampal theta current source density with regression score comprising (Below) predicted power meter spectral densities for frequencies comparable to harmonics of the Schumann resonance. Note the elevated peaks at around 7.8 and 40 Hz..... 111

Figure 4.3 (Top) Scattergram depicting the correlation between microstate disturbance with regression score comprising (Below) predicted power meter spectral densities for frequencies comparable to harmonics of the Schumann resonance. Note the elevated peaks at around 40 and 46 Hz. 112

Figure 5.1 Absolute potential difference ($\Delta\mu V^2 \cdot Hz^{-1}$) plotted as a function of frequency for the rostral-caudal and left-right measurements during QEEG for 177 subjects measured over a three year period..... 126

Figure 5.2 Scattergram of the correlation ($r=0.82$) between the discrete potential difference values for the caudal-rostral vs left-right potential differences. 126

Figure 5.3 Means of the z-scores of the spectral density ($\mu V^2 \cdot Hz^{-1}$) of the measurements as a function of frequency for the rostral-caudal and left-right measurements. 127

Figure 5.4 Log of spectral density of various frequencies reflecting the Schumann resonance for all 237 records. 129

Figure 5.6 Variance explained of all classic microstates as a function of the intensity of the Schumann resonance (first three harmonics) within the EEG. N indicates numbers of records per post hoc group. 132

Figure 6.1 (Above) Sample power spectra of a classical quantitative EEG of an average person and (Below) Schumann resonance profile associated with the same segment of quantitative electroencephalographic activity. 151

Figure 6.2 Cylinder containing the induction magnetometer “Herbert” by which local Schumann resonances were measured. 158

Figure 6.3 The magnetometer during stages of wrapping the copper wire. There were between 96,000 to 97,000 turns. 159

Figure 6.4 Calibration of the “Herbert” induction coil magnetometer demonstrating that the peak intensities at the harmonics were consistent with the measures of other stations. The mean peak values around 8 Hz is approximately 2 pT, within the range of other measurements. 159

Figure 6.5 Log of spectral power density for Schumann resonances as a function of frequency from our local station recorded using a USB soundcard. The relative harmonic peaks in arbitrary units (au) are veridical. 160

Figure 6.6 Spectral density over the caudal region (temporal-T5 T6, occipital O1 O2 and parietal, P3, P4, Pz) of 34 subjects whose brain activity was measured while sitting in a quiet Faraday chamber. 161

Figure 6.7 Pattern of spindle-like activity recorded locally by a Schumann unit after filtration within each of the Schumann resonance modes. Each line represents a harmonic of the Schumann resonance starting with the fundamental 7.8Hz (top line) and ending with the 7th harmonic 45Hz (bottom line). 163

Figure 6.8 Frequency pattern within each envelope or spindle from Figure 6 after Hilbert transformation..... 163

Figure 6.9 Demonstration of a type of fugal coupling between the various harmonics of the Schumann values. This example depicts coupling specifically between the first and seventh Schumann harmonics. Red and yellow areas indicate cross-frequency coherence intervals..... 164

Figure 6.10 Correlation between the coherence strength between the left (T3) and right (T4) temporal lobes for subjects whose QEEGs were measured in Sudbury, Ontario and the electric field strength of the first two Schumann harmonics in California.. 173

Figure 6.11 Correlation between the intensity of the contemporary fundamental electric field of the Schumann resonance in California and the net difference in current density as measured by sLORETA for the 9 to 10 Hz band between the left and right parahippocampal regions for 49 subjects whose QEEGs were measured between 2009 and 2010..... 177

Figure 6.12 The effect size (correlation coefficient squared) for the association between the caudal 14.7 Hz QEEG activity in Sudbury and Schumann E field spectral density in Italy and the frequency band of the E field. Note the strongest correlation for the first three harmonics of the Schumann resonance. 180

Figure 6.13 Sample (about 5 s) electroencephalographic voltage pattern from the different sensor sites over the skull (indicated by traditional identifiers) and the voltage fluctuations associated with the simultaneous recording of the Schumann. 186

Figure 6.14 Sample record (about 10 s) of the composite EEG from the caudal portions of the subject’s cerebrum (EEG) and the Schumann resonance (EM) measured 1 m away. The horizontal axis is real time in ms while the vertical axis is frequency. The first, second and third harmonic of the Schumann resonance measured with the magnetometer were coherent with the 8, 13, and 20Hz activity occurring within the integrated caudal root-mean-square signal. The yellow indicates weak (0.30 coherence while the red indicates stronger (0.5 to 0.7) coherence. In the first panel (below the raw data) the coherence durations in the indicated frequencies occurred primarily as brief periods between 0.3 s to about 2 s. The phase shift is noted in the lower panel. The phase shift for this event at 7.8 Hz with cerebral activity was equivalent to about 41.9 ms. “Harmonic synchrony” or simultaneous coherence across two or more harmonics (possibly 4 or 5 with different magnitudes of coherence) is indicated by the vertical dotted line. 187

Figure 7.1 Examples of harmonic synchrony observed between a male and female participant during simultaneous measurements of their EEG and ELF activity measured with a magnetometer locally in Sudbury, Canada..... 207

Figure 7.2 Examples of harmonic synchrony observed between a male and female participant during simultaneous measurements of their EEG and ELF activity measured with a magnetometer non-locally in Cumiana, Italy. 208

Figure 7.3 Averaged coherence between the caudal root-mean-square and ELF activity recorded in Italy plotted as a function of frequency. 209

Figure 7.4 (A) Topographical maps of clusters before (top line) and during (middle line) the onset of harmonic synchronous events. NC refers to the number of clusters

contributing to the grand mean cluster. (B) Standardized differences between the two conditions (bottom line). Colour bar indicates z-score. 211

List of Tables

Table 1-1 Nomenclature for geomagnetic micropulsations with their associated frequencies and intensities. Adapted from Bianchi and Meloni (2007).....	15
Table 5-1 Range of the standardized (z-score) for the raw spectral density values for the peak band (in Hz) for the 10 randomly selected subjects. The “band width” for the peak band range is also shown.	128
Table 5-2 Means and Standard Errors of the Means (in parentheses) for current source density ($\mu\text{A}\cdot\text{mm}^{-2}$) of the parahippocampal gyrus within the classical frequency bands.	132

Chapter 1

Introduction

1.0 General Introduction

The possibility of a harmonic connection between all natural phenomena, ranging from the circling of subatomic particles around a nucleus to the orbit of the planets around the sun has gradually become more and more substantive (Persinger and Lavallee 2012; Persinger, 2012). During the time of Pythagoras, Ancient Greeks were already aware of a *musica universalis*, or Harmony of the Spheres, which proposed the idea that the orbit of planets followed a geometrical proportionality around the center of the galaxy. Today we now know that gravitational and electromagnetic forces propel the planets around the sun in a quasi-periodic fashion that is also influenced by the planet's size and mass. We now also understand that living creatures existing on Earth display changes (such as hibernation and food consumption) in accordance with the season. In addition, we now understand that environmental conditions, such as weather and the geomagnetic field, which are both influenced by solar activity, can influence subtle biological processes like the behaviour of an organism. Finally, we are now beginning to understand how behaviour and structure of cellular constituents of the organism are dynamically interconnected such that behaviour (X) can influence cellular processes (Y) and vice versa. In conclusion, life on earth together with the environment that influences it is also a part of a 'cosmic dance' that exists within the universe itself (Capra, 1976). Human subjective experiences, such as observation, are then reflections of changes

within any of the aforementioned levels of discourse and exist on a continuum of macro-to-microcosm.

The coupling between the macroscopic and microscopic levels may be exemplified through modeling it as a fugue (Hofstadter, 1979). A fugue is a type of musical piece that was popular during the Baroque era and retained some popularity amongst some composers well into the 20th century (Menhuin and Davis, 1979). The fugue itself consists of a subject melody, stated explicitly at the beginning and through modulation and imitation is repeated in many ways throughout the piece, but always in harmony with other lines of melody. The main subject line of a fugue can be imitated in many ways. One way is to simply restate the same information in a different key signature (Figure 1.1). Another way is to invert the subject to produce a 'mirror image' so that it sounds 'upside-down'. In perhaps a way more pertinent to the 'harmony of the spheres', the melody is stretched out over multiple bars, such as in a bass line, and has shorter repetitions placed within the larger, a technique called diminution (Figure 1.2). This would be complimentary to how revolutions of individual planets around the sun may be described, with planets closer to the sun completing one full cycle with a frequency greater than planets in outer orbits.

Nikola Tesla is once said to have remarked that to understand the secrets of the universe, one need only think in terms of energy, vibration and frequency. Frequency (Hz or s^{-1}), or cycles per second cps, is the amount of oscillations of a particular substance occurring in one second and might be thought of as information when it is patterned over time. As an example, sound, from a psychophysical perspective, is a psychological experience that occurs when air molecules are displaced with certain frequencies. Depending upon the source of sound, information in the form of sound

waves produces vibrations of the tympanic membrane of the ear that are registered by stereocilia cells within the cochlea and ultimately translated into action potentials that are then processed by the temporal lobes of the brain.

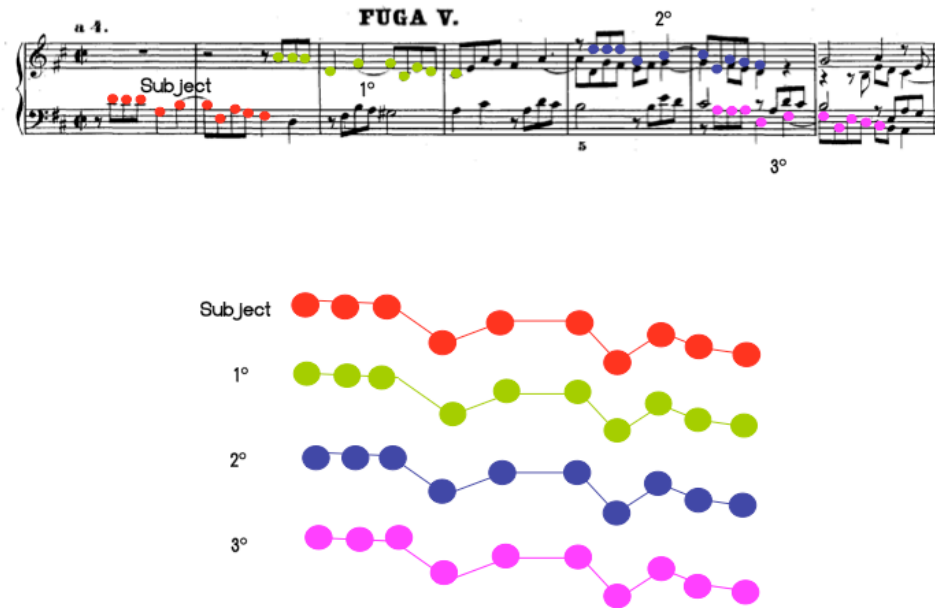


Figure 1.1 Fugue in D Major from “The Well-Tempered Clavier, Book 2”. In this fugal passage, the subject melody (red) is repeated verbatim in 3 other voices.

The concept of frequency is important for many reasons, but not the least of which is its importance for understanding the connection between macro and microscopic levels. For example, the frequency of the observation of some-thing can lead to pattern recognition of particular phenomena, such as tidal waves occurring from gravitational forces between the earth and the moon; another instructive example would be the frequency with which the earth rotates. Frequency also allows for the discovery of vibrations produced of particular molecules. This is useful to define the ‘state’ of an atom, in particular whether the atom is in a stable state (less likely to bind other atoms to

produce derivative molecules) or excited state (more likely to form bonds with other atoms).

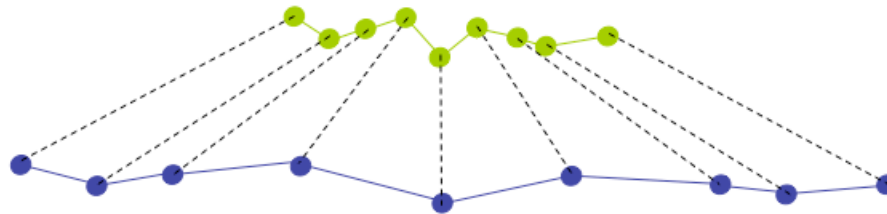


Figure 1.2 Fugue in C-Minor from “The Well-Tempered Clavier, Book 2”. The subject in this passage is stated along two different speeds (green=fast, blue=slow) in a way that can be likened to celestial bodies rotating around the sun with different temporal periods.

Frequency is also an important feature when discussed within the context of behavioural and geophysical sciences. One of the most useful tools for understanding the distributions of frequencies is spectral analysis. Given a time-series x with observations made at regular intervals, spectral analysis can be used to decompose the time-series into a series of sine waves in order to predict the occurrence of a phenomenon, such as brain waves.

It will be proposed in this dissertation that ‘fugal’ relationship exists between the electromagnetic activity generated within the earth and the electromagnetic activity

generated within the human brain. As Persinger has discussed on many occasions, the special and temporal properties of the earth are all within the same range as those measured frequently by the brain and might indicate a scale-invariant or fractal relationship between both (Persinger, 2008; Persinger et al., 2008; Persinger 2012, Persinger, 2013). One way that this harmony of the spheres (earth and brain) could exist is because of the coupling of frequency, namely that the natural resonant electromagnetic frequencies of the earth are similar in magnitude and intensity to those generated within the brain, specifically within the extremely-low frequency domain of 0.1 to 100Hz.

2.0 Basic Concepts

2.1 Natural Magnetic Fields

2.1.1 Description of Electromagnetic Fields

Electromagnetic fields can be described as a force exerted on particulate matter and exist in all points of space. A classic way of describing the electric field, for example, is the force a point charge (almost always positively-charged particle such as a proton) will experience when immersed within a field (Serway and Jewett, 2004). Whereas the velocity, or drift velocity, of an electron within a given substance is about 1 mm/s due to resistive and capacitive characteristics within the medium, the velocity of an electromagnetic field approaches the speed of light and extends everywhere in space (Giancoli, 1984). Therefore, stated simply, electromagnetic fields influence the consequence of matter immersed within it.

An electric field can be described in terms of the units $V \cdot m^{-1}$, or $kg \cdot m \cdot A^{-1} s^{-3}$. An electric field or electric force of one particle due to the proximity of another particle can be described by the equation $F_E = q_1 \cdot q_2 / 4 \cdot \pi \cdot \epsilon \cdot r^2$, which is very similar to the formula for gravitation, where q is charge of the particle, and ϵ is the electric permittivity of free-space (Serway and Jewett, 2004). One can see from the formula that the electric field strength at any point is proportional to the inverse square of the distance separating the two charges. A classic example of an electric field is depicted in Figure 1.3 where lines of force connect a positively-charged particle to a negatively-charged particle. Similarly, moving electrical charges, which produce an electric field, also simultaneously produce a magnetic field perpendicular to the direction of the current flow by the principle of

electromagnetic induction developed originally by Faraday (Serway and Jewett, 2004). The intensity of the magnetic field, which can be ascribed the unit Tesla or $\text{kg}\cdot\text{A}^{-1}\cdot\text{s}^{-2}$, can be calculated using the formula $B=\mu\cdot I/2\pi r^2$ where μ is the permeability of free space, I is the electrical current strength and r is the radial distance from the current source.

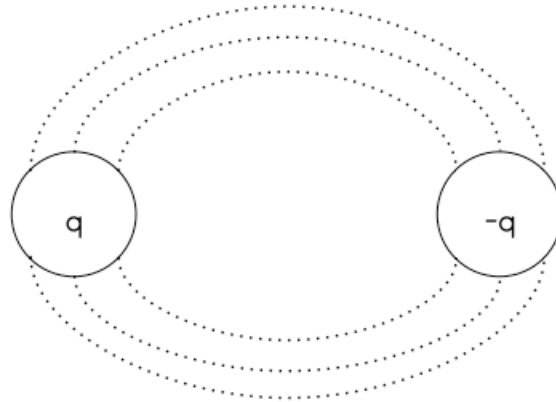


Figure 1.3 Classical example of electric fields generated by a positively-charged (proton) and negatively-charged (electron) particles.

2.1.2 Geomagnetic Field

Surrounding the earth there exists a magnetic field. There are many theories as to how this field is generated, but it is generally accepted that the earth's magnetic field is generated by electrical current loops produced by moving liquid iron within the earth's outer core (Roberts, 1992). Due to convection and temperature disparities between the earth's core and the layer containing the metallic fluid, the fluid moves around the solid iron core and generates an electrical current loop that in turn produces a magnetic field.

Around the earth outside of the earth's atmosphere exists a region that is known as the magnetosphere that hugs the earth and rejoins to form the magnetotail (Figure 1.4). The dynamics of this region are influenced by the solar wind, which can be described as a steady 'laminar' flow of particles (mostly protons) similar to a stream of water moving around a rock (Bleil, 1964). The study of the interaction between the solar wind and its associated magnetic field with the earth, which is about 1-5 nanoTesla, is known as electromagnetic hydrodynamics.

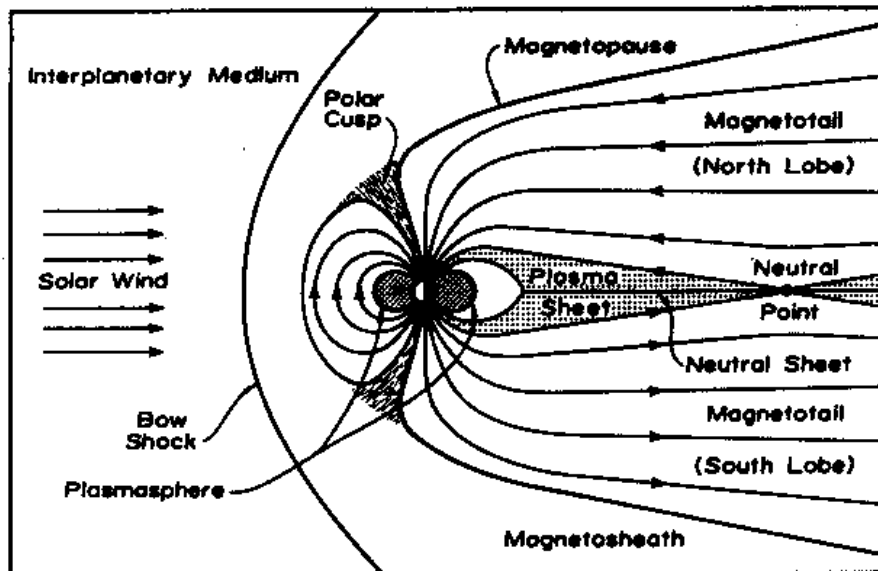


Fig. 2. A schematic noon-midnight meridian cross-section of the terrestrial magnetosphere (Russell, 1972).

Figure 1.4 The magnetosphere and associated boundaries. Picture from (Russell, 1972).

The strength of the earth's magnetic field, measured in Teslas or $\text{kg}\cdot\text{A}^{-1}\cdot\text{s}^2$ is usually measured with a digital magnetometer. Due to the three-dimensional nature of magnetic fields, there are usually three measurements that are required to more accurately describe its intensity, namely the x, y, and z-components. In addition, two

other measures describe the angle of the flux lines with respect to the horizontal component, called declination, as well as the angle from which it deviates around the earth's meridian, called inclination (Chapman and Bartels, 1940).

The typical intensity of the geomagnetic field is approximately 20-60 microTesla, or 20,000 to 60,000 nanoTesla depending upon what component is measured (Chapman and Bartels, 1940). This intensity varies in time depending upon geographical location and external solar forces such as proton storms generated from coronal mass ejections. It is generally accepted that the strength of the field increases as a function of latitude, with highest intensities recorded in aurora regions of the Northern hemisphere relative to the equator.

The sun periodically produces coronal mass ejections, which are high-energy bursts of protons that can interact with the earth's geomagnetic field to produce geomagnetic storms. These bursts of energy travel via the solar wind with velocities that can range from about 300-400 km·s⁻¹ background velocities to about 600-900 km·s⁻¹ (Matsushita and Campbell, 1967). Due to the higher density of protons and the increase in speed of the solar wind, it produces a disturbance in the geomagnetic field and displaces the background geomagnetic field from anywhere between 30-300 nanoTesla (Bleil, 1964). Julius Bartels developed a scale by which the strength of the geomagnetic disturbance could be quantified and is called the K-index. K-indices below 4 are commonly known as 'low disturbance', whereas K-indices at 4 or above 4 are regarded as moderate to active-level disturbances respectively.

While the initial displacement can take place anywhere between seconds and minutes, there is usually a longer 'recovery' time which can last anywhere from days to

weeks in some instances (Bleil, 1964). These periods of geomagnetic disturbance can be visualized on magnetometers as an initial spike (as in the case of a 'sudden' commencement) with a displacement of the field known as the 'main phase' period followed by a slow recovery back to normal levels (Figure 1.5). It is at these times where lights called aurorae can be seen with the naked eye, particularly in higher latitude areas and especially in auroral regions of the earth.

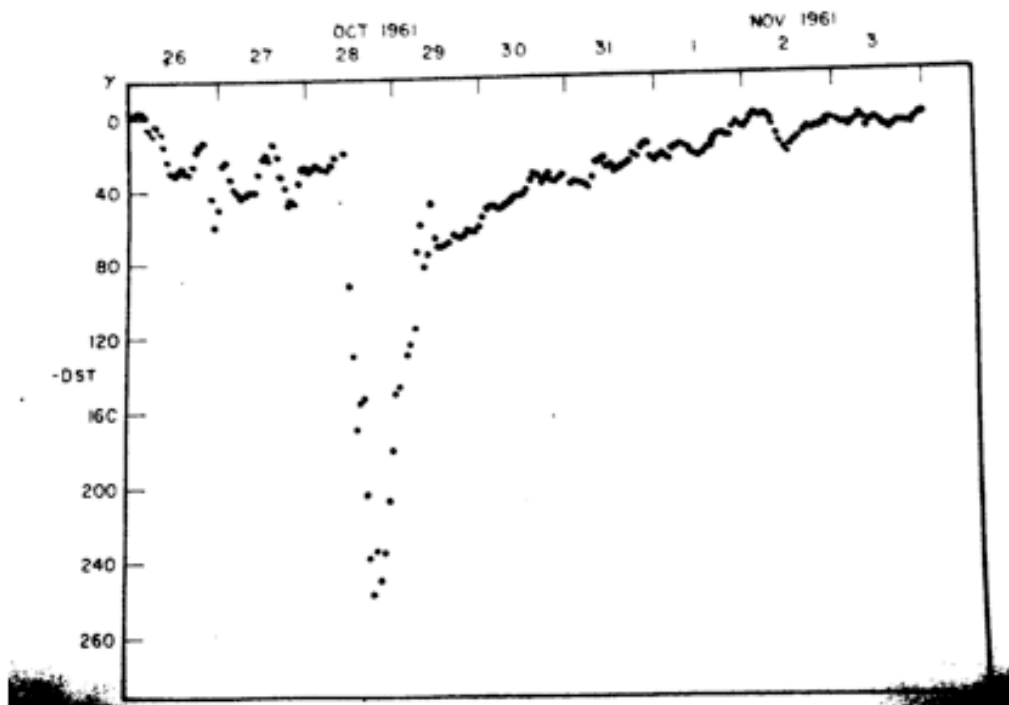


Figure 1.5 Example of a geomagnetic storm. The y-axis refers to gammas (each gamma represents one nanoTesla) and x-axis is time. Picture in (Bleil, 1964).

2.1.3 Earth-Ionospheric Schumann Resonance

In between the surface of the earth and the lower layer of the ionosphere, there exists a cavity with which electromagnetic waves can resonate (Figure 1.6) (Sentman, 1995). This cavity exists because the density of protons in the D-layer of the ionosphere acts as a boundary with low conductivity that allows electromagnetic fields to bounce back and forth (Schlegel and Fullekrug, 1999). This capacity of the earth-ionospheric cavity is exploited for propagation of short-wave radio (within kilohertz range) as well as to determine the ionospheric proton density. In the latter, megahertz radio frequencies are beamed into the ionosphere and are refracted back to the earth. Because proton density is related to the passing of certain frequencies, the frequency of radio waves that penetrates into space and does not deflect back to earth can be used to estimate the proton density of at a given altitude.

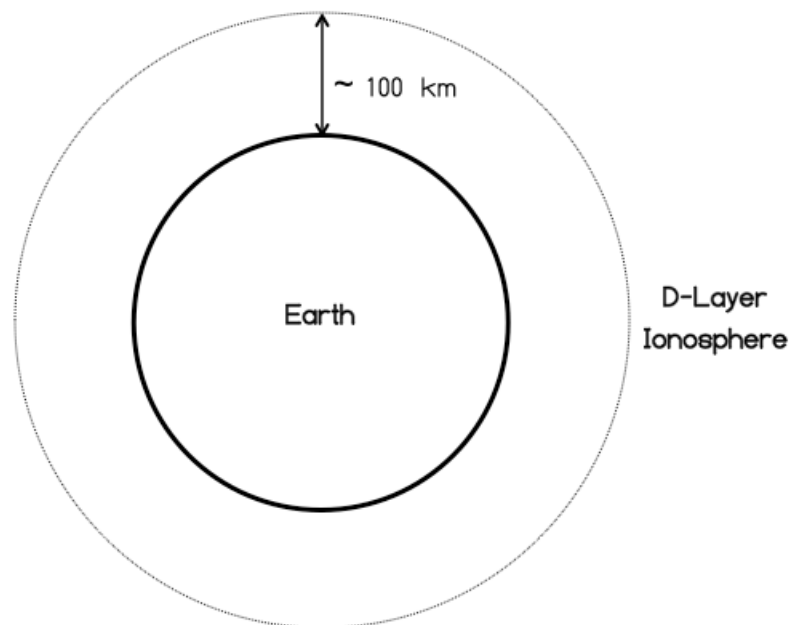


Figure 1.6 Schematic diagram of the cavity bounded by the earth and the ionosphere.

In the 1950s Winfried Otto Schumann predicted that the boundaries formed by the earth and the ionosphere could function as a waveguide for resonant electromagnetic frequencies (Besser, 2007). Resonance can be expressed as a property of all matter such that its physical characteristics produce a structure that allows the object to oscillate at particular frequencies. A common example would be that of a wine glass. When a particular frequency of sound is injected into the glass, it produces standing waves with the structure of the silica. Depending upon the amplitude of the injected sound at a resonant frequency, the standing waves can become so large that it shatters the glass.

Because electromagnetic waves travel at a velocity similar to light, and because of the circumference of the earth is approximately 40000 kilometers, one can obtain a frequency by inserting these two values into the classic equation for velocity of a wave $v=f\lambda$ where v is velocity ($m\cdot s^{-1}$), f is frequency (s^{-1}) and λ is wavelength (m). Solving for the frequency one obtains $3\cdot 10^8$ divided by $4\cdot 10^7m$ to yield a frequency of approximately 7.5Hz. This theoretical fundamental frequency of this cavity has since been measured many times to be approximately 7.8Hz, however like all natural phenomena the fundamental frequency is organized along a normal distribution such that the it can vary between 7.3 and 8.3Hz.

Harmonics of a fundamental frequency can be explained as octaves of the same pitch within a musical context. For example if one pictured middle C on a piano, the C occurring one octave above could, for demonstrative purposes, be considered a harmonic of middle C. Just like most standing waves, the Schumann resonance fundamental frequency has harmonic frequencies spaced by approximately 6Hz intervals to yield harmonics of approximately 14, 20, 26, 33, 39, 45 and 51 Hz (Figure 1.7) (Rakov

and Uman, 2003). Typically harmonics measured above the 40Hz harmonic are rarely measured because of electromagnetic interference from human-constructed power systems (i.e. 60Hz) as well as telephone ring currents (Konig, 1981). When they are not sufficiently far away from these sources, constructive and destructive interference can produce uncharacteristic signals when measured by ground-based magnetometers (Nickolaenko and Hayakawa, 2014).

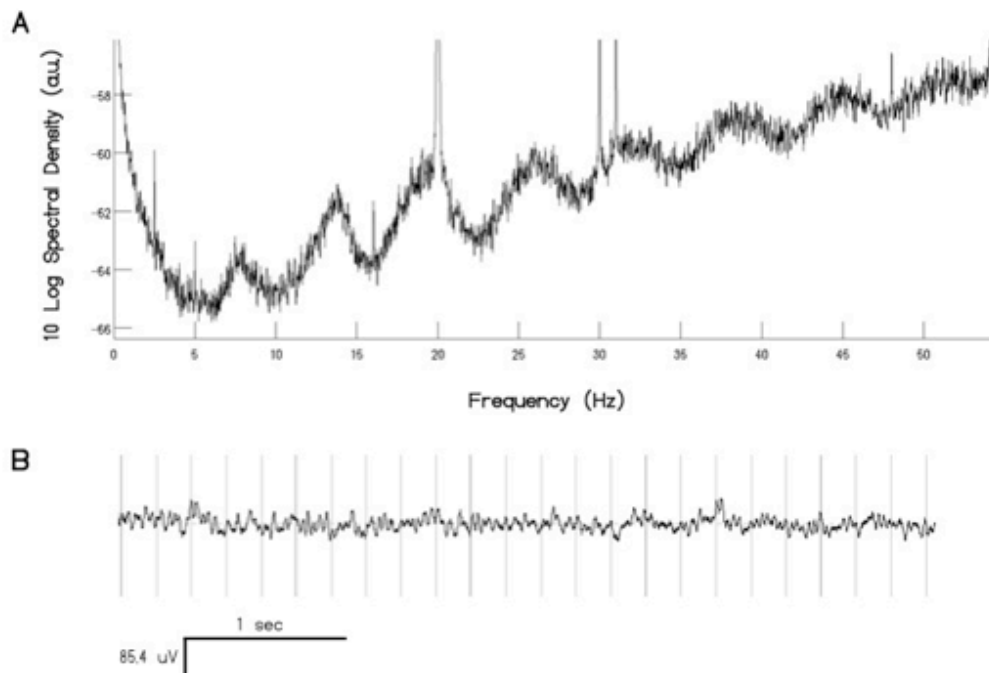


Figure 1.7 (A) Spectral density profile of the Schumann resonance (B) Exemplary time-series from which Schumann resonance spectra are obtained.

The magnetic component of the Schumann resonance is typically measured with air-coil or induction coil magnetometers with sensitivities in the picoTesla range, usually expressed in dimensional units of $\text{pT}^2 \cdot \text{Hz}^{-1}$ (Greenberg and Price, 2007, Heckman et al., 1998)). To appreciate this sensitivity, a typical electromagnetic intensity measured from

a computer screen is about a microTesla, or a million times stronger than the Schumann resonance whereas typical magnetic resonance imaging devices are within the order of 1-2 Teslas, or a trillion times stronger than natural earth background 'noise'. The induction coil itself is a cylinder wrapped with tens to hundreds of thousands of thin copper wire (with approximately .2-.3 millimeter diameter). A paramagnetic material, such as mu-metal, is then inserted into the center coil to increase its inductance (ability to attract a magnetic field) by a factor of 100 to 1000 times. Because a time-varying electrical current is associated with a time-varying magnetic field by electromagnetic induction, the magnetic field picked-up within the coil produces electric current within the copper wire. The time-varying voltages are then fed into equipment that filters out unwanted artifacts and magnifies the signal. The resultant time-series (signal) is then recorded on a computer and is entered into software that can analyze the frequency characteristics of the signal.

The Schumann resonance displays peak intensities at times that roughly correspond to peak thunderstorm activity at equatorial levels, such as Southeast Asia and Africa (Price and Melnikov, 2004). Konig found that the Schumann resonance was stronger during daytime periods (Konig, 1974); other researchers later confirmed this finding (Price and Melnikov, 2004). In addition, the Schumann resonance displays a characteristic seasonal variation with the highest variation in the first fundamental frequencies occurring in the winter as opposed to the summer (Satori, 1996). The Schumann resonance can also be used as a measure to infer global temperature (Sekiguchi et al, 2006).

2.1.4 Geomagnetic Micropulsations

Geomagnetic micropulsations are visualized in strip-chart recordings of the earth's time-varying electromagnetic field as periodic fluctuations with intensities of about 1 to 5 nanoTesla (Bleil, 1964). They are generated by changes in solar wind and their nomenclature can be divided into two classes of occurrences (Jacobs, 1970). Micropulsations with a regular periodicity are labeled as 'continuous' (Pc) whereas micropulsations that appear to be spontaneously arranged are called 'irregular' (Pi). These two classes can be further broken down as a function of their frequency. A table listing the general characteristics of the types of micropulsations can be found in Table 1 and is adapted from Bianchi and Meloni (2007).

Table 1-1 Nomenclature for geomagnetic micropulsations with their associated frequencies and intensities. Adapted from Bianchi and Meloni (2007).

	Continuous pulsations					Irregular pulsations	
Pulsation	Pc1	Pc1	Pc3	Pc4	Pc5	Pi1	Pi2
Class							
Period (s)	0.2-5	5-10	10-45	45-150	150-600	1-40	40-150
Frequency (mHz)	200-5000	100-200	22-100	7-22	2-7	25-1000	2-25
Intensity (nT)	1	3	10	<300	300	10	100

The most commonly recorded micropulsations are Pc1s (Figure 8) and can be measured with instruments sensitive enough to measure time-varying magnetic fields

with intensities within the nanoTesla range, such as with induction coil magnetometers. Because of their periodicity and fine-structure, they have been labeled as ‘pearls’ due to their resemblance to a pearl necklace (Kangas et al., 1998). These micropulsations appear more frequently during nighttime recordings at mid-latitude regions, regardless of geographic location and possess polarity inversion at conjugate geographical locations (i.e. locations on the earth with similarities in geomagnetic flux). During a Pc1 event, the ‘inter-stimulus’ time between adjacent pearls is approximately 5-10 minutes with fine-structure frequencies of about 0.1 to 5Hz (Figure 1.8) with an event duration that can last from minutes to hours.

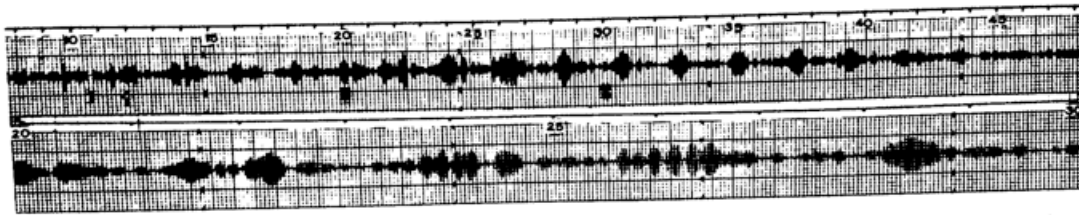


FIG. 7. Example of amplitude variation for *pc* 1 event at Macquarie Island from 0008 to 0048 UT on 10 February 1962 (upper trace). An expanded 10 min of the upper record appears as the bottom trace [Campbell and Stiltner, 1965].

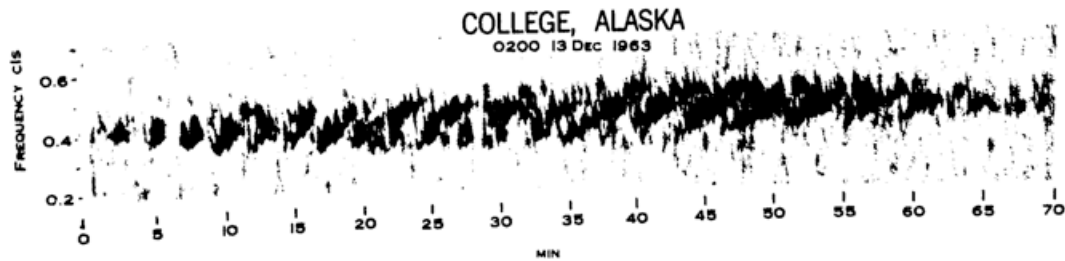


FIG. 8. Representative emission at College, Alaska, 13 December 1963 [Campbell and Stiltner, 1965].

Figure 1.8 (Above) Time-series and (Below) sonogram of a Pc1 micropulsation event showing ‘rising-tones’ in the range of 0.4 to 0.5Hz. Picture in Volume 2 of Matsushita and Campbell (1967).

2.2 Quantitative Electroencephalography (QEEG)

2.2.1 Equipment and Methods

The quantitative electroencephalograph is a modified version of the electroencephalograph discovered by Hans Berger and allows for the digital recording of voltages that are recorded from the surface of the scalp (Millett, 2001; Niedermeyer 2005). Whereas during the discovery of the electroencephalograph data analysis was performed mostly by qualitative visual inspection or coarse frequency approximation by counting the number of peaks per second (indication of frequency), in a modern context computers are used to record raw voltages at high sampling frequencies (the number of recordings per second) which allows researchers to quantify the 'peaks and valleys' of electrical activity from the brain in terms of frequency and amplitude. Most contemporary quantitative electroencephalographs are battery-operated and fed into laptop computers making them portable and adaptable to most conceivable experimental settings.

In standard procedures, sensors with an approximate diameter of 1 cm are placed on the scalp with some conductive paste (usually a compound containing sodium) sandwiched between the sensor and the scalp. In some QEEG apparatuses, the sensors are embedded in a cap that can simply be applied over the scalp. Each sensor is then placed according to standardized sensor placements, known more commonly as the 10-20 International Standard of Electrode Placement. This standardization ensures that results are generalizable to other researchers and also facilitates replicability within different laboratories.

Once the sensors/cap have been applied and impedances of each sensor have been appropriately set (by adding or subtracting the conductive paste), measurements of

voltages at a fixed sampling rate are collected and digitized, with a digital-to-analog converter system, and recorded by a computer system.

2.2.2 Nature of the Data

The intensities of the voltages typically recorded with the QEEG are within the range of 50-100 microvolts, or $10^{-6} \text{ kg}\cdot\text{m}^2\cdot\text{A}^{-1}\cdot\text{s}^{-3}$. For comparative purposes, this voltage is approximately a million times less than batteries that supply power for television remote controls. The intensity of the scalp recordings is approximately proportional to the numbers of action potentials, whose voltages are within the order of 10^{-3} volts of neurons firing synchronously. It may seem counter-intuitive that the voltage associated with neuronal assemblies is a thousand times less than the voltage associated with one action potential; however scalp voltages are not only attenuated by the physical impedance by the skull and cerebrospinal fluid, but also by constructive and destructive interference (adding and subtracting) of proximal neuronal discharges. The mechanism by which the 'squiggles' observed in the strip chart are generated has been summarized in Figure 1.9 which shows that the voltage of the local field potentials (recorded within a defined area of the scalp) are approximately proportional to the integrated neuronal activity below the surface.

2.2.3 Spectral Analysis

The obtained signal can be expressed in terms of a time-series and is thus entered into appropriate statistical analysis. One of the most common techniques for understanding the frequency characteristics of the time-series is to apply a Fast Fourier

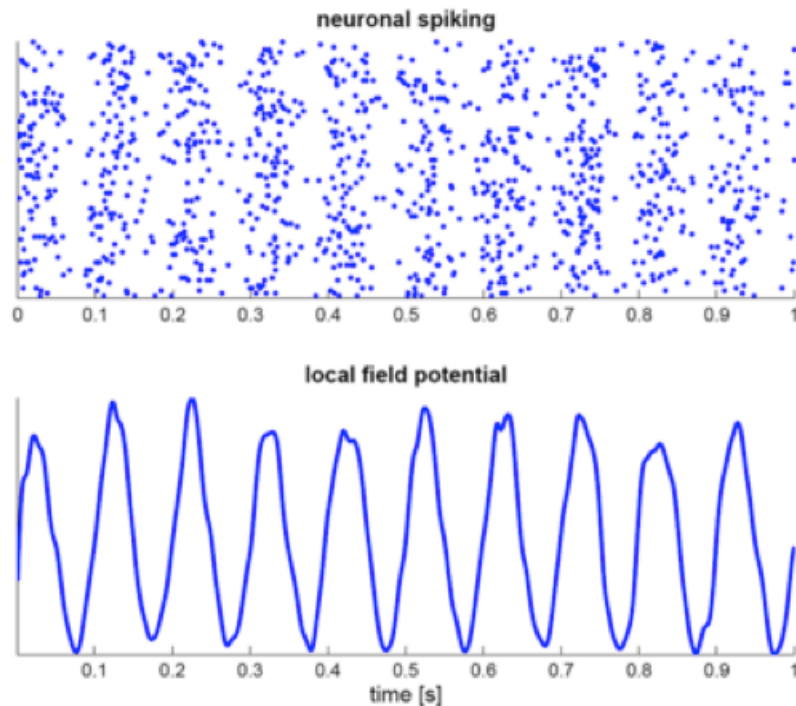


Figure 1.9 Theoretical simultaneous spiking of many neurons contributing to (Below) local field potentials measured from sensors on the scalp. From en.wikipedia.org/wiki/Neural_Oscillation.

Transform. This equation models the ‘irregular’ time-series into a series of sinusoidal waves of increasing frequency and then calculates the spectral density of each sinusoidal component. A summary of the FFT procedure is depicted in Figure 1.10. Due to the nature of the algorithm as well as the Nyquist limit, the maximum frequency of a given time-series that can be characterized is dependent upon sampling rate such that the upper limit is one-half the original sampling rate, or expressed more consisely $F_s/2$ where F_s is the sampling frequency. Therefore sampling the observed voltages at higher frequencies allows a greater characterization of the signal’s spectral characteristics.

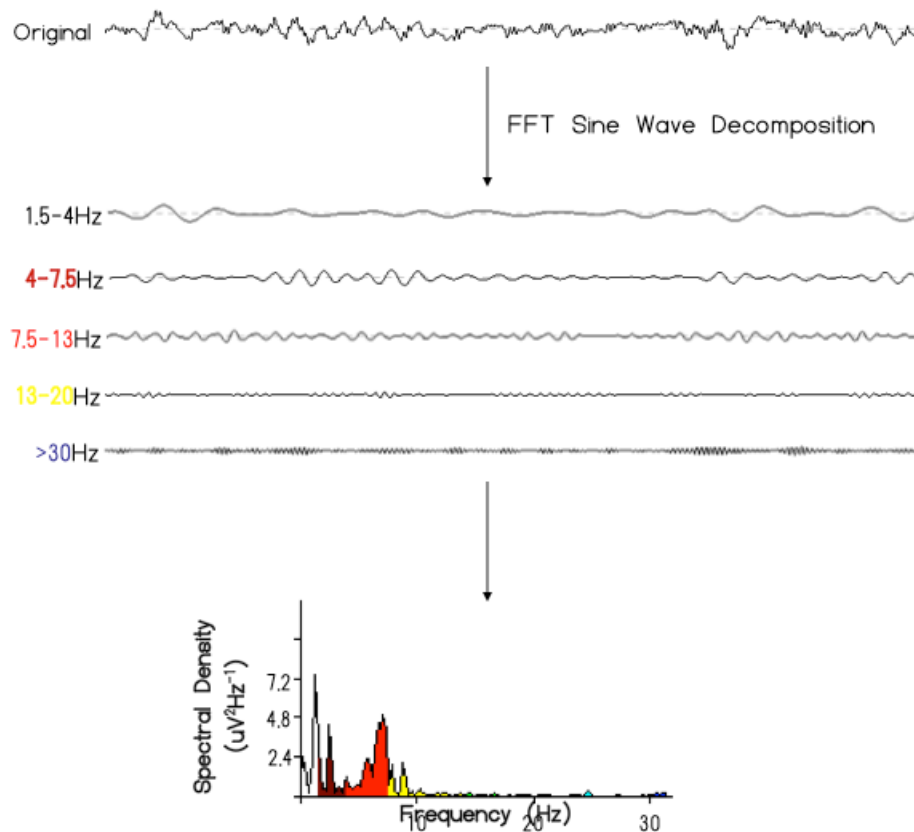


Figure 1.10 Schematic of a typical spectral analysis performed on quantitative EEG data. The original signal (top) is modeled after a series of sine waves (middle) and the area under the curve of each signal is then calculated and graphed (bottom).

It is common to divide the observed spectral densities in terms of frequency bands, or summated spectral densities of multiple frequencies. The classic frequency bands are delta (1.5-4Hz), theta (4-7.5Hz), low-alpha (7.5-10Hz), high-alpha (10-13Hz), beta₁ (13-20Hz), beta₂ (20-25Hz), beta₃ (25-30Hz) and gamma (>30Hz). In each case, the bandwidth represents the sum of the spectral densities ($\text{uV}^2 \cdot \text{Hz}^{-1}$) of the discrete frequencies within the given frequency range. This categorization is largely based upon qualitative brain-behaviour relationships of individuals discerned years ago. For example, Hans Berger observed that when individuals, as well as animals such as dogs, closed their eyes there was a preponderance of 'spindles' observed in the strip chart.

These spindles are usually between 8-13Hz and are now classified as 'alpha' activity. In contrast when individuals are asked to mentally solve mathematical problems, the strip-charts of the individuals displayed fast-frequency activity, now characterized under 'beta' and 'gamma' frequency domains.

2.2.4 Brain Microstates

The shape of the electric field of the brain can be modeled with isocontour lines similar to those used in demarcating geographic altitudes in mapping. The isocontour lines, rather than height in the example of geography, indicate voltage gradients. The lines are then connected where the voltage is roughly approximate, which is almost the exact same process used to map the electric and magnetic flux lines outlined in examples from the physical sciences and is a popular technique in electroencephalography (Duffy, 1986).

While there are many algorithms that can model the contour lines, one of the most popular methods reported in the literature was described by Lehmann and Koenig (2004) almost 20 years ago and almost 40 years ago by Skrandies and Lehmann (1980). The basic idea was to treat the arrangement of sensors on the scalp as probes of an electric field and study the resulting shapes that were produced during experiments designed to elicit a response to a visual stimulus. By computing a spatial standard deviation, which is more popularly known within the literature as global field potential, a reference-free indication of the global output of the brain could be obtained, independent on the choice of reference electrodes at the time of measurement (Skrandies, 1990). Originally, it was found that this measure correlated significantly with changes in the electric field of the brain evoked with images. Thus, when a visual stimulus was

presented to the participant, a peak in global field power was observed. The 'shape' of the 'electric field landscape' was then visualized by computing a Principal Components Analysis on all channels recorded simultaneously. PCA is similar to factor analysis in that it is used to reduce a set of variables into mutually exclusive 'factors'. For example, in principle a PCA, when looking at the complexity of different musical songs, might be able to categorize them into "electronic", "country", "classical" and "rock and roll". In the case of EEG, the electric field inferred from multiple recording can be factored into a handful of basic shapes.

In a paper published by Koenig and Lehmann in *NeuroImage* in 2002, the authors reported that 4 classes or shapes of electric fields (Figure 1.11) represented ~80% of the variance in cortical electric field topographies; these shapes have been confirmed by many other researchers. These electric field microstates have a mean duration of about 80-100 milliseconds whose duration changes as a function of age. In addition, the occurrence or frequency of each microstate as well as the time spent in one microstate versus the other 4 also change as a function of age, and also in certain clinical populations. For example, the average microstate duration was found to be shorter in people who exhibited symptoms of schizophrenia, as well as general cognitive impairment (Lehmann et al., 2005; Stretlets et al., 2003; Koenig et al., 1999). Recently, Corradini and Persinger (2014) showed that the average microstate duration was significantly correlated with measures of global impairment as inferred by psychometric indicators of cerebral assessment.

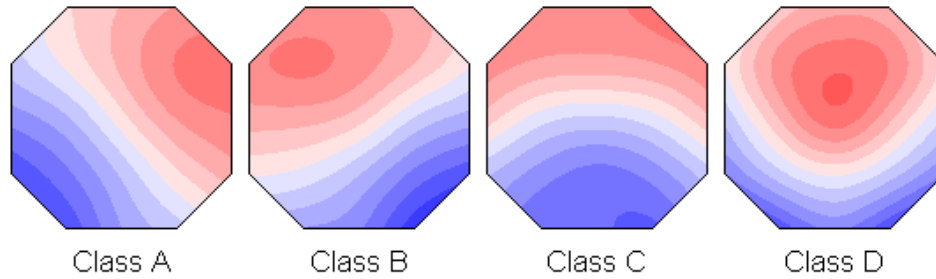


Figure 1.11 The 4 classes of normative microstates as originally discovered by Koenig and Lehmann (2002).

That dynamic changes occur within assemblies of neurons can be modeled with microstates is beneficial for a plethora of reasons. First, if it is assumed that consciousness is the result of coherent oscillations which merge between distinct parts of the brain to produce the sensation of a percept, these microstates allow for quantitative descriptions of the shapes that might be associated with them. In other words, the study of the electrical components of consciousness is not just relegated to the frequency domain, as is more commonly employed in electrophysiology, but can also be explored in terms of spatial patterns. For example, one of the common metaphors applied to this type of analysis is that the 4 microstates might represent the 4 'building blocks' of thinking. In this respect, all thinking that occurs in one second within the individual is a combination of these 4 basic patterns represented in the shape and duration of the brain electric field.

2.2.5 Coherence

In statistics, two variables x and y are said to be correlated if they vary together. If an increase in x is associated with an increase in y the correlation is positive (+); conversely if an increase in x is associated with a decrease in y the correlation is

negative (-). The concept of correlation can also be extended to describe functional connectivity between two recording sites of an EEG and is called coherence. Coherence measures the strength of the relationship between two EEG recording sites recorded simultaneously. It can also be described as harmonies of the brain. In this case the two EEG recording sites can be expressed as a violin and a cello. The amount of consonance between the two instruments would be a metaphor for coherence.

If the brain is assumed to have distinct areas, based upon cytoarchitecture or function, then coherence can be described as how these brain areas interact over time. For example a conversation might be described as coherence between the left temporal and left frontal regions. While activation within the left temporal region, more specifically Wernicke's area, is classically associated with the reception of speech, the left frontal region, called Broca's area, is associated with initiating speech. Because conversation is an interaction between listening to and understanding language (left temporal) and responding (left frontal), one might expect that the coherence between these two regions is significant.

Coherence analyses have been used in many research endeavors to characterize the functional connectivity of the brain when individuals perform a multitude of different tasks. For example, a recent study investigated coherence of the brain when individuals were asked to discern the emotional prosody of speech (Rusalova et al., 2014). It was found that overall coherence was decreased for individuals who could sense the emotional component of speech more easily. In a study investigating 'resting' state EEG, it was found that coherence between the pre-motor cortex and the parietal lobe could predict with ~85% accuracy how fast an individual could acquire a specific motor skill (.

Coherence analyses have also been used to assess responses to electromagnetic stimuli when applied to the brain. Recently, Saroka and Persinger (2013) found that when individuals experience a sensed presence there is greater coherence within the alpha band between the left and right temporal lobes of the brain. Hill and Saroka (2010) utilized coherence analysis to discern functional connectivity changes in individuals who listened to binaural recordings of 'sacred sites' found within Canada. They found that there was increased coherence between the left temporal and right frontal regions). Finally, it has also been found that coherence between the left and right temporal regions increases as a function of the disturbance of the static geomagnetic field (2014). In this study, coherence measures derived from approximately 200 individual recordings of 'resting-state' eyes closed electroencephalographic baselines were used.

Coherence is usually expressed in terms of its frequency characteristics and ranges between 0 (no coherence) and 1 (perfectly coherent). Mathematically coherence C_{xy} between two EEG recording sites x and y is described as $C_{xy} = S_{xy} / \sqrt{S_x S_y}$ where the numerator is equal to the square-root of the cross-spectrum of the two signals and the denominator is the product of the spectrums of x and y (Knott and Mahoney, 2001). An example is depicted in Figure 1.12. In the upper part of the figure, two signals recorded from the left and right parietal recording sites are shown. Already, one can see how the voltages in both signals seem to increase and decrease together. The bottom part of the figure shows the results of the analysis. It is clear that these two signals are coherent at 10Hz by inspecting two components of the figure; the left side of the figure depicts the coherence magnitude peaks at 10Hz and the spectrogram shows a band of yellow, red, blue, and green occurring at the same 10Hz component where the x-axis indicates time.

The colours can be compared to real coherence values by reference to the colour legend on the right.

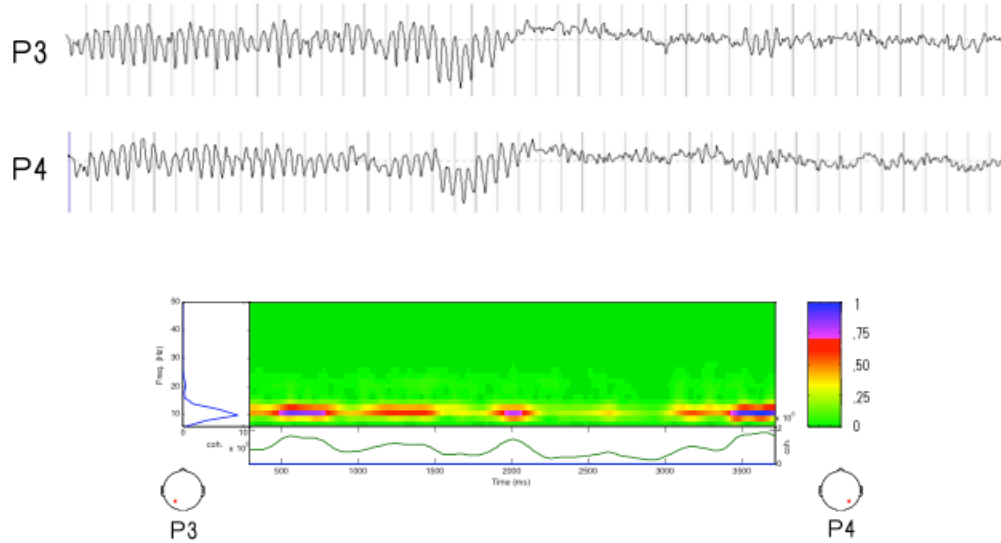


Figure 1.12 (Top) Two signals derived from P3 and P4 sensors on the scalp show evident synchronicity (Bottom) Coherence analysis indicating that both sensors are periodically coherent within the 9-10Hz range.

2.2.6 Source Localization

Source localization is a relatively new technique for the quantitative electroencephalograph and is used to discern “where” a particular kind of activity was derived from. Because fluctuations within the electric field of the brain can be highly redundant, source localization provides a way of discerning the source of a particular type of activity. While the spatial resolution is dependent upon the number of sensors sampling the brain’s electric field, it is a relatively accurate tool with quantitative electroencephalographs with as little as 16-19 sensors. The unit of measure for source localization is current source density (μAmm^{-2}) and can range from anywhere between 50 and 2000 units.

One of the most commonly used software for source localization analysis is called sLORETA, which is short for standardized low-resolution electromagnetic tomography (Pascual-Marqui, 2002). The software itself is free to use for any researcher and comes equipped with many different functions that allow for statistical comparisons to be performed between two groups, utilities that can save activation of specific regions of the brain for implementation into other statistical packages like SPSS, as well as explorer tools that can be used for visual mapping and computation of functional connectivity of distinct brain regions. This software has been reliably tested against other measures such as fMRI. For example, one EEG-fMRI study has shown that an increase in alpha electrical activity measured with the QEEG over the occipital regions when analyzed using source localization techniques is also associated with a decrease in blood-oxygenation visualized with fMRI.

Source localization, specifically using sLORETA, may also be a valid indicator of brain function within clinical settings. Corradini and Persinger (2013) performed a study which assessed the accuracy with which sLORETA could localize specific sources of activity while performing various neuropsychological tests from the Halstead-Reitan battery. It was found that many of the tests assessing function of specific regions of the brain were congruent with sLORETA activations during the time of the performance of those tests.

2.3 Biological Effects of Natural and Experimental Electromagnetic Fields

Because all matter, including living organisms, is composed of particles the importance of the influence of electromagnetic fields on biological systems can be appreciated. In addition, because living systems are aggregates of particles, the study of electromagnetic fields on biology and behavior can help to understand how they influence living systems macroscopically.

Over the past few decades an abundant literature has been created suggesting that brain activity and behavior can be influenced by applying weak-intensity electromagnetic fields within the microTesla range. In 2009, Tsang and Persinger published a study showing that subjective mood, as measured by the Profile of Mood States questionnaire, is significantly affected by application of different patterns of electromagnetic activity. Changes in depression and fatigue were both significantly decreased by the application of a particular pattern modeled after burst-firing neurons recorded from the amygdala. This pattern was also employed by Baker-Price and Persinger in a study investigating the possible treatment of depressed individuals following closed-head injury (Baker-Price and Persinger, 1996; Baker-Price and Persinger, 2003). The results showed that symptoms of depression, inferred using the Beck Inventory for Depression, significantly decreased during a 6-week program in which BurstX was applied for 50 minutes once per week.

Weak-intensity electromagnetic fields, when applied across the bilateral temporal regions, have also been shown to induce the sensed presence and out-of-body experiences experimentally. Saroka and Persinger (2013) showed that individuals who experienced a sensed presence also displayed changes in brain activity. The sensed

presence protocol consists of a 30-minute bilateral temporo-parietal application of a frequency-modulated pattern (also called the Thomas pattern), followed by a 30-minute application of the BurstX pattern. Individuals who experienced a sensed presence also displayed an increase in bilateral-temporal coherence after approximately 10-15 minutes after the initial frequency-modulated application. This change was also accompanied by an increase in right frontal theta (4-7Hz) activity. This finding replicated previous work showing that the sensed presence is more probable when there is coherence between the right and left temporal lobes whereas out-of-body experiences are associated with increased coherence within the left-temporal lobe and the right-frontal lobe.

In a study published in 1999 Cook and Persinger showed that the experience of subjective time could be influenced by the application of a frequency-modulated pattern (Thomas pulse) with a device called the Octopus. This device is comprised of 8 solenoids that are arranged around the head. Upon initiation of a field pattern, each solenoid is activated in a counter-clockwise manner individually for a period of time. Using the same device, Lavalley and Persinger (2011) showed that application of a suite of patterns (each 5 minutes in duration) not only affected microstate descriptors but also produced the sensed presence in individuals exposed to the 'forward' as opposed to the same set of patterns presented in reverse. This finding further confirmed that the presentation of the patterns is of critical importance for the elicitation of experiences within subjects.

The electromagnetic field strengths are about 1000 times less than those used in conventional studies investigating transcranial magnetic stimulation (TMS). Whereas the former have intensities within the milliTesla to Tesla range, those employed in the above cited studies are within microTesla range. One of the suspected reasons for their

efficacy is that the patterns mimic natural processes within the brain, whereas TMS studies usually employ simple sine waves that the brain may habituate to in a matter of seconds due to their intrinsic redundancy (1995).

Changes in the static geomagnetic field have also been demonstrated to be correlated with changes in brain activity has been suggested by many individuals. In a series of experiments Mulligan and Persinger (2010) showed that geomagnetic disturbances influence brain activity. The first correlative study replicated a previous study conducted by Babayev and Allahverdiyeva (2007) and indicated that 'resting' theta (4-7Hz) and gamma (40+ Hz) activity occurring within the right prefrontal cortex while individuals were sitting with eyes-closed was highly correlated with the atmospheric power obtained from polar orbiting satellites. In a second experimental study complimenting the first, Mulligan and Persinger (2012) applied electromagnetic fields (comparable in pattern and strength to natural geomagnetic storms) to individuals while their brain activity was monitored with a quantitative electroencephalograph. The results indicated that the individuals exposed to the 20 nT simulated geomagnetic storm showed an increase in theta activity within the right parietal and a suppression by application of 70 nT strength geomagnetic simulations.

Dr. Neil Cherry published many manuscripts investigating the relationship between the strengths of the Schumann resonances and human health (Cherry, 2002; Cherry, 2003). In particular he has found that increases in sunspot number, which he has shown to be positively correlated with Schumann resonance intensity, is also highly correlated with induced and accidental death rates in Thailand. As was demonstrated by Cosic (2006) who showed that the spinal cord exhibits its own selective response profile with frequencies similar to the Schumann resonance, Cherry further extrapolated on the

apparent similarity between the spectral densities of the Schumann resonance and the brain synthesized originally by Konig (1974, 1984). Based upon these observations in combination with works by other researchers including Wever (1974) who demonstrated that human circadian rhythms are disrupted by insulation from the natural ELF electromagnetic activity, Dr. Cherry proposed that human biological systems are synchronized with the Schumann resonance and that disruption in the connection can produce deleterious effects on human health.

3.0 Apparent Earth-Ionosphere-Brain Connection

3.1 Experimental Motivations for Investigation

Shortly after Winfried Otto Schumann published theoretical calculations proposing that the cavity between the earth and ionosphere would act as a waveguide to support electromagnetic standing waves, Dr. Herbert Konig, who was Schumann's doctoral student, was able to measure the time-varying signals of the earth's Schumann resonance; its validity was verified later multiple independent researchers (Balsler and Wagner, 1960; Chapman and Jones, 1964; Madden and Thompson, 1965). In multiple published books, including Persinger's VLF-ELF effects, Konig showed that the signals recorded with magnetometers were similar in shape to those recorded from the electroencephalograms of people (Konig, 1974). He noted two types of signals that roughly approximated 1) the alpha rhythm which he called "Type I" signal, and 2) delta activity which was called "Type II". The original picture comparing the two signals is illustrated in Figure 113.

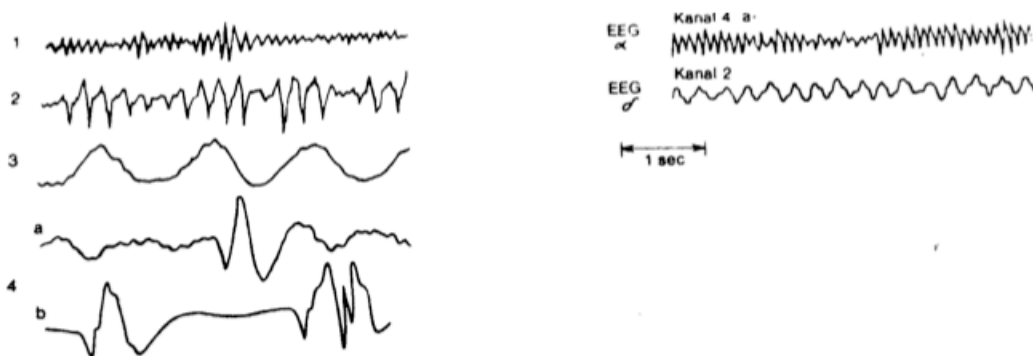


Figure 1.13 Original comparison between electromagnetic signals (Left) and signals derived from human electroencephalograms (right) made by Konig. Picture found in Persinger (1974).

To assess how the Schumann resonance may influence human behavior, Konig measured the reaction times of people as well as the Schumann resonance simultaneously. The analysis indicated that human reaction time was significantly correlated with the intensity of the Type I signal. In particular he found that as the relative intensity of the Type I signal increased, human reaction time (measured in milliseconds) decreased.

Since this time, multiple papers have been published on the convergence between brain electrical activity and the Schumann resonance. In 1995, Paul Nunez published a theoretical chapter on classical physics models and brain activity (Nunez, 1995). In the chapter, Nunez drew a direct comparison to standing waves, a type of physical wave produced by constructive/destructive interference of two waves with similar amplitude and frequency, generated by the earth-ionosphere and theoretical standing waves that might be produced by the cavity formed between the brain and the skull. A standing-wave can be visualized when one pictures an individual holding a string at which is fixed to a wall. If one oscillates the string up and down with a stable frequency and amplitude, one would observe that that the string seems to produce a steady wave that does not oscillate between + and – but rather seems to ‘stand’.

Standing waves can be described in terms of their fundamental frequency (f_0) and its harmonics (f_n). Depending upon the shape of the cavity, the harmonics of the fundamental frequency may vary. This property is utilized in the formation of musical instruments such as guitars and violins. By changing the shape of the cavity within which the pitch resonates, the timbre or tone of the plucked string changes. A classic example would be the differences in tones generated by an electrical guitar (without amplification or cavity) and a classical or acoustic guitar. Whereas the electrical guitar

may be described as sounding 'tinny', the acoustic guitar would be described as having 'tone'.

3.2 Quantitative Motivations for Investigation

Employing dimensional analyses and quantification of known physical aspects of geophysical and cerebral function, Persinger (2012b) predicted that there is a fundamental scale-invariant relationship between processes that occur globally around the earth during lightning storms (with comparable current densities as action potentials as they travel along the axon when diameter is accommodated) and within the brain itself. For example, the operating intensity of brain activity as well as the Schumann resonances are both within picoTesla range. In addition, using an average bulk velocity of ~ 4.5 ms divided by the average circumference of the human brain, Persinger obtained a fundamental frequency of approximately 7.8Hz.

This relationship may not just be coincidental. The average intensity of the time-varying magnetic field measured from the scalp is about 0.1 to 2 picoTeslas. These fields have been hypothesized to originate from activity perpendicular to the electric field, in accordance with the general relationship between electric and magnetic fields. Similarly the average intensity of the magnetic field recorded by the earth-ionosphere is between 0.1 and 1 picoTesla. Therefore despite the differences in size between the brain and the earth, there might exist a harmonic relationship between the two by means of average intensities.

To continue further, electric field strengths of the Schumann resonance have been measured to be between .1 and $1 \text{ mV}\cdot\text{m}^{-1}$. Paul Nunez in his book *Electric Fields of the Brain* (1984) models the cortex after a dipole layer with positive charge located ventrally towards the underlying white matter and negative charge located close to layer

I of the cortex (Figure 1.14). If this model is extended, it resembles the classic example of the electric field characteristics between two parallel plates with opposite charge (Figure 1B). As such it may be possible to calculate an electric field equivalent for comparison against intensities recorded in other natural phenomena.

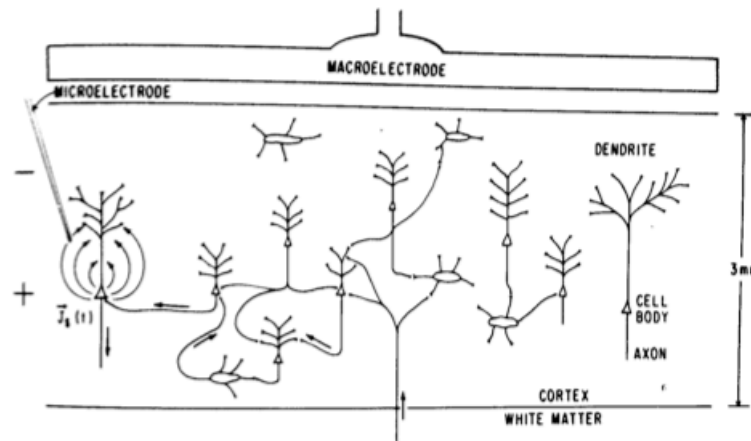


Figure 1.14 Schematic diagram of a section of neocortex that can be modeled as two parallel plates with the positive plate closer to cortex/white matter interface and the negative plate closer to the surface of the cortex. Taken from Nunez, 1984.

Relatively large fields of brain activity can be calculated by computing the root-mean-square of channels measuring posterior sites of the brain. The average spectral density is approximately $.3 \mu\text{V}^2 \cdot \text{Hz}^{-1}$ at a frequency of 7.8Hz for a population of 18 randomly selected baseline measurements. When this voltage is multiplied by frequency and square-rooted, a voltage of about $1.5 \mu\text{V}$ is obtained. If the assumption that the cortex (not considering gyrification) is dipolar is valid, dividing this voltage by the average thickness of the cortex of 3 mm results in an electric field strength of about 0.56 mV/m, well within the average range of electric field perturbations measured with devices like a Marconi or ball antenna.

4.0 Interdisciplinary Approach

Ultimately all knowledge is acquired, codified, interpreted, and communicated by processes that exist within the human brain. According to Nunez only about 5-10 percent of all white matter fibers in the brain, which relay information from one region to another, are purely sensory (Nunez, 1995). This would suggest that most aspects of 'objective' reality are the result of internal processes that have been acquired and developed through the experiences of the individual; however the possibility that only 5-10 percent is sufficient to gain an understanding of this reality cannot be dismissed. Either way, this fact would seem to indicate that perceived differences between concepts such as mono versus interdisciplinarity are the function of how the human brain constructs the environment and in this particular case the distinction. If this is the case, it would be advantageous to describe the two phenomena as though they were variables displaced from context. For example, a relationship between 'x' and 'y' may not exist until it is framed within a field of study, such as mathematics or molecular biology.

4.1 Disciplinarity

The concept of 'disciplinarity' has been explored from multiple perspectives. Within the context of epistemology and political science Turner (2000) has likened the idea of a discipline to a 'cartel' in a market. Such a comparison would imply that members of a particular discipline utilize standardized tools to produce knowledge that is largely communicable only amongst those who are immersed within the discipline. Because of the social structure of the discipline, languages are conceived to act as heuristics in communicating information from one research institute to another.

Others have argued that 'disciplinarity' is like a machine (Chettiparamb, 2007), similar to Newton's mechanistic model of the universe. In this sense, disciplines are necessarily a set of algorithms that allow for production of information by specializing in one particular function or set of problems. As a result a constricted view of how 'nature' functions could be built rapidly to allow for further technological advancements where needed. This conception of the term 'discipline' was potentially born historically out of the necessity in Germany to train individuals as technicians and professionals for industry (Salter and Hearn, 1996, p.19). As such, the concept of a discipline could be defined more generally as a collection of 'axioms' or rules that attempt to provide structure for the conception, acquisition, and realization of knowledge/information of a particular topic. The major thrust in the case of disciplinarity is the methodology and 'where' best to study a particular topic (Chettiparamb, 2007).

It has been suggested that the conception of the problem, eventually leading to the attained knowledge, is largely based upon the perceived boundaries of a given topic and how it may be categorized into a particular field (Moran, 2010). For example, understanding the morphology of bone structures within the mandibles of the mouth are best suited to taxonomic methods that currently exist within the genre of 'biology'. The acquisition phase would then be described as the methods of analysis used by that discipline to get some answer or output. Finally the output of the analysis would then enter a 'realization' phase by which the problem, the analysis, and the implications are framed within a literary work that is communicable to other members of the same discipline. This process is largely formalized, but plastic, depending upon shared beliefs and traditions, and by extension the language embedded within an associated discipline. In a sense, as described by Chandler (2009), there can be imposed a distinction

between what constitutes a doctrine and a discipline, the former having associated with it the concepts of subscription to some assumption; he revisits this idea by recapitulating Cohen's response of the irrelevance of association with a particular discipline where the necessary 'becoming embarrassed' of one's own practices suggests an attachment of identity of the researcher which perpetuates the notion of the 'sense of self' in part defined by the discipline. In short, a discipline is defined by the formalized process by which information is organized. While usually applied within the context of academia, one could extend this definition within art-forms. For example, what defines musical genres (here paralleled with discipline-concept) is the instrumentation, the intervals between different pitches and temporal and linguistic patterns that are employed in composition.

This 'self-concept' that defines the discipline can then be taken to represent the left hemispheric processes of the brain that act as a filter by which relevant information is acquired, organized and communicated. Not surprisingly, left hemispheric functions include logic, mathematical reasoning, verbal reasoning and other linear processes that can be likened to the linear process of 'knowledge production' within the discipline and are all required for deductive processes involved within the sciences in general.

4.2 Interdisciplinarity

In a chapter written on holistic approaches to research, Sarewitz (2010) discusses the possibility that the boundaries found at the edges of a discipline are inherently a result of perception. In this case, there is no 'real' boundary between discipline X and discipline Y, and that the boundaries that do exist are simply illusions imposed by the cognitive structure of the inquisitor. The approach of 'blurring' is echoed

by Geertz (1983) who observed that many of the social sciences began to 'role-play' by the usage of analogies derived from other fields including literature and theatre; his thoughtful treatise demonstrated that the acquisition of knowledge can be facilitated through examination of the relationship between disciplines such that for example, a scientific problem could be viewed 'from the lense' of a fiction writer. Indeed if one were to apply a statistical 'analysis of covariance' for language imbued by each discipline, one might find that fundamental patterns exist between disciplines. For example, consider the concepts of harmony in music, correlation in statistics and coherence in physics. In all three cases the implied meaning is that there is an aesthetic or mathematical relationship between two sets of variables-in the case of harmony two consonant melodic lines, in the case of correlation and coherence two variables-that are linear. Thus, it might be suggested that if boundary lines do exist between predefined disciplines, they exist because of the language used to describe a fundamental process.

In some respects the interdisciplinarity, a concept that has been paired synonymously with 'creativity', 'crossing-boundaries' and 'blending' (Frodeman, Klein and Mictcham, 2010; Klein, 2005, Geertz, 1980), that began to emerge in the 1960s (Newell, 2008), possesses ideals that were explored by many early Greek philosophers such as Socrates and Pythagorus as well as individuals during the Renaissance period from which the concept of the 'polymath' or 'Renaissance man' originated (Klein, 2005). In such methods of education and learning, a wide variety of topics such as mathematics, music, geometry, and philosophy were studied simultaneously. These ideas were then later explored by physiologists and physicists in the 19th century. Individuals such as Hermann von Helmholtz, the developer of the theory of conservation of energy, and Thomas Young, who demonstrated that Newton's particle theory of light

could also be accommodated by wave-physics and would later attempt to study the interaction between light and sound (Young, 1800), both integrated aspects of different 'disciplines' to understand aspects of others.

Interdisciplinarity, as it is regarded today, is thought to have been born out of a necessity to solve big-picture problems that cannot be adequately assessed through the lens of one discipline alone. With the increased specialization observed within the disciplines, individuals began to assess applicability to 'real-world' situations (Shailer, 2005). As such, while disciplinary research can be described as focal and rigorous methodology as it pertains to a given 'territory' of reality, interdisciplinary research attempts to exploit the holistic ability within the human brain to integrate seemingly disparate knowledge to explore topics that are by nature complex by application of multiple processes used throughout the disciplines. Thus in contrast to 'disciplinarity' as it has been outlined here, interdisciplinary research is not rigid or stereotyped, but flexible to allow for as many different possibilities to gain a more complete understanding of the problem.

According to Salter and Hearn (1996) as well as Repko (2008), there are two types of interdisciplinary categories by which research is conducted. The first is called 'conceptual' interdisciplinarity and is epistemological in nature and deals with understanding the limitations of the insights of a problem explored by a single discipline. The second is called "instrumental interdisciplinarity", in which the concepts, knowledge and methods from "two or more" disciplines are borrowed in order to solve a problem that cannot be addressed by one field alone; in this way the disciplines fuse together seamlessly. According to Aboelela and colleagues' (2007) qualitative review of the literature surrounding the definition of interdisciplinarity, a variant of this conception or

“positivist” interpretation would likely to be endorsed by the physical and social sciences. Disciplines are then viewed as a foundational starting point for interdisciplinary studies such that the “perspectives, epistemologies, assumptions, theories, concepts, methods that inform our ability as humans to understand our world” (Repko 2008, p. 21) are not deteriorated.

Such a view has exhaustive implications for the advancement of creative ideas and consolidation of information. For example studies within the neurosciences have demonstrated that what is called “creativity” may be ‘cross-wiring’ between brain regions that are rarely connected. Synaesthesia, a common condition reported by composers like Alexander Scriabin, in which individuals can “hear” colour or “taste” music, has been hypothesized to be caused by enhancement of connections between regions of the brain that normally process sound and colour separately (Brang and Ramachandran, 2011). If this is the case, then exploring the same problem from different disciplinary paradigms, such as mathematics commonly linked to the left cerebral hemisphere and music which is traditionally associated with the right hemisphere, could allow for the enhancement of ‘accidents’ to occur that allow for creative insights observed biologically as the expansion or re-molding of dendritic spines.

As has been stated from the outset, there is sufficient evidence to suggest that information is largely organized by the structure and function of the human brain. Therefore, if the processes inherent in a discipline are taken metaphorically to function as the left-hemisphere where linear processes, such as those engaged by the disciplines, are largely performed, it is tempting to equate the seemingly parallel processes involved in interdisciplinary research to represent the right hemisphere which is by nature spatial and pattern based. Consequently from a sociological standpoint the

emergence of interdisciplinary studies could be interpreted as an expansion and development of right-left hemispheric coherence within the human brain. From this perspective the differences between mono-and inter-disciplinarity would be described by functional differences between the left and right hemispheres of the brain.

If one of the major thrusts for interdisciplinary research is to enhance creativity, the aforementioned analogy to left and right hemispheric processes for disciplinarity and interdisciplinarity is apt. One major finding is that the sensed presence is the product of coherence between the left and right hemispheres. As Persinger and Makarec (1992) have previously stated, the sensed presence may be the process by which the muses were experienced by Greek artists. If this is the case, then creativity is necessarily a left and right hemispheric process and by definition experience in both disciplinary and interdisciplinary endeavors are required for creativity to flourish, or stated alternatively by Repko (2012, p.71) "intuition and method". It may be relevant that according to Simonton's (1975) quantitative review of creative individuals, there appears to be 3 major 'factors' of interdisciplinary individuals who fall into the categories of discursive creativity (with the physical, biological, chemical sciences), presentational creativity (i.e. painting architecture), and rational-mystic creativity (physical sciences, religion, and general philosophy); these clusters may highlight that the propensity for interdisciplinary studies is innate and that learning one particular discipline already allows 'cross-talk' to occur with others.

This view of creativity is recapitulated by Morin (2008) who synthesizes many Eastern philosophies on his views of complexity within the natural and social sciences; complexity here is synonymous with the term 'predictability' and relates to Strathern's (2004) reiteration of cold (unpredictability but with a 'strategic plan' in the case of events)

and hot (unpredictability arising from the interactions of multiple factors not originally incorporated into an equation) situations. Complexity, a necessary and perhaps impending change in thought processes accompanying the acquisition of information, is thought to be accompanied by the integration of opposites, in the same way that would have been described by Hegel and within the psychology of Jung (1959) who emphasized 'individuation' as a necessary process of merging the 'unconscious' with the 'conscious' for individual development. This view is also echoed by other contemporary authors, such as Tononi and Edelman (1998), who describe consciousness as a process that is simultaneously integrating and differentiating experiences acquired subjectively and whose process may be described mathematically, like Morin's perspective, by Shannonian information theory, or entropy. In this vein and to extrapolate, science is not only objective, but also subjective. Perhaps one important example of the relationship between subject-object can be found within the domain of quantum physics. Whereas a mechanistic and seemingly objective model of the universe, with a natural order that could be formalized, pervaded much of scientific thought up until time 19th century, discoveries within quantum physics included the observer as part of the interaction between the molecules that composed the universe where the observer can affect the consequences of the experiment.

4.3 Interdisciplinary Requirement and Methodology

The topic that has been chosen for the thesis is a comparative exploration between the processes that are observed naturally within the context of geomagnetism and processes observed with brain function. Multiple research endeavours have been conducted that demonstrate that the earth's geomagnetic field influences human behaviour, and more specifically, brain activity. For example Mulligan et al. (2010)

demonstrated that regions of the brain involved with decision making are strongly correlated with increases in the geomagnetic field. The topic can best be described therefore as a continuation of research conducted by Dr. Herbert Konig who, with Anker-muller (1960), demonstrated that the signals received by a magnetometer that measures ultra-low frequency activity (ULF) of the earth overlaps with naturally occurring oscillations in voltage recorded from the human brain. Unfortunately since that time, not much exploration of possible connectivity has been conducted, with perhaps one exception; the work of Pobachenko demonstrated increased 'non-time-locked' coherence between the strength of alpha activity occurring within the brain and alpha-range activity occurring in the atmosphere (Pobachenko et al., 2006). Sample questions that would need answering are: How is this connection possible? Is the connection with the earth synchronous? What are the implications of such a connection if it exists?

Since the time of the initial comparison, many investigators have demonstrated theoretically that there may be a functional link between electromagnetic processes that occur in the brain and those that occur within nature. From an integratory perspective that defines interdisciplinary studies (Repko, 2012), information gleaned from the emergence of data supporting this connection could shape the way that neuroscientists, who understand "40 Hz binding" as a strong "neural correlate of consciousness", view the process of consciousness itself. For example, Persinger (2012) demonstrated that the frequency and current magnitudes of lightning strikes when scaled appropriately contain the same intrinsic electrical current density as those of action potentials and the frequency of lightning strikes, which is about 44 +/- 5 strikes per second or '40 Hz' (Christian et al., 2003), approaches the 'binding' feature of consciousness (Llinás and Ribary, 1993). Nunez (1995) successfully described the processes that occur in the

brain by using fundamental models, similar to the models approached by von Bekesey in trying to discern the psychophysics of hearing. In Nunez's approach he treated the brain and skull as an earth-ionospheric cavity and predicted a dominant frequency, ~10 cycles per second, using the bulk velocity of action potentials.

The current dissertation is designed to continue assessing the potential earth-brain connection by using modern technology that is portable and readily available. From a cursory review, multiple methods and knowledges from backgrounds such as electrophysiology, geomagnetism, signal processing, mathematics, electronics and geophysics are required in order to make an accurate assessment. Repko (2008) described a 10-step 'nonlinear and iterative' process, similar to Szostak's 12-step process, for steps on possible ways to conduct interdisciplinary research; this process has been used with degrees of success for studies in linguistics (van der Lecq, 2012), understanding the cognitive science of action understanding in humans (Keestra, 2012), and understanding stress episodes as experienced by NHL hockey players (Battochio, 2013). According to Repko, the process of identifying disciplines (Step 3) is necessary in order to achieve some integration of the insights drawn amongst the disparate knowledges.

The principle thrust can thus be described as convergence rather than divergence, with the patterns observed in the brain and the earth linking both. The fundamental 'connection' points, or concepts, associating the disciplines explored within this project are frequency and intensity. The principle operating frequency of electrical potentials recorded with an electroencephalogram is approximately 8-13 Hz. Depending upon approaches, the associated electric and magnetic field strengths of the 8-13Hz activity recorded over the back of the brain when individuals have their eyes

closed is approximately .4-.5 mV/m and 1-2 picoTesla. As it turns out, the Schumann resonance, which is a global resonance affecting all regions of the earth, displays a peak frequency of about 8Hz (Balsler and Wagner, 1960) with electric field and magnetic field strengths approaching .1-1 mV/m and 1-3 picoTesla. This convergence suggests that there may be indeed a connection between the two processes occurring at a micro (the human brain) and a macro (the earth) level (Figure 1C).

This approach to interdisciplinarity might best be described as Mode I according to criteria outlined by Chettiparamb (2006). In this mode, "...the attempt is to demonstrate that two things are actually the manifestation of the same structure...". This method is also related to one of Morin's (2008) principles for a framework by which complexity can be used as a mode of scientific inquiry; here he specifies the idea of a holographic relationship wherein the individual components of an object contain the information of the whole, as in the case of the fractal mathematical set known as the Sierpinski triangle (Figure 1.15A). The relationships that will be investigated within the dissertation are modeled after the "fugue" musical form (Figure 1.15B), which at its core relies upon recapitulation and imitation of a central melodic theme (Menuhim, 1986). Based upon the quantitative and qualitative convergences of the two phenomena outlined above one might speculate that the two processes (brain and earth) are derived from the same source of variance.

The overall methodology to be employed within the dissertation is a combination of statistical and analytical techniques widely practiced within the social and physical sciences. Spectral analysis, a tool that is used in a broad array of natural sciences, is slowly becoming the 'universal tool' for communicating discrete quantifications between different fields and observes the conception of the "methodology" as a stand-alone

procedure external to a particular discipline (Chandler, 2009). The central tenet in spectral analysis is to quantify frequency to obtain information on predictability and periodicity and can be used to examine the patterns of space and time. As such one could see its applicability to discerning natural periodicities, such as tidal waves, as well as within the musical studio, to control the distribution of tones within a recording.

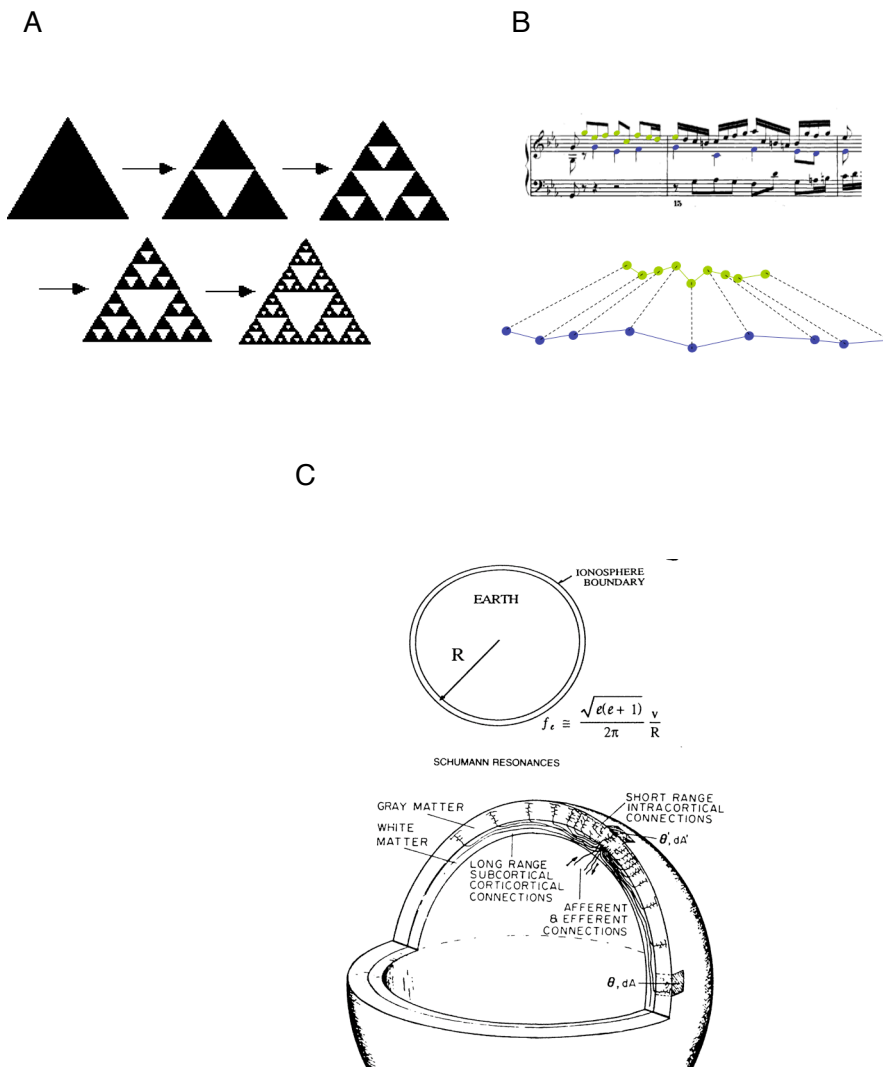


Figure 1.15 The 'holographic', or fractal relationships explored in a mathematical set (A), a musical fugue (B), and the proposed connection between electromagnetic processes of the human brain and the earth-ionosphere (C). (A) Example of a fractal mathematical set known as the Sierpinski Triangle. The process shows how the information within one component of the object can be

broken down into constituent parts, each possessing the same informational content. (Image Source: <http://math.bu.edu/DYSYS/chaos-game/node2.html>) (B) Fugue in C-Minor from “The Well-Tempered Clavier, Book 2 ”. The subject in this passage is stated along two different speeds (green=fast, blue=slow) in a way that can be likened to celestial bodies rotating around the sun with different temporal periods. (C) Relationship between standing waves formed within the earth-ionosphere cavity and the human brain. (Image Source: Nunez (1995), p.83)

The second major technique that will be featured within the topic is that of coherence/correlational analysis. Coherence, as has been previously described, is a technique usually applied to discern how two signals vary as a function of time and is widely used in the physical sciences (Rusalova et al, 2014). This technique should allow for ‘functional connectivities’ to be discerned, if they are present, between signals generated naturally by the earth and those generated by the human brain.

Finally, microstate analysis, usually employed in electrophysiological explorations of the time-varying components of voltages recorded from multiple sensors of the human head (Koenig et al, 2002), will be used in order to assess general patterns of ‘geo-states’ that may or may not exist according to static DC geomagnetic recordings made at several laboratories around the world. In this case, the recordings at each site represent one ‘channel’ in a quantitative electroencephalograph and by employing large datasets (approximately one year) of multiple ‘channels, shapes of the DC magnetic field of the earth can be mapped. In all cases the statistical and analytical tools will be used interchangeably to study both qualitative and quantitative aspects of patterns that may or may not exist between the earth’s geomagnetic field and the electric field of the human brain. While a general methodology is implied, there are of course findings that may warrant reconsideration of the tools used to accomplish the analysis. This approach, according to Strathern (2004), could be called ‘ethnographic’ in the sense that

methodologies are devised 'after the fact' in order to cater to the individual needs of the data.

5.0 Proposed Research and Methods

Given the research cited above, which by no means is complete, demonstrating connections between the earth's time-varying and static geomagnetic field and brain activity, and also given the paucity of research showing direct connections between the naturally generated Schumann resonance and brain activity, the research will attempt to continue to investigate for other possible interfaces between the two phenomena. The principle method of the research will be investigating measures derived from magnetometers, measuring both static and time-varying components of the earth's magnetic field, in combination with various statistical and analytical techniques using the QEEG. While there have been indicators suggesting that a 'fugal' relationship between the two phenomena exists, few studies have investigated a direct one-to-one correspondence between earth-generated time-varying electromagnetic fields and human brain activity.

5.1 Relationships between brain activity and measures of the static geomagnetic field

This research will continue in the same vein as that already performed by Mulligan and Persinger. Over the last 3-4 years, an extensive database of QEEG baselines from approximately 180 individuals has accumulated from various experiments performed within the Neuroscience Research Group laboratory. These eyes-closed 'resting' baselines will be employed to discern additional potential relationships between the geomagnetic field and human brain-activity.

The general methodology will be simple. Simultaneous measurements of the brain's electrical activity as well as the earth's magnetic field will be recorded. The resultant signals will be subjected to a myriad of different analytical techniques in order to discern if additional relationships exist. Data representing the state of the geomagnetic activity at the time of each measurement will be obtained from various online monitoring stations. Variables such as the K-index and measures of solar sunspot numbers will be obtained from these databases and correlational analyses will be performed to discern relationships between the two general classes of phenomena: brain activity and earth static geomagnetic field.

5.2 Explorative Application of QEEG-related Methods to Investigate the Static Geomagnetic Field

To further characterize the potential 'fugal' relationship between brain activity and the earth's geomagnetic field, the application of methodologies typically employed in quantitative electroencephalography will be engaged. If both phenomena are related or produce or are produced from shared sources of variance, then the inter-mingling of methods should produce comparable time and space dependent properties when scale is accommodated.

In this very exploratory study, approximately one-year of the static geomagnetic field, sampled at once per minute, will be extracted from online repositories from 8 regions roughly approximating the scaled-locations of sensors typically placed on the scalp to measure brain-generated electrical activity. These 'geo-channels' will be synchronized into one record and microstate analyses will be employed to discern the

spatial orientation of the field to produce 'geostate' maps. In addition, coherence analyses typical of QEEG research will be applied to discern periods 'geo-synchronicity' between distant locations around the earth.

5.3 Relationships between brain activity and measures of background AC magnetic fields

While the earth's DC geomagnetic field is relatively static (with the exception of normal diurnal variations in its intensity), there also exists smaller time-coupled perturbations that are within nanoTesla to picoTesla range. Research investigating potential influences of 60Hz electromagnetic fields in North America on biological systems, generated primarily from AC power line electricity delivery systems, is copious and many studies have suggested that that they can effect biology. Within rural environments 60-Hz power-line frequencies, with electric field intensities ranging between between 10^{-2} - 10^{-4} V/m depending upon source distance and have discrete harmonics produced according to basic physical principles, and magnetic fields generated by electronics may produce changes in physiology. There have been extensive correlative researches demonstrating that some residents living proximal to powerline generators show increased incidences of leukemia, breast-cancer, and general malaise and fatigue. With this motivation, one proposed study would be to investigate the changes in the AC background and measure real-time relationships with brain activity.

The methodology in this research will require simultaneous recordings of the AC-background electromagnetic field and brain activity monitored with a QEEG. Indicators

of the background AC field will be measured with a power meter, a standard device typically used in laboratories to measure electromagnetic field strengths in milliGauss units where 1 milliGauss is equal to 100 nanoTesla. This same sensor has previously been utilized in a study investigating the transmission of artificial time-varying electromagnetic fields through simulated skull. This sensor will be connected to a laptop that will record the perturbations in the local electromagnetic field inside of an acoustic sound-proof chamber while the brain activity of individuals situated inside the chamber is monitored simultaneously.

The general statistical approach will be correlational and spectral densities ($\text{milliGauss}^2\text{Hz}^{-1}$) from the time-varying AC magnetic field will be correlated with a variety of time-frequency dependent changes in brain activity (i.e. spectral density, coherence).

5.4 Schumann Resonance Signatures in the Human Brain

In 1979, Dr. Konig published a chapter within Persinger's ELF and VLF Electromagnetic Effects discussing extremely-low and very-low electromagnetic frequencies occurring naturally with possible connections with biology. In particular he discussed the concepts of ELF-VLF frequencies within the context of holographic memory and electroencephalography. Figure 15 depicts a condensed spectral array of an electroencephalographic recording of an individual who has been monitored during their sleep found within his chapter in "Electromagnetic Bio-Information" (Popp, 1984). It is obvious that there are two major peaks that occur together and apart: peaks at 8 and 14 Hz. These two frequencies constitute the first and second harmonics of the Schumann resonance.

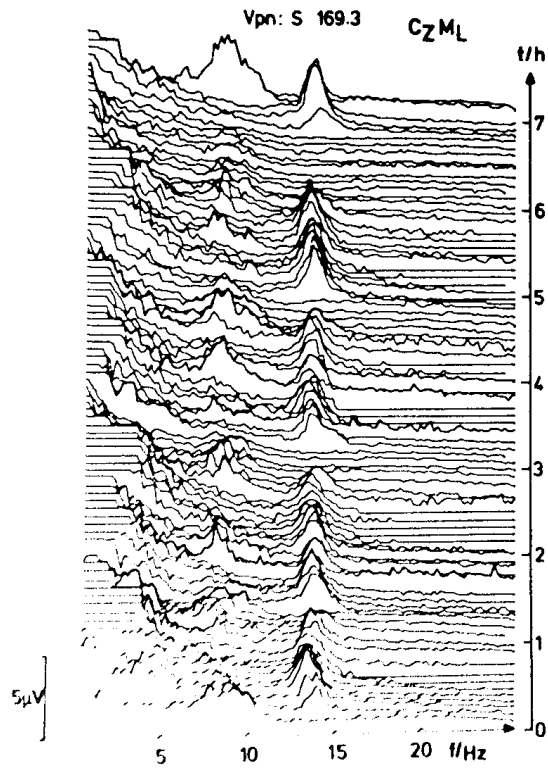


Figure 1.16 Temporal courses of amplitude frequency spectra averaged over five minutes (from Kloppel in Popp, 1979).

In this study, a dataset of approximately 237 cases of eyes-closed baselines will be used to explore other potential signatures that may be apparent within brain activity alone. Spectral analyses will be the major method used to decompose the signal into select frequencies and statistical analysis with the use of other derived QEEG variables (i.e. microstates, source localization) will be used to explore the derived Schumann resonance signature to understand any intrinsic relationships. Just as Cosic has found that Schumann-like frequencies occur within the activity of the spinal cord, they may also be found within the electrical field of the brain.

5.5 Relationships Between Extremely-Low Frequency Spectral Density and Human Brain Activity and Construction and Characterization of an Induction Coil Magnetometer For Measuring Extremely-Low Frequency Earth-Ionospheric Perturbations

While reading the studies written by Dr. Neil Cherry on human health relationships to the Schumann resonance and sunspot numbers, a database from which he was able derive intensities of extremely-low frequency spectral densities was discovered. Perusing the site further, it contains not only magnetic and electric field time-series sampled at 40Hz, but also seismometers (sampled at 80Hz), geophones and other instruments used to study earthquake activity for prediction. The site is a joint collaboration between many geophysical laboratories within California, including USGS and Berkeley. Access to data from at least 1995 can be found at <http://ncedc.org/ncedc/other-geophysical-datasets.html>. The data can be requested at lengths up to a couple of years and software (rdseed) can be used to extract specific times of interest.

Because there is a large dataset of baseline eyes-closed encephalograms available, this study will attempt to draw a relationship between the strength of various quantitative electroencephalographic measures and extreme-low frequency spectral densities obtained from the aforementioned database in California. The study will fundamentally be correlational. Multiple linear regressions will be performed in order to predict fundamental Schumann frequency intensities from the database of eyes-closed baselines.

5.6 Construction and Characterization of an Induction Coil Magnetometer For Measuring Extremely-Low Frequency Earth-Ionospheric Perturbations

The intensity of extremely-low frequency (0.1-100Hz) electromagnetic activity generated within the earth-ionosphere cavity is about one million times less than the geomagnetic field and is typically measured within the picoTesla range. As a result, specialized sensors are required in order to measure time-dependent changes within the scale of seconds. This component of the dissertation will describe the methodology used to construct an induction-coil manometer, an instrument typically utilized within the field of geophysics, and its characterization using raw electronic components.

The purpose of constructing the magnetometer is two-fold. One reason for its construction is that the Schumann resonance and micropulsations can be monitored daily with the hope of further applying time-frequency methods typically employed in QEEG research to discern more information about the nature of the phenomena. While a vast literature on the topic of the Schumann resonance has accrued, there has been little research investigating 'phase-coherence' relationships between the different harmonics. For example, one potential avenue for research is to investigate how often the fundamental 7.8 Hz becomes coherent with the 39Hz harmonic. The relationship between these two frequencies in particular has been thoroughly investigated within the context of neuroscience where 7 Hz frequencies generated within the hippocampus, also known as the 'gateway to memory', are correlated with 40Hz ripples which are superimposed upon the fundamental 7Hz carrier frequency and often correlated with the 'binding' factor required to produce a cohesive consolidation of various sensory components of consciousness. Investigating the phase relationships between these two

frequencies within the context of geophysics may be of relevance for its comparison to human consciousness.

5.7 Simultaneous Measurements of the Schumann Resonance and Brain

Activity

The second reason for constructing a magnetometer sensitive enough to measure extremely-low frequency electromagnetic fields is to discern if real-time or time-lagged coupling exists between the Schumann resonance and human brain activity. While many publications have appeared suggesting a coherence between the two phenomena, few have investigated the basic physical units in real-time. One exception is the study performed by Konig who discovered a relationship between reaction times of people the occurrence or intensity of Type 1 natural electromagnetic signals that also overlap with brain activity.

The approach to this component of the dissertation will be to measure both signals (brain and earth) simultaneously by feeding the perturbations in ELF-range electromagnetic recordings into the QEEG to be measured as a channel appearing amongst the array of sensors recording the electric field of the brain. As with other proposed methods, both time-series will be decomposed according to frequency and other derived QEEG-measures (i.e. source localization, coherence) to investigate a potential coupling of the two phenomena.

6.0 References

- Aboelela SW et al. (2007). Defining Interdisciplinary Research: Conclusions from a Critical Review of the Literature. *Health Services Research* 42: 329-346.
- Babayev, E. S., & Allahverdiyeva, A. A. (2007). Effects of geomagnetic activity variations on the physiological and psychological state of functionally healthy humans: some results of Azerbaijani studies. *Advances in Space Research*, 40(12), 1941-1951.
- Baker-Price, L. A., and Michael A. Persinger. "Weak, but complex pulsed magnetic fields may reduce depression following traumatic brain injury." *Perceptual and motor skills* 83.2 (1996): 491-498.
- Baker-Price, L., & Persinger, M. A. (2003). Intermittent burst-firing weak (1 microTesla) magnetic fields reduce psychometric depression in patients who sustained closed head injuries: A replication and electroencephalographic validation. *Perceptual and motor skills*, 96(3), 965-974.
- Balser, M., & Wagner, C. A. (1960). Observations of Earth-ionosphere cavity resonances. *Nature*, 188(4751), 638-641.
- Battochio RC. (2013). An Interdisciplinary Take on Stress, Coping, and Adaptation in the National Hockey League. In Reguigui A (Ed): *Perspectives sur l'interdisciplinarité / Perspectives on Interdisciplinarity*, Sudbury, Série monographique en sciences humaines / Human Sciences Monograph Series, vol 13, 2013.

- Brang D and Ramachandran VS. (2011). Survival of the Synaesthesia Gene: Why Do People Hear Colors and Taste Words? PLoS Biology 9: e1001205.
- Besser, B. P. (2007). Synopsis of the historical development of Schumann resonances. Radio Science, 42(2).
- Bianchi, C. (2007). Natural and man-made terrestrial electromagnetic noise: an outlook. Annals of Geophysics.
- Bleil, D. F. (1964). Natural electromagnetic phenomena below 30 kc/s. In Natural Electromagnetic Phenomena (Vol. 1).
- Capra, F. (1976). The Tao of Physics. London: Fontana.
- Chandler J. (2009). Introduction: Doctrines, Disciplines, Discourses, Departments. Critical Inquiry 35: 729:746.
- Chapman, F. W., & Jones, D. L. (1964). Observations of earth-ionosphere cavity resonances and their interpretation in terms of a two-layer ionosphere model. Radio Science, Journal of Research National Bureau of Standards D, 68(11), 1177-1185.
- Chapman, S., & Bartels, J. (1940). Geomagnetism. Oxford: Clarendon Press.
- Cherry, N. (2002). Schumann Resonances, a plausible biophysical mechanism for the human health effects of Solar. Natural Hazards, 26(3), 279-331.
- Cherry, N. (2003). Schumann resonance and sunspot relations to human health effects in Thailand. Natural hazards, 29(1), 1-11.

- Chettiparamb A. (2007). *Interdisciplinarity: A Literature Review*, Southampton (UK), The Higher Education Academy, Interdisciplinary Teaching and Learning Group.
- Christian HJ et al. (2003). Global frequency and distribution of lightning as observed from space by the Optical Transient Detector. *Journal of Geophysical Research* 108.D1: ACL-4.
- Cook, C. M., Koren, S. A., & Persinger, M. A. (1999). Subjective time estimation by humans is increased by counterclockwise but not clockwise circumcerebral rotations of phase-shifting magnetic pulses in the horizontal plane. *Neuroscience Letters*, 268(2), 61-64.
- Corradini, P. L., & Persinger, M. A. (2013). Standardized Low Resolution Electromagnetic Tomography (s_LORETA) is a Sensitive Indicator of Protracted Neuropsychological Impairments Following “Mild”(Concussive) Traumatic Brain Injury. *Journal of Neurology & Neurophysiology*.
- Corradini, P. L., & Persinger, M. A. (2014). Spectral power, source localization and microstates to quantify chronic deficits from 'mild' closed head injury: Correlation with classic neuropsychological tests. *Brain Injury*, (0), 1-11.
- Ćosić, I., Cvetković, D., Fang, Q., & Lazoura, H. (2006). Human electrophysiological signal responses to ELF Schumann resonance and artificial electromagnetic fields. *FME Transactions*, 34(2), 93-103.

- Duffy, F. H. (1986). Topographic mapping of brain electrical activity. In *The impetus for this volume was an international symposium, "Progress in Topographic Mapping of Neurophysiological Data,"* held in Boston, MA at The Children's Hospital, Harvard Medical School on Oct 16-17, 1984.. Butterworth Publishers.
- Frodeman R, Klein JT, Mitcham C. (2010). *The Oxford Handbook of Interdisciplinarity*. Oxford, Oxford Press.
- Geertz C. (1980). Blurred Genres: The Reconfiguration of Social Thought. *The American Scholar* 49, 165-179.
- Giancoli, D. C. (1984). *General physics* (p. 503). Englewood Cliffs, NJ: Prentice-Hall.
- Greenberg, E., & Price, C. (2007). Diurnal variations of ELF transients and background noise in the Schumann resonance band. *Radio Science*, 42(2).
- Heckman, S. J., Williams, E., & Boldi, B. (1998). Total global lightning inferred from Schumann resonance measurements. *Journal of Geophysical Research: Atmospheres*(1984–2012), 103(D24), 31775-31779.
- Hill, D. R., & Saroka, K. S. (2010). *Sonic Patterns, Spirituality and Brain Function: The Sound Component of Neurotheology*. *NeuroQuantology*, 8(4).
- Hofstadter, D. R. (2000). *Godel, Escher, Bach* (p. 168). Penguin.
- Jacobs, J. A. (1970). *Geomagnetic micropulsations*. New York: Springer-Verlag.

- Jung CG. (1959). Conscious, Unconscious, and Individuation. In Read H, Fordham M and Adler G (Eds) *The Collected Works of C.G. Jung: The Archetypes and The Collective Unconscious* (pp. 275-289). New York, Pantheon Books.
- Kangas, J., Guglielmi, A., & Pokhotelov, O. (1998). Morphology and physics of short-period magnetic pulsations. *Space Science Reviews*, 83(3-4), 435-512.
- Keestra M. (2012). Understanding Human Action: Integrating Meanings, Mechanisms, Causes and Contexts. In Repko AF, Newell WH, Szostak R (Eds): *Case Studies in Interdisciplinary Research*. Thousand Oaks (CA), Sage.
- Klein JT. (2005). *Humanities, Culture, and Interdisciplinarity*. New York, State University of New York Press.
- Koenig, T., Lehmann, D., Merlo, M. C., Kochi, K., Hell, D., & Koukkou, M. (1999). A deviant EEG brain microstate in acute, neuroleptic-naive schizophrenics at rest. *European archives of psychiatry and clinical neuroscience*, 249(4), 205-211.
- Koenig, T., Prichep, L., Lehmann, D., Sosa, P. V., Braeker, E., Kleinlogel, H., ... & John, E. R. (2002). Millisecond by millisecond, year by year: normative EEG microstates and developmental stages. *Neuroimage*, 16(1), 41-48.
- König, H. L. (1974). ELF and VLF signal properties: Physical characteristics. In Persinger (Ed.) *ELF and VLF electromagnetic field effects* (pp. 9-34). Springer US.

- König, H. L. (1974). Behavioural changes in human subjects associated with ELF electric fields. In Persinger (Ed.) ELF and VLF Electromagnetic Field Effects (pp. 81-99). Springer US.
- König, H., & Ankermüller, F. (1960). Über den Einfluss besonders niederfrequenter elektrischer Vorgänge in der Atmosphäre auf den Menschen. *Naturwissenschaften*, 47(21), 486-490.
- König, H. L., Krueger, A. P., Lang, S., & Sönning, W. (1981). *Biologic effects of environmental electromagnetism*. New York, Inc: Springer-Verlag.
- Knott, V., Mahoney, C., Kennedy, S., & Evans, K. (2001). EEG power, frequency, asymmetry and coherence in male depression. *Psychiatry Research: Neuroimaging*, 106(2), 123-140.
- Lavallée, C. (2011). *Cerebral Dynamics Characterizing Normal and Altered States of Consciousness and Cognition*.
- Lehmann, D., & Skrandies, W. (1980). Reference-free identification of components of checkerboard-evoked multichannel potential fields. *Electroencephalography and clinical neurophysiology*, 48(6), 609-621.
- Lehmann, D., Faber, P. L., Galderisi, S., Herrmann, W. M., Kinoshita, T., Koukkou, M., ... & Koenig, T. (2005). EEG microstate duration and syntax in acute, medication-naive, first-episode schizophrenia: a multi-center study. *Psychiatry Research: Neuroimaging*, 138(2), 141-156.

- Llinás R and Ribary U. (1993). Coherent 40-Hz oscillation characterizes dream state in humans. *Proc. Natl. Acad. Sci.* 90: 2078-2081.
- Madden, T., & Thompson, W. (1965). Low-frequency electromagnetic oscillations of the Earth-ionosphere cavity. *Reviews of Geophysics*, 3(2), 211-254.
- Matsushita, S., and Campbell, W. H. (1967). *Physics of geomagnetic phenomena* (Vol. 2). Academic Press.
- Menuhin, Y., & Davis, C. W. (1986). *The Music of Man*. Methuen.
- Millett, D. (2001). Hans Berger: From psychic energy to the EEG. *Perspectives in biology and medicine*, 44(4), 522-542.
- Moran, Joe, *Interdisciplinarity*, 2nd ed., London, Routledge, 2010.
- Morin E. (2008). *On Complexity*. New Jersey, Hampton Press.
- Mulligan, B. P., Hunter, M. D., & Persinger, M. A. (2010). Effects of geomagnetic activity and atmospheric power variations on quantitative measures of brain activity: replication of the Azerbaijani studies. *Advances in Space Research*, 45(7), 940-948.
- Mulligan, B. P., & Persinger, M. A. (2012). Experimental simulation of the effects of sudden increases in geomagnetic activity upon quantitative measures of human brain activity: validation of correlational studies. *Neuroscience letters*, 516(1), 54-56.

- Newell WH. (2008). The Intertwined History of Interdisciplinary Undergraduate Education and the Association for Integrative Studies: An Insider's View. *Issues in Integrative Studies* 26, 1-59.
- Nickolaenko, A., & Hayakawa, M. (2014). *Schumann Resonance for Tyros: Essentials of Global Electromagnetic Resonance in the Earth-ionosphere Cavity*. Springer.
- Niedermeyer, E., & da Silva, F. L. (Eds.). (2005). *Electroencephalography: basic principles, clinical applications, and related fields*. Lippincott Williams & Wilkins.
- Nunez, P. L., & Srinivasan, R. (1984). *Electric fields of the brain: the neurophysics of EEG*. Oxford university press.
- Nunez, P. L. (1995). *Neocortical dynamics and human EEG rhythms*. Oxford University Press, USA.
- Pascual-Marqui, R. D. (2002). Standardized low-resolution brain electromagnetic tomography (sLORETA): technical details. *Methods Find Exp Clin Pharmacol*, 24(Suppl D), 5-12.
- Persinger, M. A. (1995). On the possibility of directly accessing every human brain by electromagnetic induction of fundamental algorithms. *Perceptual and Motor Skills*, 80(3), 791-799.
- Persinger, M. A. (2008). On the possible representation of the electromagnetic equivalents of all human memory within the earth's magnetic field: implications for theoretical biology. *Theoretical Biology Insights*, 1, 3-11.

- Persinger, M. A. (2012). Brain electromagnetic activity and lightning: potentially congruent scale-invariant quantitative properties. *Frontiers in integrative neuroscience*, 6.
- Persinger, M. A. (2013). Billions of human brains immersed within a shared geomagnetic field: Quantitative solutions and implications for future adaptations. *Open Biology Journal*, 6, 8-13.
- Persinger, M. A., Koren, S. A., & Lafreniere, G. F. (2008). A neuroquantologic approach to how human thought might affect the universe. *NeuroQuantology*, 6(3).
- Persinger, M. A., & Lavallee, C. (2012) . The sum of $n = n$ concept and the quantitative support for the cerebral-holographic and electromagnetic configuration of consciousness. *Journal of Consciousness Studies*, 19, 128-153.
- Persinger MA and Makarec K. (2002). The feeling of a presence and verbal meaningfulness in context of temporal lobe function: Factor analytic verification of the muses? *Brain and Cognition*, 20(2); 217-226.
- Pobachenko SV, Kolesnik AG, Borodin AS, and Kalyuzhin VV. (2006). The contingency of parameters of human encephalograms and Schumann Resonance Electromagnetic Fields Revealed in Monitoring Studies. *Journal of Biophysics*, 51: 480-483.
- Popp, F. A., & Becker, G. (1989). *Electromagnetic Bio-Information*.

- Price, C., & Melnikov, A. (2004). Diurnal, seasonal and inter-annual variations in the Schumann resonance parameters. *Journal of atmospheric and solar-terrestrial physics*, 66(13), 1179-1185.
- Rakov, V. A., & Uman, M. A. (2003). *Lightning: physics and effects*. Cambridge University Press.
- Repko AF. (2012). *Interdisciplinary Research: Process and Theory*, 2nd Edition. Thousand Oaks (CA), Sage.
- Roberts, P. H. (1992). Dynamo theory. In *Chaotic processes in the geological sciences* (pp. 237-280). Springer US.
- Rusalova, M. N., Kislova, O. O., & Obraztsova, G. V. (2014). Dynamics of EEG Coherence Connections in Humans with Different Abilities to Recognize Emotional Expression in Speech. *Neuroscience and Behavioral Physiology*, 44(1), 93-100.
- Russell, C. T.: 1972, in E. R. Dyer (ed.), *Critical Problems of Magnetospheric Physics*, IUCSTP Secretariat, Washington, D.C., p. 1.
- Salter L and Hearn A. (1996). *Outside the Lines: Issues in Interdisciplinary Research*, Montreal, McGill-Queen's Press.
- Saretz D. Against Holism. In Frodeman R, Klein JT, and Mitcham (Eds.) *The Oxford Handbook of Interdisciplinarity* (pp. 65-75).

- Saroka, K. S., & Persinger, M. A. (2013). Potential production of Hughlings Jackson's "parasitic consciousness" by physiologically-patterned weak transcerebral magnetic fields: QEEG and source localization. *Epilepsy & Behavior*, 28(3), 395-407.
- Saroka, K. S., Caswell, J. M., Lapointe, A., & Persinger, M. A. (2014). Greater electroencephalographic coherence between left and right temporal lobe structures during increased geomagnetic activity. *Neuroscience letters*, 560, 126-130.
- Satori, G. (1996). Monitoring schumann resonances-11. Daily and seasonal frequencyvariations. *Journal of Atmospheric and Terrestrial Physics*, 58(13), 1483-1488.
- Schlegel, K., & Füllekrug, M. (1999). Schumann resonance parameter changes during high-energy particle precipitation. *Journal of Geophysical Research: Space Physics* (1978–2012), 104(A5), 10111-10118.
- Sekiguchi, M., Hayakawa, M., Nickolaenko, A. P., & Hobara, Y. (2006, August). Evidence on a link between the intensity of Schumann resonance and global surface temperature. In *Annales geophysicae* (Vol. 24, No. 7, pp. 1809-1817).
- Sentman, D. D. (1995). Schumann resonances: In Volland, H. (Ed.). (1995). *Handbook of atmospheric electrodynamics* (Vol. 1). CRC Press.
- Serway, R. A., & Jewett, J. W. (2004). *Physics for scientists and engineers* (6th edn.) Thomson Learning.

- Shailer K. (2005). Interdisciplinarity in a Disciplinary Universe: A Review of Key Issues. Faculty of Liberal Studies, Ontario College of Art and Design. Item 7a.
- Simonton, D.K. (1975). Interdisciplinary Creativity Over Historical Time: A Correlational Analysis of Generational Fluctuations. *Social Behaviour and Personality*, 3(2): 181-188.
- Skrandies, W. (1990). Global field power and topographic similarity. *Brain topography*, 3(1), 137-141.
- Strathern, M. (2004). *Commons and Borderlands: Working Papers on Interdisciplinarity, Accountability and the Flow of Knowledge*. Oxon, Sean Kingston Publishing.
- Strelets, V., Faber, P. L., Golikova, J., Novototsky-Vlasov, V., Koenig, T., Gianotti, L. R. R., ... & Lehmann, D. (2003). Chronic schizophrenics with positive symptomatology have shortened EEG microstate durations. *Clinical Neurophysiology*, 114(11), 2043-2051.
- Szostak R. (2002). How to do Interdisciplinarity: Integrating the Deabte. *Issues in Integrative Studies*, 20: 103:122.
- Tononi G and Edelman GM. (1998). Consciousness and Complexity. *Science* 282:1846-1851.
- Tsang, E. W., Koren, S. A., & Persinger, M. A. (2009). Specific patterns of weak (1 microTesla) transcerebral complex magnetic fields differentially affect depression, fatigue, and confusion in normal volunteers. *Electromagnetic biology and medicine*, 28(4), 365-373.

Turner S (2000). What are Disciplines? And How Is Interdisciplinarity Different?. In Weingart P and Stehr N (Eds.) Practising Interdisciplinarity (pp. 46-p. 65). University of Toronto Press.

Van der Lecq R. (2012). Why we talk: An interdisciplinary approach to the Evolutionary Origin of Language. In Repko AF, Newell WH, Szostak R (Eds): Case Studies in Interdisciplinary Research. Thousand Oaks (CA), Sage.

Wever, R. (1974). ELF-effects on human circadian rhythms. In Persinger (Ed) ELF and VLF electromagnetic field effects (pp. 101-144). Springer US.

Young T. (1800). Outlines of Experiments and Inquiries Respecting Sound and Light. Philisophical Transactions of the Royal Society of London 90, 106-150.

Chapter 2

Greater electroencephalographic coherence between left and right temporal lobe structures during increased geomagnetic activity

Published in Neuroscience Letters

Co-Authors: Joey Caswell, Adnrew Lapointe and Michael Persinger

2.1 Abstract

Interhemispheric coherence for 19 channel EEG activity collected over a three year period from 184 men and women who relaxed in a quiet, darkened chamber showed significant increased coherence between caudal temporal regions for the 11 Hz frequency band during increased (>8 nT) global geomagnetic activity at the time of measurement. Detailed analyses from source-localization indicated that a likely origin was the parahippocampal regions whose net differences at 10, 11 and 12 Hz intervals were significantly correlated with geomagnetic activity. Analyses of residuals to obtain a “purer” measure of parahippocampal contributions indicated that interhemispheric temporal lobe coherence across unit increments between 1 and 40Hz revealed the most statistically significant peaks at 7.5Hz and 19.5 Hz. These weak but reliable correlations between global geomagnetic activity and the degree of inter-temporal lobe coherence for normal people relaxing in a dark, quiet area are consistent with the results of multiple studies indicating that intrusive experiences such as “presences” or “hallucinations” are more frequent when global geomagnetic activity increases above $\sim 15-20$ nT.

2.2 Introduction

Although the static magnetic field of the earth averages ~50,000 nT perturbations more than 1000 times smaller in magnitude are associated with significant changes in the incidence rates of broad classes of behavior (Bureau and Persinger, 1992; Michon and Persinger, 1997; Persinger et al., 2013; Subrahmanyam et al., 1985). Small increases (>20 nT) in global geomagnetic intensity have been correlated with increased display of epileptic convulsions in clinical patients (Rajaram and Mitra, 1981) as well as rats in which epilepsy has been induced experimentally (Persinger, 1995). That the effects were associated with the magnetic field component rather than the multiple correlative variables such as proton flux and electric field changes was demonstrated with experimental simulations (Michon and Persinger, 1997; St-Pierre et al., 2007). Human experiences, often described as hallucinations or “altered states” (Persinger, 1988; Randall and Randall, 1991) that are consistent with increased electrical activity within the temporal lobes have also been correlated with increases in daily geomagnetic activity. Reports of bereavement apparitions occurred on days when the mean global perturbation was ~28 nT compared to days before or after (as well as monthly averages) that averaged 20–21 nT (Persinger, 1988).

The development of easily available quantitative electroencephalographic (QEEG) techniques and the statistical software to effectively extract information concerning specific activity has shown that the human brains, or at least a subset of them, display clear changes in power within specific frequency bands over specific regions during very intense geomagnetic activity (Babyev and Allahverdiyeva, 2007). Mulligan et al. (2010) showed that even daily global changes in aa (average antipodal

indices) values of between 20 and 50 nT were associated with robust changes in electroencephalographic power in normal volunteers. Young adults whose whole bodies were exposed to experimental simulation of components of geomagnetic activity at natural intensities exhibited changes in QEEG patterns within a few minutes (Mulligan and Persinger, 2012).

The preferential sensitivity of the right hemisphere to subtle increases in geomagnetic activity has been reported (Booth et al, 2005). For decades neurosurgeons and epileptologists have reported that individuals who exhibit electrical foci within the right temporal lobe were more likely to report unusual experiences such as “sensed presences”, detachment, and exotic experiences including frank hallucinations (Babb et al., 1987; Persinger and Saroka, 2013). Over the last 20 years we have been examining the hypothesis that differential exposure of the right hemispheres of volunteers to physiologically patterned, weak magnetic fields followed by bilateral stimulation enhances the report of intrusive experiences of “presences” and other representations of the “right hemispheric sense of self” (Persinger, 2003; Persinger et al, 2010; St-Pierre and Persinger, 2006; Saroka and Persinger, 2013).

In other words the experimental protocol (Saroka et al., 2010) produces a condition that is similar to that during enhanced geomagnetic activity which has been shown to be correlated with “out-of-body” experiences in certain populations (Persinger, 1995). Persinger and Richards (1995) reported a threshold for the enhanced numbers of reports for a cluster of items which involved “vestibular themes”, i.e., detachment, floating. These experiences markedly increased when the global geomagnetic activity increased over a K_p (‘kennziffer’ or index of the logarithm of a number) of 3 or between 15nT and 25 nT.

Within the last five years we have measured hundreds of subjects within various experimental settings by 19 channel QEEG and discerned source localizations with Low Resolution Electromagnetic Tomography (sLORETA). We reasoned that if increased geomagnetic activity was associated with enhanced coherence between the right and left hemispheres (and this condition was primarily involved with the report of vestibular experiences and often the “detection” of a sensed presence) then recent computational software with greater sensitivity that measures enhanced interhemispheric coherence should reveal a comparable threshold. Here we show that within a population of 184 subjects tested over a period of several years this coherence increased significantly when the global geomagnetic activity increased beyond 20 nT.

2.3 Methods and Materials

A total of 184 men and women, ages 20 through 80 years, were tested singly over a 3.5 year period as a part of a larger study involved with examining source localizations during periods of relaxation in quiet settings when the eyes were opened or closed. Because a subset of these subjects had been measured several times under different experimental conditions, 233 records were available for this study.

Quantitative electroencephalographic (QEEG) recordings were collected with a Mitsar-201 amplifier connected to a Dell laptop equipped with WinEEG v. 2.8. Each subject wore a 19-channel Electro-Cap, which recorded activity from 19 sites (Fp1, Fp2, F7, F3, Fz, F4, F8, T3, C3, Cz, C4, T4, T5, P3, Pz, P4, T6, O1, O2) commensurate with the International Standard of Electrode Placement. All electrode impedances were maintained below 5k Ω . For each subject, sixteen-second segments of artifact free eyes closed data was extracted and filtered between 1.5 and 40 Hz.

Spectral analyses were completed with MATLAB software equipped with EEGLab (Delorme and Makeig, 2004). We used the `bandpower.m` function to compute spectral power for each sensor within the delta (1.5–4 Hz), theta (4–7.5 Hz), low-alpha (7.5–10 Hz), high-alpha (10–13 Hz), beta-1 (13–20 Hz), beta-2 (20–25 Hz) beta-3 (25–30 Hz) gamma-1 (30–35 Hz) and gamma-2 (35–40 Hz) bands. Coherence analyses were also completed using the EEGLab toolbox. Specifically, we used the `coherence.m` function (script available at <http://sccn.ucsd.edu/pipermail/eeglablist/2005/001056.html>) to calculate coherence between the left (T5) and right (T6) posterior temporal sites. Both the spectral power and the coherence magnitudes for each individual were saved for further analysis with SPSS.

Source localization using sLORETA (Pasqual-Marquis, 2002) software was employed to infer bilateral activation within the parahippocampal gyri. sLORETA software models the current source density ($\mu\text{A}/\text{mm}^2$) distribution [9] of activity recorded from scalp electrodes onto a 3D reconstruction of the human brain. For this study, we first translated the 19-channel time-series into the frequency-domain by means of cross-spectral analysis within discrete 1-Hz frequency bins from 1 to 40 Hz using the EEG to Cross-Spectrum function. Current source density was then computed using Cross-Spectrum to sLORETA. The results of this computation were then entered into the sLORETA to ROI function to obtain regional-specific activation of the bilateral parahippocampal gyri using its approximate MNI co-ordinates (right: X = 28, Y = -40, Z = -12; left: X = -28, Y = -40, Z = -12). As a result both left and right parahippocampal sLORETA activation scores were obtained for discrete 1-Hz frequency bins from 1 to 40 Hz. These scores were also saved and imported into SPSS for further analyses.

Considering the frequent occurrence of increased activation within the right parahippocampal region as inferred by source localization (sLORETA) during conditions associated with both sensed presences and increased geomagnetic activity (Saroka and Persinger, 2013), we computed net differences between the left and right parahippocampal scores as a function of 1 Hz increments by subtracting activation in the left parahippocampal gyrus from the right; therefore the scores reflected right parahippocampal activation with respect to the left and positive values indicated greater right parahippocampal involvement. Preliminary analyses of variance (described below) suggested similar effects for the 10, 11, and 12 Hz bands, which also comprise what is commonly known as the “high-alpha” band. Hence the sum of the activation of 10, 11, and 12Hz bands for the net changes in parahippocampal activation was employed as the predictor and all channels and bands were employed as independent variables in a step-wise multiple regression. In order to discern the intrinsic activity in right parahippocampal regions after the removal of cortical components, the residuals were analyzed as a function of the different levels of K values at the time of the measurement. Because activation of intracortical regions inferred by sLORETA is ultimately based upon electrical activity derived from the outer surface of the brain, we reasoned that controlling for cortical activity by removing shared sources of variance contributed by the sensors would provide a more accurate representation of activity within the parahippocampal region. Finally the strength (Rho^2) of the correlations between this residual and the T5–T6 coherence values for each of the frequencies between 1 and 40 Hz were completed. All analyses involved PC SPSS 16 software.

2.4 Results

The numbers of people (in parentheses) measured during times of various levels of geomagnetic disturbance were $K_p=0$ (N=47), $K_p=1$ (N=105), $K_p=2$ (N=51), $K_p=3$ (N=23) $K_p\geq 4$ (N=7). The results of the coherence analyses are shown in Fig 3.1. The mean coherence between the left (T5) and right (T6) posterior temporal regions significantly increased ($F_{4,228}= 4.97$, $p < .01$, Ω^2 estimate = .08) when the contemporary geomagnetic activity, as inferred by 3 h K-indices, was 2 or greater which is equivalent to >6 to 9 nT at the time of the measurement. The coherence was also specific to the 11 Hz frequency band and was not evident for increments below or above this value.

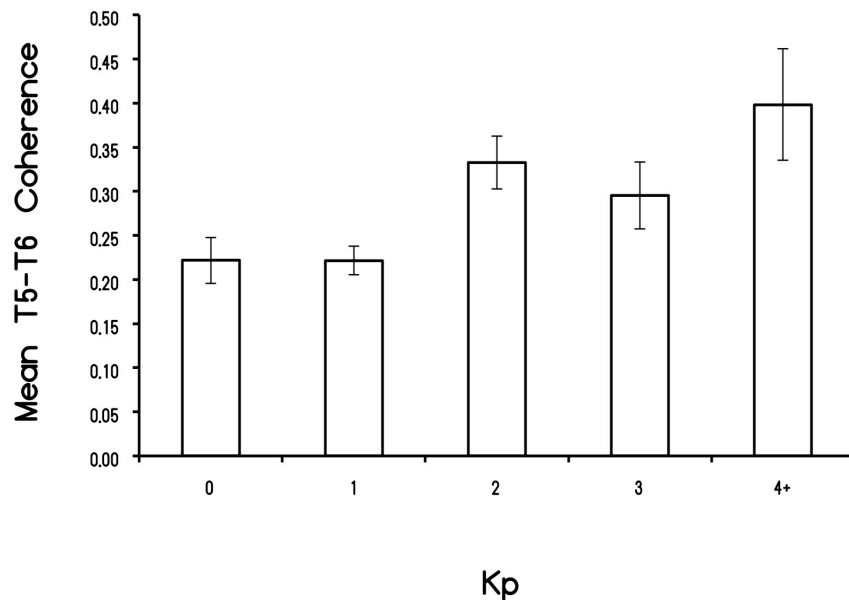


Figure 2.1 Mean coherence score between the left (T5) and right (T6) temporal lobes as a function of the global geomagnetic (K_p) during the 3 h period of the measurements. The numbers of subjects (parentheses) per group intensity were: 0 (47), 1 (105), 2 (51), 3(23) and >4 (7); they were tested over a 3.5 years period. Vertical bars indicate SEM.

The effect sizes for the correlations between the K indices and the net differences in current source density between the left and right parahippocampal regions for each 1 Hz increment are shown in Figure 3.2. Oneway analyses of variance indicated statistically significant correlations only for the adjacent 10, 11, and 12 Hz bands as well as a smaller 30 Hz frequency.

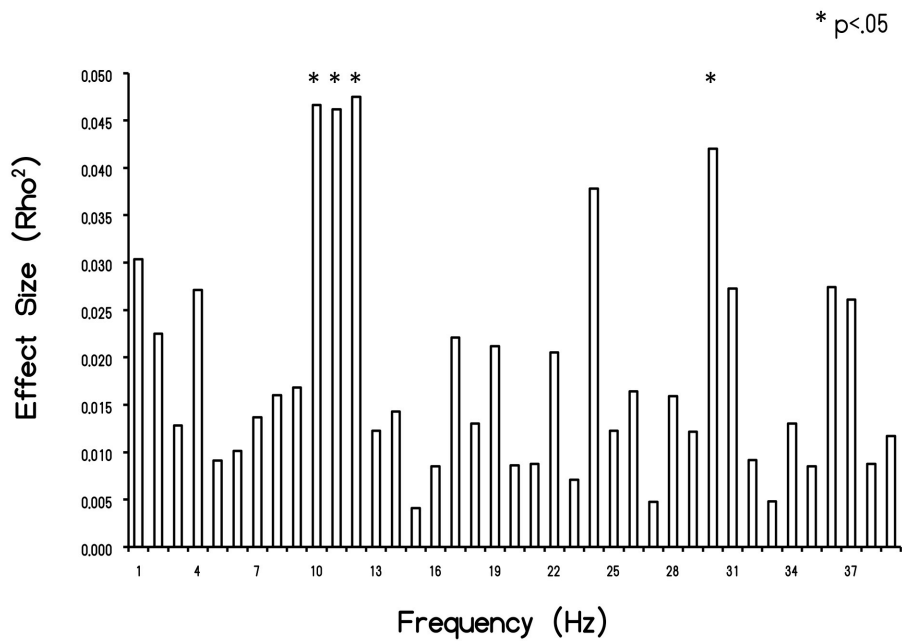


Figure 2.2 Effect sizes for the correlation between the K indices at the time of the measurements and the net differences in power between the left and right parahippocampal regions for each 1 Hz increment.

The only variables that entered the equation for the sum of the activation within the 10, 11, and 12 Hz ($\Sigma_{10,12}$) bands were high-alpha from the right posterior temporal (RPT- α 2) regions and the left posterior temporal region within the theta (LPT- Θ) and high- alpha (LPT- α 2) frequency bands. The multiple r was 0.62 and the results are summarized in Eq. (1).

$$\sum_{10,12} = 339.28(\text{RPT}-\alpha_2) - 264.14(\text{LPT}-\alpha_2) - 80.85(\text{LPT}-\Theta) + 6.83(1) \quad (\text{Eq. 1})$$

When the standardized residuals for this equation (which we interpreted as an indicator of the difference between the two parahippocampal regions not attributed to concomitant cortical activity) were compared by one way analysis [$F_{4,228} = 4.36$, $p < .01$; Ω^2 estimate=.07] of variance there was a significant increase in this residual as a function of the K value at the time of measurement (Figure 3.3). Post hoc Tukey analyses set at a significance level of $p < .05$ indicated that the mean residual was highest during the time of a K = 4 geomagnetic storm when compared against K = 0 or K = 1. Fig. 4 shows the effect size of the correlation between these standardized residuals with the coherence measures between T5 and T6 across all frequencies. The strongest effect sizes occurred ~7.5 Hz and 19.5 Hz.

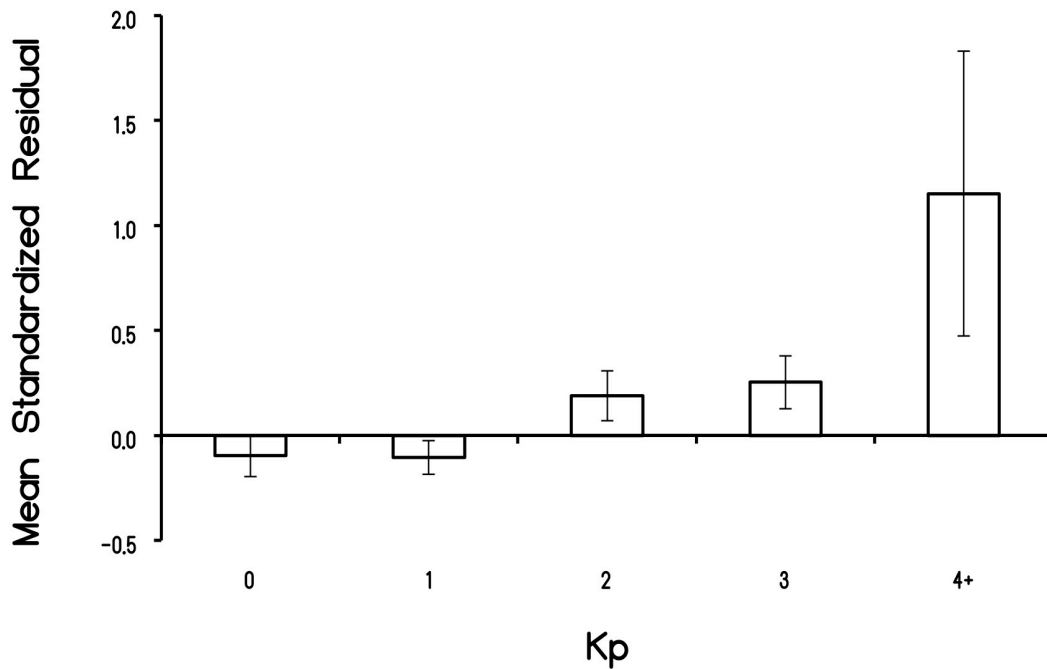


Figure 2.3 Mean standardized residuals for the difference between the two parahippocampal regions extracted by sLORETA after removal of variance associated with cortical activity as a function of geomagnetic activity. Vertical bars are SEM.

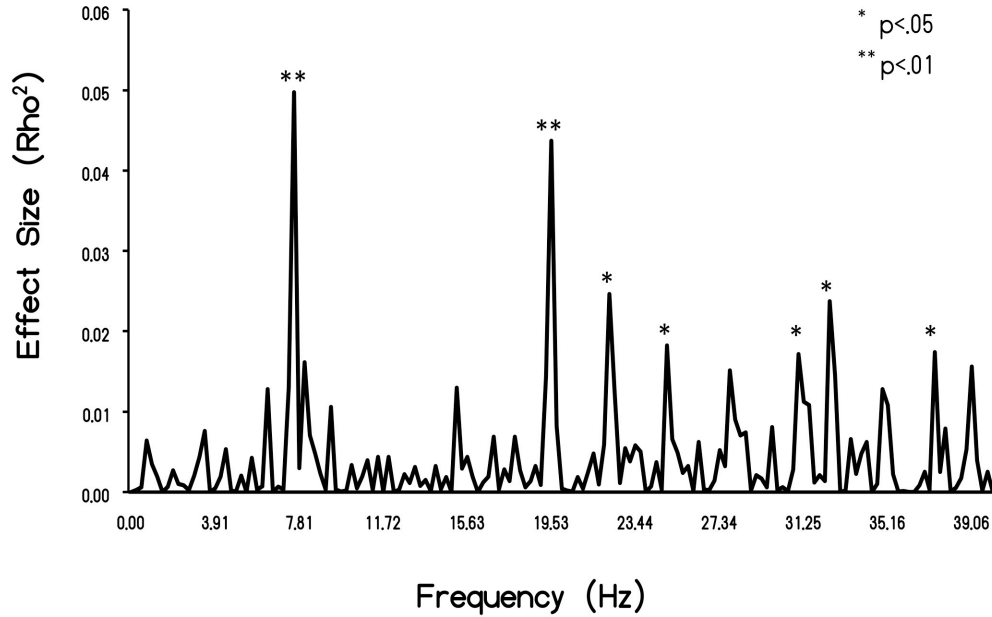


Figure 2.4 Effect sizes for the correlations between standardized residuals from Figure 3 with the coherence measures between T5 and T6 across all frequencies. The first two peaks are ~7.6 Hz and ~19.6 Hz.

3.5 Discussion and Conclusion

The association between increased epileptic phenomena in mammals and increased geomagnetic activity has been reported by several authors. In general the strength of the association (r^2) indicates that the variables share about 25% of the variance. Experimental simulations of geomagnetic activity with electrical labile animal brains, such as seized rats, indicate that the intensity of the applied fields and the proportions of increased numbers of seizures approximate the natural condition (Michon and Persinger, 1996; Persinger, 1995). Quantitative EEG measurements for human

subjects have revealed consistent correlations between the intensity of global geomagnetic activity and the proportion of power within specific frequency bands (usually theta and gamma) particularly over the right hemisphere (Babayev and Allahverdiyeva, 2007; Mulligan and Persinger, 2010). Again, comparable effects in the change in cerebral EEG power over similar regions of the right hemisphere have been reproduced experimentally (Mulligan and Persinger, 2012).

The results of the present study replicate and extend the threshold values for significant changes in biological measurements that have been observed for a number of species. Increased aggression between rats with seizure-induced brain damage (Persinger, 1997), mortality of rats with acute epileptic limbic lability (Bureau and Persinger, 1995) and the occurrence of “spontaneous” seizures in populations of epileptic rats (Persinger, 1995) have indicated thresholds of >15 nT for global geomagnetic activity at the time of the behaviors.

In the original Persinger and Richards (1995) study involving 127 human subjects, most of whom were exposed to weak transcerebral fields, the report of vestibular experiences were conspicuously increased while sitting blind folded within the same acoustic chamber employed in this study. However in that study the effect was most associated with the activity during the night before the experiment. In the present study the increased coherence between the left and right posterior temporal lobes was directly associated with the global geomagnetic activity at the time of the QEEG measurements. All of these volunteers were sitting quietly in the darkened chamber, were not blind folded, and did not receive any transcerebral weak magnetic fields.

The increased coherence between the left and right temporal lobes in normal

subjects simply sitting alone in a quiet, darkened place during periods when geomagnetic activity increased above 6–9nT suggests that more direct quantitative brain measurements are most sensitive to ambient geomagnetic activity or that transcerebral magnetic fields compete for similar processes and hence increase the threshold (15–20 nT) for the detection of any effect. We suggest a continuum might exist similar to that reported for surgical stimulation between the proportion of coherence of neuronal populations and the intensity of the effect. Babb et al. (1987) reported that as more and more neurons became coherent the subject’s experiences shifted along a continuum from “normal ideation” to vestibular and powerful thoughts, to “vivid perceptual experiences” and ultimately to convulsions. That discrete cerebral changes can occur without awareness of discernable changes in subjective experiences is well documented (Berns et al., 1997).

The increased coherence between the left and right posterior temporal lobes, given the functional correlates of this region, should encourage visual and auditory phenomena. The report of bereavement apparitions are more likely to occur when the ambient geomagnetic activity during the experience increases from about 20–28 nT, an average increase of about 8 nT. A similar observation was reported by Randall and Randall (1991). It may be relevant to note that the magnitude of the 11 Hz posterior temporal coherence displayed by individuals measured on days where the geomagnetic disturbance exceeded ~8nT approximated the magnitude of the 10–13 Hz anterior temporal coherence displayed by individuals who had experienced an experimentally-induced sensed presence approximately 5–10 min following exposure to a frequency-modulated electromagnetic field (St-Pierre and Persinger, 2006; Saroka and Persinger, 2013).

The particular involvement of the parahippocampal region is important for several reasons. First it contains structures, the hippocampus and amygdala, which were the regions from which “hallucinations” or experiences have been most easily evoked by direct surgical stimulation (Persinger et al., 2013; Persinger et al, 2010). Second this area includes the perirhinal and entorhinal cortices, the “gatekeepers” of the hippocampus, that mediate input that originates from large areas of the cerebral cortices and visa versa (Gloor, 1997). Because it relays spatial information and receives more powerful inputs from the frontal and cingulate regions, second-order visual and auditory association areas, and the parietal and temporoparietal multimodal centers for language (of the dominant hemisphere) the role of expectation, linguistic labels and visuo-auditory spatial details would be expected to dominate subjective experiences when it is activated.

We have postulated that the prototype for many mystical experiences involves a “sensed presence” which has been interpreted as the awareness of the right hemispheric equivalent of the left hemispheric sense of self (Persinger, 2003; St-Pierre and Persinger, 2006). Although there were many inferential studies, recent source-localization and QEEG vectorial measurements have indicated that these experiences when elicited by transcerebral magnetic fields within the laboratory involve a right temporal to left temporal lobe direction (Persinger et al, 2010). That geomagnetic activity above ~8 nT at the time of the measurements increased coherence may increase our understanding of how these experiences might be encouraged by subtle ambient forces and energies.

The neurophysical mechanisms by which the presumed effects from the

increased geomagnetic activity produced the increased coherence measured in this study must still be identified. The traditional limits of “kT boundaries” may not be applicable (Cifra et al., 2010). There would certainly be sufficient energy available. Modified calculations from Mulligan et al. (Kesser et al., 2011) indicates that increased perturbations of 10nT would be associated with ~10 J within the average human brain. Assuming $\sim 10^{-20}$ J per action potential (Persinger, 2010) this increased energy would be equivalent to one million neurons each discharging around 10 Hz.

3.6 References

- Babb TL, Wilson CL, Isokawa-Akesson M, Firing patterns of human limbic neurons during stereocephalography (SSEG) and clinical temporal lobe seizures, *Electroencephalography and Clinical Neurophysiology* 66 (1987) 467–482.
- Babayev ES, Allahverdiyeva AA. Effects of geomagnetic activity variations on the physiological and psychological state of functionally healthy humans: some results of the Azerbaijani studies. *Advances in Space Research* 40 (2007) 1941–1951.
- Berns GS, Cohen JD, Mintun MA. Brain regions responsive to novelty in the absence of awareness. *Science* 276 (1997) 1272–1275.
- Booth JN, Koren SA, Persinger MA. Increased feelings of the sensed presence and increased geomagnetic activity at the time of the experience during exposure to transcerebral weak magnetic fields. *International Journal of Neuroscience* 115 (2005) 1053–1079.
- Bureau YR, Persinger MA. Geomagnetic activity and enhanced mortality in rats with acute (epileptic) limbic lability. *International Journal of Biometeorology* 36 (1992) 226–232.

- Cifra M, Fields JZ, Farhadi A. Electromagnetic cellular interactions. *Progress in Biophysics and Molecular Biology* 105 (2010) 223–246.
- Delorme A, Makeig S. EEGLAB: an open source toolbox for analysis of single-trial EEG dynamics including independent component analysis. *Journal of Neuroscience Methods* 134 (2004) 9–21.
- Gloor P. *The Temporal Lobe and Limbic System*. Oxford University Press, N.Y, 1997.
- Keiser D, Padberg F, Reisinger E, Pogarell O, Kirsch V, Palm U, Karch V, Möller HJ, Nitsche MA, Mulert C. Prefrontal direct current stimulation modulates resting EEG and event-related potentials in healthy subjects: a standardized low resolution tomography (sLORETA) study. *NeuroImage* 55 (2011) 644–657.
- Michon AL, Persinger MA. Experimental simulation of the effects of increased geomagnetic activity upon nocturnal seizures in rats. *Neuroscience Letters* 224 (1997) 53–56.
- Mulligan BP, Hunter MD, Persinger MA. Effects of geomagnetic activity and atmospheric power variations on quantitative measures of brain activity: replication of the Azerbaijani studies. *Advances in Space Research* 45 (2010) 940–948.
- Mulligan BP, Persinger MA. Experimental simulation of the effects of sudden increases in geomagnetic activity upon quantitative measures of human brain activity: validation of correlational studies. *Neuroscience Letters* 516 (2012) 54–56.
- Pasqual-Marquis RD. Standardized low resolution brain electromagnetic tomography (sLORETA): technical details. *Methods and Findings in Experimental Pharmacology* 24 (2002) D5–D12.
- Persinger MA. Increased geomagnetic activity and the occurrence of bereavement hallucinations: evidence for melatonin-mediated microseizuring in the temporal lobe. *Neuroscience Letters* 88 (1988) 271–274.

- Persinger MA. Geophysical variables and behavior: LXXIX. Overt limbic seizures are associated with concurrent and premidscotophase geomagnetic activity: synchronization by prenocturnal feeding. *Perceptual and Motor Skills* 81 (1995) 83–93.
- Persinger MA. Out-of-body-like experiences are more probable in people with elevated complex partial epileptic-like signs during periods of enhanced geo- magnetic activity: a non-linear effect. *Perceptual and Motor Skills* 80 (1995) 563–569.
- Persinger MA. Geomagnetic variables and behavior: LXXXIII. Increased geo- magnetic activity and group aggression in chronic epileptic rats. *Perceptual and Motor Skills* 85 (1997) 395–402.
- Persinger MA. The sensed presence within experimental settings: implication for the male and female concept of self. *The Journal of Psychology* 137 (2003) 5–16.
- Persinger MA. 10^{-20} Joules as a neuromolecular quantum in medicinal chemistry: an alternative approach to myriad molecular pathways. *Current Medicinal Chemistry* 17 (2010) 3094–3098.
- Persinger MA, Dotta BT, Saroka KS, Scott MA. Congruence of energies for cerebral photon emissions, quantitative EEG activities and ~5 nT changes in proximal geomagnetic field support spin-based hypothesis of consciousness. *Journal of Consciousness Exploration and Research* 4 (2013) 1–24.
- Persinger MA, Saroka KS. Comparable proportions of classes of experiences and intracerebral consequences for surgical stimulation and external application of weak magnetic field patterns: implications for converging effects in complex partial seizures. *Epilepsy and Behavior* 27 (2013) 220–224.
- Persinger MA, Saroka KS, Koren SA, St-Pierre LS. The electromagnetic induction of

- mystical and altered states within the laboratory. *Journal of Consciousness Exploration and Research* 1 (2010) 808–830.
- Persinger MA, Richards PM. Vestibular experiences of humans during brief periods of partial sensory deprivation are enhanced when daily geomagnetic activity exceeds 15–20 nT. *Neuroscience Letters* 194 (1995) 69–72.
- Rajaram M, Mitra S. Correlations between convulsive seizure and geomagnetic activity. *Neuroscience Letters* 24 (1981) 187–191.
- Randall W, Randall S. The solar wind and hallucinations – a possible relation due to magnetic disturbances. *Bioelectromagnetism* 12 (1991) 67–70.
- St-Pierre LS, Parker GH, Bubenik GA, Persinger MA. Enhanced mortality of rat pups following inductions of epileptic seizures after perinatal exposures to 5 nT, 7 Hz, magnetic fields. *Life Sciences* 81 (2007) 1496–1500.
- St-Pierre LS, Persinger MA. Experimental facilitation of the sensed presence is predicted by specific patterns of applied magnetic fields not by suggestibility: re-analysis of 19 experiments. *International Journal of Neuroscience* 116 (2006) 1–18.
- Saroka KS, Mulligan BP, Murphy TR, Persinger MA. Experimental elicitation of an out of body experience and concomitant cross-hemispheric electroencephalographic coherence. *Neuroquantology* 8 (2010) 466–477.
- Saroka KS, Persinger MA. Potential production of Hughling Jackson's parasitic consciousness by physiologically-patterned weak transcerebral magnetic fields: QEEG and source localization. *Epilepsy and Behavior* 28 (2013) 395–407.
- Subrahmanyam S, Sanker PV, Narayan, Srinivasan TM. Effects of magnetic micropulsations on biological systems: a bioenvironmental effect. *International Journal of Biometeorology* 29 (1985) 293–305.

Chapter 3

Assessment of Geomagnetic Coherence and Topographic Landscapes of the Static Geomagnetic Field in Relation to the Human Brain Employing Electroencephalographic Methodology

3.1 Introduction

The earth is surrounded by a geomagnetic field that is influenced by solar activity. The average intensity of the earth's magnetic field is approximately 50,000 nT (Chapman and Bartels, 1940), which is approximately a million times stronger than the intensities of the earth's intrinsic Schumann resonance. During geomagnetic storms, precipitated by changes in the solar wind which is comprised of protons, the geomagnetic field displays sudden shifts in its activity that can deviate by approximately 200-300 nT during extreme storms or 20-30 nT during low-level disturbances (Bleil, 1964).

One property of the brain is that sudden disturbances (i.e. closed head injuries, seizures) can change the electrical landscape of its electric field topography. We have found that post-concussion, alpha activity of one individual displayed a 'ring' type pattern when measurements were taken everyday for 7-8 days post-injury. This "ringing" has also been observed for several hours to days after a sudden impulse of protons that disturb the static geomagnetic field and are typically observed after sudden storm commencements particularly in high latitudes (Bleil 1964) with durations that are approximately proportional to the degree of geomagnetic disturbance.

One approach to scientific inquiry is that processes that occur at a microscopic level are related to processes that occur at a macroscopic scale. For example, small changes in molecular concentration of certain neurochemical compounds can alter the way that the individual experiences his or her environment as in the case with psychotropic substances. Scale invariance, or fractal geometry, assumes that an object retains its geometrical (either in space or time) shape as one proceeds to “zoom in” or “zoom out”. In this case, the introduction of selective serotonin reuptake inhibitors to some depressed individuals minimizes a negative bias towards experience. Thus, small microscopic molecular differences influence macroscopic behaviour.

Such scale-invariance can be found within a variety of natural settings. For example, if one were to view the landscape of Northern coniferous trees from a distance of some kilometers above the tree line, the trees would look like moss that can be found buried deep within its forests. Modern quantitative electroencephalographic techniques now employ measures of fractal geometry (Georgiev et al., 2009). When such algorithms are applied to time-series signals such as EEG, one can discern the “level of consciousness” of individuals who are under the influence of anaesthetic compounds (Nan and Jingua, 1988).

Theoretically the concept of a connection between processes that influence the earth and those that influence the brain has been demonstrated quantitatively. Persinger (2012) demonstrated that the electrical properties of lightning strikes are similar to those produced naturally within the brain during action potentials when scale, or size, is accommodated. In addition, the intensity and resonant frequencies of the cavity generated between brain tissue and the skull are similar to those produced in the

cavity between the upper-layers of the ionosphere and the earth's surface (Nunez, 1995).

It may not be spurious that the geomagnetic field and the brain's electrical field can be described as "dipolar", with North and South poles of the brain oriented depending upon its geometric placement within the earth's geomagnetic field. For example, there is evidence to suggest that animals such as birds orient along flux lines of the geomagnetic field for the purpose of migration (Thalau et al., 2005). In the case of birds, there may be evidence to suggest that they can actually "see" the flux lines due to over-expression of a protein known as cryptochrome (Ritz et al., 2009). In addition it has been reported that latency to REM sleep changes as a function of orientation of the supine individual within the earth's geomagnetic field (Ruhstroth-Bauer et al., 1987).

Ideally, if two systems at separate levels are connected then algorithms and analytical techniques applied to one level should produce comparable outcomes in the other. The following analysis was conducted in order to apply methodologies commonly employed in quantitative encephalographic studies to geomagnetic field signals recorded simultaneously from distant regions around the earth. The first analysis, coherence, can be thought of as the degree to which two signals, or time-series, are harmonious. If both display similar changes over time in "peaks and troughs", they are said to be coherent. Such coherence within the brain is thought to be vital for 'binding' the separate components of experience into a percept.

The second analysis describes the geometrical landscape of electric fields and is known as microstate analysis (Koenig et al., 1999). These microstates normally last between 80-120 milliseconds in humans and are thought to be the 'atoms of thought',

similar to base pairs in a sequence of DNA. Theoretically a sequence of these states could be the language with which information generated exogenously and endogenously is consolidated, described and ultimately communicated within a social setting.

3.2 Materials and Methods

Approximately one year of the X-component of the static geomagnetic field was collected from IntraMagnet from locations depicted in Figure 3.1A for years 2013 and 2014. The sampling rate of this data was 1/60Hz, or one observation per minute. This data was then imported into MATLAB software where the magnetic field measurements of 8 regions were consolidated into one variable. Because intensities of the static geomagnetic field were stronger in certain geographical regions, within-channel z-scores were obtained so as to normalize the measurements.

The resultant 8-channel time series was then imported into EEGLab (Delorme and Makeig, 2004) software for visualization and artifact correction (i.e. power outages) using an interpolation method which identified points in the time-series with z-scores greater than 3, removed them, and then interpolated an average. The resultant time-series was then 100 points constituted one days worth of data therefore 1 second was equivalent to 10 days. Once artifacts were removed and the data was re-sampled it was saved as an ASCII text file for later importation into MapWin software.

Based upon earlier findings indicating greater coherence between the left and right temporal region during times of geomagnetic disturbance (Saroka et al., 2013) coherence was computed for each bi-channel combination (total=28) for each day (N=715) between January 1, 2013 and December 15, 2014. 1/604800. Coherence

within the 0 to 1 microHertz (approximately equivalent to 7 days) bandwidth was then averaged. Global averages of coherence were computed from obtaining the mean of all 28 possible bivariate combinations of channels for each channel.

Within MapWin software, a specialized but approximate montage was defined based upon the geographical locations of the magnetometers. This montage can be viewed in Figure 3.1B. The entire ~35 earth-second epoch was imported into MapWin with a pass-band filter of 0-20Hz, as is employed regularly in the literature. Microstate clusters were computed using the “Construct Microstate Maps” option, forcing the analysis to produce 4 clusters with pre-cluster normalization. To compute inferences of coverage, occurrence and duration of each of the 4 classes of microstate, the 35 second record was segmented according to each day (i.e. 350 days). The microstate clusters produced in the original analysis were then applied to each segment individually and conventional microstate parameters were then saved for further SPSS analysis.

To compare the results of the microstate analysis against some measure of validity, the daily Kp index was obtained from the OMNI online geophysical database (<http://omniweb.gsfc.nasa.gov/form/dx1.html>) for each day for both years.

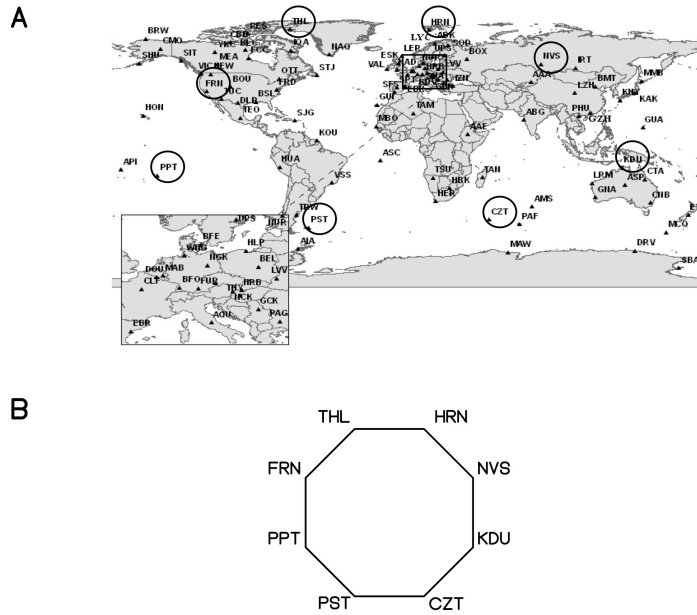


Figure 3.1 (A) Geographical regions from which samples of the geomagnetic field were sampled (B) Montage for the 8 ‘sensors’ of the world fitted to their approximate locations if they were modeled on the classic 10-20 system used regularly within electroencephalography.

3.3 Results

3.3.1 Qualitative Descriptions

The 8-channel geophysical time-series organized according to geographical region is depicted in Figure 3.2. From a qualitative perspective, the time-series resembles a standard electroencephalographic record. Clearly evident are diurnal variations in the static X-component of the geomagnetic field. A Bartel’s musical notation plot is depicted below the 8-channel record in order to compare sudden geomagnetic disturbances (i.e. impulses) with the raw data. These impulses (indicated with arrows) are discernible across most of the channels.

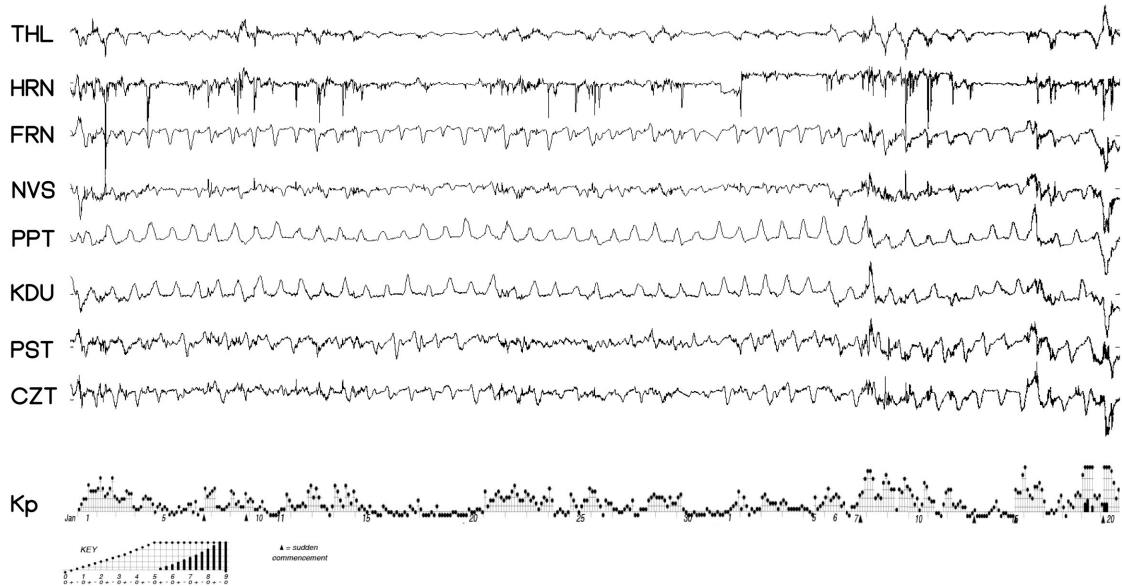


Figure 3.2 Time-series of 50 days of the geomagnetic field fluctuations sampled at the respective stations with the planetary k-index plotted at the bottom.

3.3.2 Coherence Analysis

One-way analysis of variance performed on global coherence as a function of k-index indicated that there was significantly more coherence ($F_{4,706}=20.00$, $p<.05$, ω^2 estimate=.10) during days in which the k-index was equivalent to or exceeded 4 (Figure 3.3). When the effect sizes for this effect were plotted as a function of channel-pair it was determined that coherence between PPT and KDU stations, which would roughly correspond to the T5 and T6 sensors on a standard 10-20 montage, displayed the strongest effect (Figure 3.4).

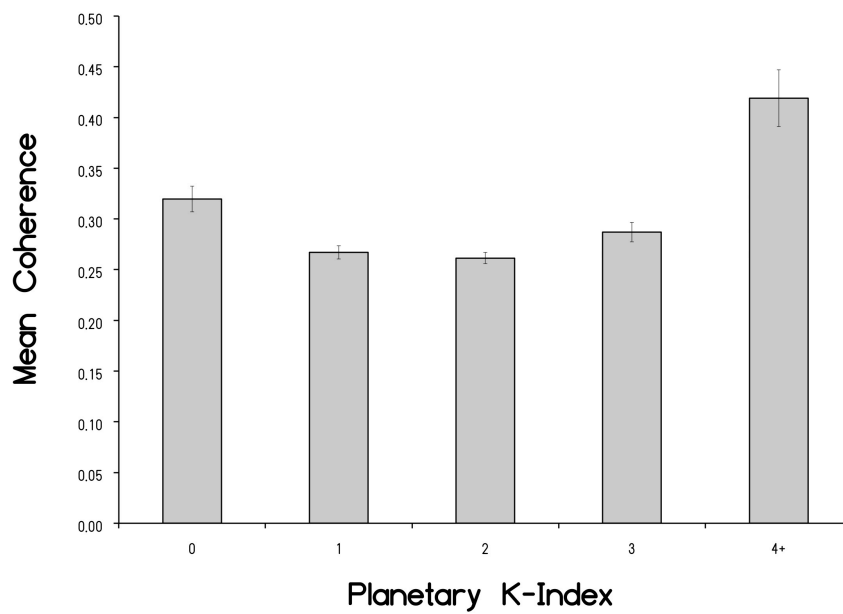


Figure 3.3 Mean global coherence plotted as a function of the planetary k-index showing that mean global geomagnetic coherence is strongest during days when the k-index is greater than or equal to 4.

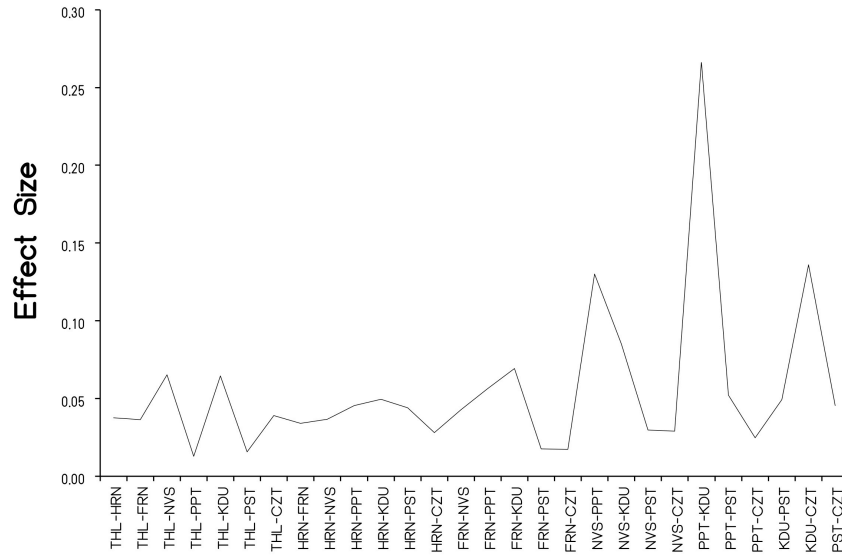


Figure 3.4 Effect sizes for the 28 bivariate combinations coherence. The strongest effect size was observed between the PPT and KDU sites.

3.3.3 Microstate Analysis

Microstate analysis determined that 4 classes of topographies explained approximately 66% of the variance in fluctuations of the static geomagnetic field during the 2014 year. The microstates associated with each time point within the 350-day time series is depicted in Figure 3.5. To insure that the topographies were consistent across time, records for the year 2013 were also entered into Mapwin for topography calculation. The results for year 2013 and 2014 are depicted in Figure 3.6, which shows a high degree of similarity between the different topographies from year-to-year.

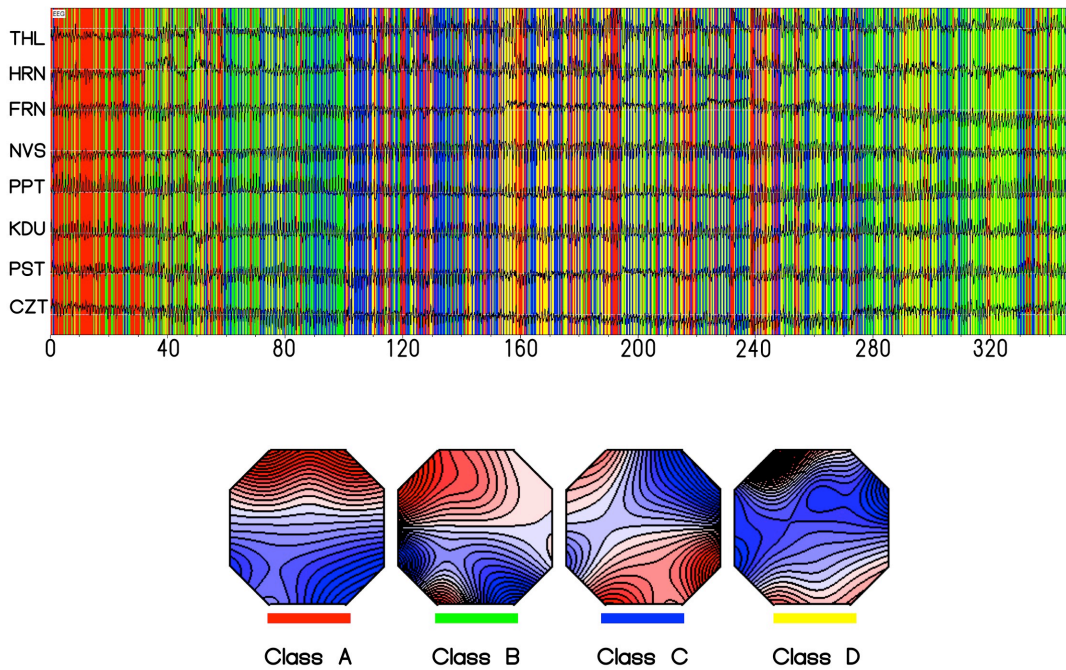


Figure 3.5 Sequence of microstates of the geomagnetic field for 350-days during year 2014.

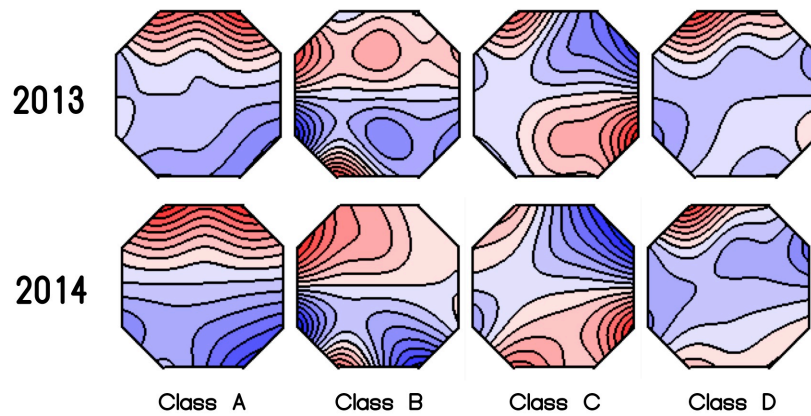


Figure 3.6 Topographies of the static geomagnetic field inferred from microstate analysis for the years 2013 and 2014 separately. The results suggest a high congruency between 'field maps' of the static geomagnetic field from year-to-year.

3.4 Discussion and Conclusion

The relationship between the earth's geomagnetic field and human brain activity has been assessed qualitatively and quantitatively. The waveforms generated by the electroencephalograms of humans show remarkable congruence with that of atmospheric noise showing on average identities in the frequency range between 0 and about 50 Hz (König and Anker Müller, 1960). Several groups have demonstrated direct coherence between the Schumann resonance, which is observable within the spectrums of human brains and strongest primarily over the caudal aspect of the cerebrum, and the brain's electric field within specific frequency ranges of about 8 to 30 Hz (Pobachenko, 2006; Saroka and Persinger, 2014). The frequency of these coherences is about 1-2 times per second with average durations of about 300 milliseconds and approximates the duration of about 2-3 microstates.

Because the basic assumption motivating this analysis was that there is a direct connection between processes occurring on both microscopic (human brain) and macroscopic (the earth) levels, we assumed that analytic methods commonly employed within one level should reveal comparable outcomes in the other. The main requirement was that these similarities should be internally consistent from year-to-year and valid within the context of the knowledge base of that level. The results of the coherence analysis indicated that average coherence of the channels recording the geomagnetic field at different sites was strongest during periods of disturbance and was pronounced between recording sites that would have been comparable to the left and right posterior temporal sites if the nasion was localized around the North pole of the earth. Increased coherence within human electroencephalographic activity between the left and right

temporal lobes has been observed during the incidences of geomagnetic disturbances (Saroka et al., 2013). The coherence between these two regions was strongest within frequency bands approaching the fundamental (~8 Hz) and third harmonic (~20 Hz) of the Schumann resonance. Pobachenko et al. (2006) previously reported that the correlation between simultaneous measurements of atmospheric noise and human electroencephalograms was strongest during periods of geomagnetic disturbance. The integration of these results with those found previously would suggest a mirrored fugal-coupling of processes occurring at both levels whereby events such as sudden commencements simultaneously produce coherences within the earth and the human brain.

The microstate analysis revealed 4 topographies that cumulatively explained between 62-66% of the variance in the variations of the topographies of the static geomagnetic field that were relatively consistent between the two years. The first microstate (Class A) reiterates that the magnetic fields are strongest at the North and South poles of the earth and resembles Class C commonly observed in human brains (Koenig et al., 2002). Class C begins to resemble isocontour maps showing that total magnetic field is strongest over the Canadian Northwest Territories and portions of Antarctica south of Australia and conversely in parts of Russia north of China and in the Pacific Ocean west of Antarctica. Interestingly Class D appears to be most sensitive to abrupt changes in the geomagnetic field that can partially be explained by the tilt of the North Pole relative to the Sun.

In conclusion, while open to speculation, the analyses conducted in this chapter support a fractal relationship between electromagnetic processes occurring within the human brain and the earth. The shapes of microstates as well as the coherencies

observed in cross-station analysis potentially demonstrate that it is possible to explore time-varying (in this case the static geomagnetic field) signals in congruous ways.

For centuries the explanation behind near-simultaneous appearances of phenomena like cave art and scientific discoveries has been labeled with various rationalizations such as impending coincidence, evolutionary adaptation and others, all of which assume random chance expectancies either through eventual transmission of ideas from region-to-region or mutations in the sequencing of DNA. However, these findings may offer an alternative, but equally compatible dimension consistent with Sheldrake's (2011) morphogenetic resonance hypothesis that implies that conspecific species of animals learn faster once the original behaviour has been performed. In this case the information in the form of electromagnetic patterns generated from the brains of individuals could produce changes within the earth's geomagnetic field that then influence other human brains through resonance processes. Therefore the geomagnetic field could function as a source of ideas in the form of energy, the transmission medium by which ideas are transferred between geographic regions, or both. Although seemingly improbable, both Persinger (2010) and Dotta (2010) have shown that stimuli applied to one person in isolation produces comparable changes in another person sitting in another room when both individuals share the same temporally-patterned and circumcerebrally rotating electromagnetic field.

3.5 References

Bleil, D. F. (1964). Natural electromagnetic phenomena below 30 kc/s. In *Natural Electromagnetic Phenomena* (Vol. 1).

- Chapman, S., & Bartels, J. (1940). *Geomagnetism*. Oxford: Clarendon Press.
- Delorme, A., & Makeig, S. (2004). EEGLAB: an open source toolbox for analysis of single-trial EEG dynamics including independent component analysis. *Journal of neuroscience methods*, 134(1), 9-21.
- Dotta, B. T., Buckner, C. A., Lafrenie, R. M., & Persinger, M. A. (2011). Photon emissions from human brain and cell culture exposed to distally rotating magnetic fields shared by separate light-stimulated brains and cells. *Brain research*, 1388, 77-88.
- Georgiev, S., Minchev, Z., Christova, C., & Philipova, D. (2009). EEG fractal dimension measurement before and after human auditory stimulation. *Bioautomation*, 12.
- Koenig, T., Prichep, L., Lehmann, D., Sosa, P. V., Braeker, E., Kleinlogel, H., ... & John, E. R. (2002). Millisecond by millisecond, year by year: normative EEG microstates and developmental stages. *Neuroimage*, 16(1), 41-48.
- Koenig, T., Lehmann, D., Merlo, M. C., Kochi, K., Hell, D., & Koukkou, M. (1999). A deviant EEG brain microstate in acute, neuroleptic-naive schizophrenics at rest. *European archives of psychiatry and clinical neuroscience*, 249(4), 205-211.
- König, H., & Anker Müller, F. (1960). Über den Einfluss besonders niederfrequenter elektrischer Vorgänge in der Atmosphäre auf den Menschen. *Naturwissenschaften*, 47(21), 486-490.

- Nan, X., & Jinghua, X. (1988). The fractal dimension of EEG as a physical measure of conscious human brain activities. *Bulletin of Mathematical Biology*, 50(5), 559-565.
- Nunez, P. L. (1995). *Neocortical dynamics and human EEG rhythms*. Oxford University Press, USA.
- Persinger, M. A. (2012). Brain electromagnetic activity and lightning: potentially congruent scale-invariant quantitative properties. *Frontiers in integrative neuroscience*, 6.
- Persinger, M. A., Saroka, K. S., Lavallee, C. F., Booth, J. N., Hunter, M. D., Mulligan, B. P., ... & Gang, N. (2010). Correlated cerebral events between physically and sensory isolated pairs of subjects exposed to yoked circumcerebral magnetic fields. *Neuroscience Letters*, 486(3), 231-234.
- Pobachenko, S. V., Kolesnik, A. G., Borodin, A. S., & Kalyuzhin, V. V. (2006). The contingency of parameters of human encephalograms and Schumann resonance electromagnetic fields revealed in monitoring studies. *Biophysics*, 51(3), 480-483.
- Ritz, T., Wiltschko, R., Hore, P. J., Rodgers, C. T., Stapput, K., Thalau, P., ... & Wiltschko, W. (2009). Magnetic compass of birds is based on a molecule with optimal directional sensitivity. *Biophysical journal*, 96(8), 3451-3457.
- Ruhenstroth-Bauer, G., R  ther, E., & Reinertshofer, T. H. (1987). Dependence of a sleeping parameter from the NS or EW sleeping direction. *Zeitschrift f  r Naturforschung C*, 42(9-10), 1140-1142.

- Saroka, K. S., Caswell, J. M., Lapointe, A., & Persinger, M. A. (2014). Greater electroencephalographic coherence between left and right temporal lobe structures during increased geomagnetic activity. *Neuroscience letters*, 560, 126-130.
- Saroka, K. S., & Persinger, M. A. (2014). Quantitative evidence for direct effects between Earth-ionosphere Schumann resonances and human cerebral cortical activity. *International Letters of Chemistry, Physics and Astronomy*, 20.
- Sheldrake, R. (2011). *The presence of the past: Morphic resonance and the habits of nature*. Icon Books.
- Thalau, P., Ritz, T., Stapput, K., Wiltschko, R., & Wiltschko, W. (2005). Magnetic compass orientation of migratory birds in the presence of a 1.315 MHz oscillating field. *Naturwissenschaften*, 92(2), 86-90.

Chapter 4

The Proximal AC Electromagnetic Environment and Human Brain Activity

4.1 Introduction

All biological systems exist within a complex environment composed of many features including electromagnetic waves. The frequency of these oscillations ranges from extremely low-frequency oscillations (~ 10 Hz) frequencies, which are not directly perceived but are produced naturally by the earth and the brain, to high-frequency $\sim 10^{14}$ Hz which are processed by the human retina and experienced psychologically as colour. As such there are frequencies that are directly perceived and many that are not.

That electromagnetic signals generated by modern technology can influence subtle changes in physiology has been explored extensively. Psychological phenomena such as the 'sensed presence', 'out-of-body experience' and pain diminishment have all been demonstrated to be influenced by application of weak-intensity physiologically-patterned magnetic fields (Saroka and Persinger, 2013; Persinger et al., 2010). Within rural environments 60-Hz power-line frequencies, with electric field intensities ranging between between 10^{-2} - 10^{-4} V/m (König, 1984) depending upon source distance and have discrete harmonics produced according to basic physical principles, and magnetic fields generated by electronics may produce changes in physiology. There have been extensive correlative researches demonstrating that some residents living proximal to powerline generators show increased incidences of leukemia, breast-cancer, and

general malaise and fatigue (Feychting and Ahibom, 1994; Feychting et al., 1998; Kaprio et al., 1997).

From a psychological viewpoint, we have shown that recordings of spoken-words which have been digitized and translated into a magnetic field equivalent can affect decision-making without direct awareness when subjects were asked to select the 'best choice' from a list of words (Healey and Persinger, 1997; Saroka and Persinger, 2011). Such simple, and perhaps subliminal, effects may be a product of brain function; it is well known that only 5% of connective fibers within the brain are associated with external sensory stimuli with the majority of 90-95% originating to and terminating within the cerebral cortices (Nunez, 1995). From a more holistic perspective, that would mean that 90-95% of the information processing within the brain is focused internally.

We have seen that disturbances within the earth's electromagnetic environment are correlated with disturbances in brain function. In a study published by Mulligan et al (2010), theta-band spectral density occurring within the right frontal cortices was elevated during times of geomagnetic storms. The same authors later found that when geomagnetic storms were simulated using devices which produce electromagnetic fields, there was an enhancement of low-frequency range activation within the brain after 15-20 minutes of continuous application (Mulligan and Persinger, 2012). We have also seen that disturbances in geomagnetic activity are also associated with changes in the coherence between the two temporal lobes. The magnitude of the coherence during these times was remarkably similar to that observed in an experiment which involved the encouragement of the sensed presence (Saroka et al., 2013).

The purpose of this study was to discern if brain activity of normal healthy individuals sitting quietly with their eyes closed show changes in brain activity that are correlated with crude measurements of the background AC-magnetic field occurring within the environment recorded simultaneously.

4.2 Methods and Materials

Participants

Participants were 4 healthy volunteers (1 male, 3 females) who were recruited from the laboratory. Each subject was asked to sit in a comfortable chair housed in an acoustic chamber which also served as a Faraday cage. Each subject was asked to remain seated with their eyes closed for 2-minutes.

Data Acquisition

Brain activation was monitored using a Mitsar-201 amplifier (sampling rate=250Hz) fitted with a 19-channel Electro-Cap that was placed on the heads of the participants. Electro-Gel was used to bridge contact between the scalp and the surface of the sensors in each channel. Voltages recorded from the cap were translated from analog-to-digital and were ultimately recorded and viewed on a Dell Inspiron laptop equipped with WinEEG v.2.82 software. The data was saved for further analysis within the MATLAB platform.

AC-generated electromagnetic activity was measured with an Alpha-Lab Milligauss meter. The milligauss meter was placed approximately 2-5 cm behind the heads (occipital notch) of each participant. Data was fed from the milligauss meter to an Apple Macbook equipped with Audacity recording software via coaxial cable. Data was recorded at a sampling rate of 250Hz and was later saved as a *.WAV file for further analysis within MATLAB software.

Signal Processing

All milligauss recordings were imported into MATLAB for processing and spectral analyses. The 120-second long records pertaining to each of the 4 participants was divided into 4-second segments. Consequently there were 30 observations available for each participant. The records were then submitted to a spectral analysis available within the EEGLab toolbox. The spectopo.m (Delorme and Makeig, 2004) function was used to generate discrete spectral densities within frequencies ranging from 1-50Hz. This spectral data was then saved and imported into SPSS for further statistical analysis with measures of brain activity.

The brain activity recorded with the QEEG was also imported into MATLAB. Each 120-second measurement was divided into 30x4-second chunks and re-filtered using a band-pass filter of 1.5-40Hz. Within MATLAB, coherence between the left anterior (T3) and right anterior (T4) as well as the left posterior (T5) and right posterior (T6) channels was calculated according to previously defined methods using the coherence.m function. The mean of the coherence values between the 7 and 10-Hz was computed and saved for later statistical analysis.

The same raw segments of EEG data were also used in a source localization analysis (Pascual-Marqui, 2002) to predict activity within the parahippocampal region. All data was imported into sLORETA and processed according to standard and previously-used techniques. The current source densities ($\mu\text{A}/\text{mm}^2$) within the classical frequency bands (delta, theta, low-alpha, high-alpha, beta-1, beta-2, beta-3 and gamma) were then saved and imported into the SPSS database already containing inferences of the background AC-magnetic field as well as the coherence.

Finally, topographies and microstate descriptors of the brain's electric field were computed using freely available MapWin software. All data was imported and re-filtered between 2-20Hz according to standard procedures (Koenig et al., 1999). Next, the microstate topographies for each of the segments were computed separately using the "Construct Microstates" function within the software without pre-standardized clustering. Next average clusters were then computed for each participant separately using the 30 available epochs. The resultant participant-specific clusters were then combined into a grandmean set of clusters and re-arranged according to the topographies published by Lehmann and Koenig. This resultant topographical template was then applied to each segment of each participant separately; descriptive microstate descriptors (i.e. duration, occurrence, coverage) were then computed separately, saved, and imported into the SPSS database.

Once all data (i.e. spectral analyses of background EM and QEEG descriptors) was consolidated, statistical analyses was performed on within-subject z-scored normalized derivations through Pearson and Spearman correlation analyses and linear multiple regression. For the dataset, a total of 120 cases (30 for each participant) were available.

4.3 Results

A linear stepwise multiple regression predicting mean 7-10Hz coherence from the spectral densities of the background EM revealed a significant ($R=.46$, $p<.05$) relationship. The frequencies of the spectral densities predicting the coherence were approximately 13, 19.5, 27 and 46Hz. The saved predicted scores were then entered into separate Spearman-rank correlational analyses separately for each individual. The correlations were significant across the sampled population. Results of the analysis can be seen in Figure 4.1.

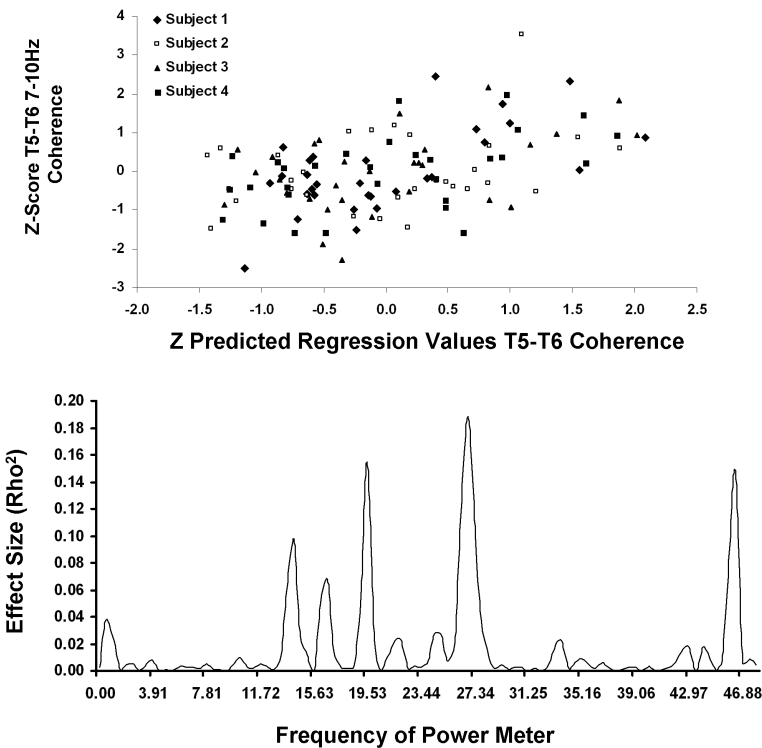


Figure 4.1 (Top) Scattergram depicting the correlation between left (T5) and right (T6) posterior temporal lobe coherence with regression score comprising (Below) predicted power meter spectral densities for frequencies comparable to harmonics of the Schumann resonance.

A separate linear stepwise linear regression was then performed predicting left-theta (4-7Hz) parahippocampal activity. The results of the analyses revealed that left-theta activity was significantly ($R=.45$) predicted by a linear combination of primarily 7.81Hz and ~ 40 Hz electromagnetic spectral densities occurring in the environment around the participant's occipital region. To insure that this correlation was not driven by one participant, separate Spearman rank-order correlations between the saved regression predicted scores and left-theta parahippocampal activity were performed. All correlations ($N=30$ for each) were significant and the results are depicted in Figure 4.2.

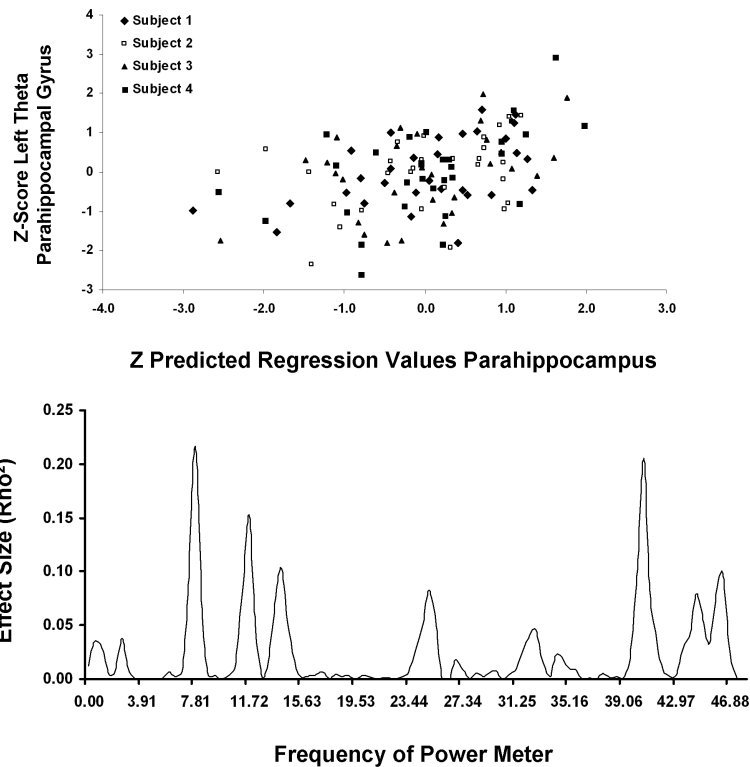


Figure 4.2 (Top) Scattergram depicting the correlation between left parahippocampal theta current source density with regression score comprising (Below) predicted power meter spectral densities for frequencies comparable to harmonics of the Schumann resonance. Note the elevated peaks at around 7.8 and 40 Hz.

A final stepwise linear multiple regression was performed to predict mean microstate disturbance from EM spectral densities occurring in the environment. Microstate disturbance is defined here as the standard deviation between the occurrences of each of the 4 classes of microstates. Hence, a greater disturbance score would indicate that one or more microstate classes occurred more frequently. The analysis revealed a significant relationship ($R=.527$, $p<.05$) existed and that microstate disturbance could be predicted from a linear combination of the EM spectral densities

occurring at 46, 40, 10 and 44Hz. The relationship was significant for each subject individually and is plotted in Figure 4.3.

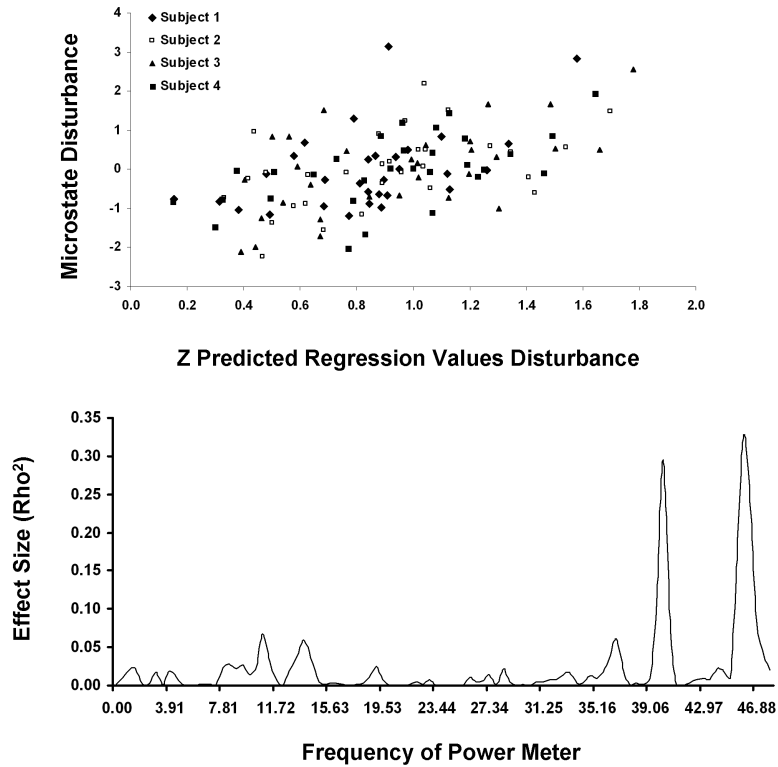


Figure 4.3 (Top) Scattergram depicting the correlation between microstate disturbance with regression score comprising (Below) predicted power meter spectral densities for frequencies comparable to harmonics of the Schumann resonance. Note the elevated peaks at around 40 and 46 Hz.

4.4 Discussion and Conclusion

The results of this study suggest that AC-electromagnetic activity occurring within the proximal environment of an individual is associated with various measurements of brain activity. In general, brain measurements presented here tended to be highly correlated with AC-electromagnetic frequencies comparable to the fundamental and eigenfrequencies of the Schumann resonance.

First, we found that 7-10Hz left-right temporal coherence was positively correlated with the electromagnetic intensity of frequencies around 20 and 27Hz. In a previous study, we observed that coherence between the left and right was elevated during times of geomagnetic storms (Saroka et al., 2013). We have also observed coherence magnitudes increases within the bilateral temporal regions increase ~10-15 minutes after the application of a frequency-modulated electromagnetic pattern for individuals who experienced a sensed presence (Saroka and Persinger, 2013).

Second, left parahippocampal activity was associated primarily with 7 and 40Hz activity occurring within the environment. This region is strongly associated with the encoding of memory because of its central location in receiving information from widespread cortical areas (Powell et al., 2004). That the left and not the right parahippocampal region was sensitive to these Schumann frequencies may be accommodated by its role in verbal encoding. For example Wagner and colleagues (1998) demonstrated that higher recall of verbal information is associated greater increases in fMRI bold activation within the left parahippocampal region. If the data presented above is applicable, then subtle changes in the electromagnetic environment could affect the consolidation of verbal information and thus influence the trajectory of future experiences of an individual.

Finally, we found that the topography of the brain's electric field was correlated with activity specifically with frequencies almost identical to the 5th and 6th harmonics of the Schumann resonance (Balsler and Wagner, 1960). Specifically, we found that 40Hz and 45Hz background electromagnetic activity was strongly correlated with displacements in the distribution of the occurrence of microstate classes. These frequencies are a candidate for the 'binding factor' suspected to consolidate all sensory

and cognitive information into a percept. Recurrent 40-Hz oscillations occurring between the thalamus and the cortex have been measured by Llinas and Ribary (1993), who also demonstrated that these gamma oscillations are also present during REM sleep when an individual is dreaming. If consciousness is considered to be highly correlated with electric, and by Faraday induction, magnetic fields the data may suggest that other extracerebral sources of information may play a stronger role in a person's experiences than previously suspected. Because the energies and frequencies for both the environment and the human brain are comparable it is unclear in which direction one is affected by the other or whether they are simultaneously affected by a third factor.

It is unclear whether the Schumann resonance generated naturally by the earth was associated with the measurements presented in this chapter. Using the same milligauss meter, we have measured an enhancement of Schumann frequencies at Agawa Provincial Park situated on Lake Superior. This special location contains rock art produced by indigenous peoples approximately 400 years ago. This recorded Schumann profile was not observed overtly within other locations around Lake Superior; however when calibration curves were calculated to discern the intensities at these Schumann peaks we found that they were within nanoTesla range, or about 1000 times that measured routinely by other investigators (Davis, 1995). While others have measured Schumann intensities within nanoTesla range, it is still uncertain whether the findings presented here are artifacts of the 60Hz power-line harmonics or other anomalous human-made signals.

Whether the measured AC-electromagnetic field is a reflection of processes produced by the earth, or whether they were generated by human intervention, the data suggests that the brains of individuals have a natural proclivity to synchronize with

frequencies similar to the Schumann Resonance. This may not be surprising given that biological systems developed in an environment where its presence is strong and that it occurs predominantly within caudal aspects of the brain during periods of eyes closed relaxation. The results may have special importance when one considers that the sub-harmonic frequencies of 60-Hz power lines extend well into frequencies resonant to the brain itself, including 10-Hz. Such findings may warrant re-consideration of the optimal frequencies of power-line transmission to minimize adverse human health effects.

4.5 References

- Balser, M., & Wagner, C. A. (1960). Observations of Earth-ionosphere cavity resonances. *Nature*, 188(4751), 638-641.
- Davis, D. (1995). Schumann resonances. *Handbook of atmospheric electrodynamics*, 1, 267.
- Delorme, A., & Makeig, S. (2004). EEGLAB: an open source toolbox for analysis of single-trial EEG dynamics including independent component analysis. *Journal of neuroscience methods*, 134(1), 9-21.
- Feychting, M., & Ahlbom, A. (1994). Magnetic fields, leukemia, and central nervous system tumors in Swedish adults residing near high-voltage power lines. *Epidemiology*, 5(5), 501-509.

- Feychting, M., Forssén, U., Rutqvist, L. E., & Ahlbom, A. (1998). Magnetic fields and breast cancer in Swedish adults residing near high-voltage power lines. *Epidemiology*, 9(4), 392-397.
- Healey, F.Y., Persinger M.A., Koren, S.A. (1997). Control of 'choice' by application of the electromagnetic equivalents of spoken words: Mediation by emotional rather than linguistic dimensions? *Perceptual and Motor Skills*, 85(3f), 1411-1418.
- Llinas, R., & Ribary, U. (1993). Coherent 40-Hz oscillation characterizes dream state in humans. *Proceedings of the National Academy of Sciences*, 90(5), 2078-2081.
- Kaprio, J., Varjonen, J., Romanov, K., Heikkilä, K., & Koskenvuo, M. (1997). Magnetic fields of transmission lines and depression. *American journal of epidemiology*, 146(12), 1037-1045.
- Koenig, T., Lehmann, D., Merlo, M. C., Kochi, K., Hell, D., & Koukkou, M. (1999). A deviant EEG brain microstate in acute, neuroleptic-naive schizophrenics at rest. *European archives of psychiatry and clinical neuroscience*, 249(4), 205-211.
- König, H. L., Krueger, A. P., Lang, S., & Sönning, W. (2012). *Biologic effects of environmental electromagnetism*. Springer Science & Business Media.
- Mulligan, B. P., Hunter, M. D., & Persinger, M. A. (2010). Effects of geomagnetic activity and atmospheric power variations on quantitative measures of brain activity: replication of the Azerbaijani studies. *Advances in Space Research*, 45(7), 940-948.

- Mulligan, B. P., & Persinger, M. A. (2012). Experimental simulation of the effects of sudden increases in geomagnetic activity upon quantitative measures of human brain activity: validation of correlational studies. *Neuroscience letters*, 516(1), 54-56.
- Nunez, P. L., & Cutillo, B. A. (Eds.). (1995). *Neocortical dynamics and human EEG rhythms*. Oxford University Press, USA.
- Pascual-Marqui, R. D. (2002). Standardized low-resolution brain electromagnetic tomography (sLORETA): technical details. *Methods Find Exp Clin Pharmacol*, 24(Suppl D), 5-12.
- Persinger, M. A., Saroka, K. S., Mulligan, B. P., & Murphy, T. R. (2010). Experimental elicitation of an out of body experience and concomitant cross-hemispheric electroencephalographic coherence. *NeuroQuantology*, 8(4).
- Saroka, K. S., Caswell, J. M., Lapointe, A., & Persinger, M. A. (2014). Greater electroencephalographic coherence between left and right temporal lobe structures during increased geomagnetic activity. *Neuroscience letters*, 560, 126-130.
- Saroka, K. S., & Persinger, M. A. (2011). Detection of electromagnetic equivalents of the emotional characteristics of words: implications for the electronic-listening generation. *Open Behavioral Sciences Journal*, 5, 24-27.
- Saroka, K. S., & Persinger, M. A. (2013). Potential production of Hughlings Jackson's "parasitic consciousness" by physiologically-patterned weak transcerebral

magnetic fields: QEEG and source localization. *Epilepsy & Behavior*, 28(3), 395-407.

Powell, H. W. R., Guye, M., Parker, G. J. M., Symms, M. R., Boulby, P., Koepp, M. J., ... & Duncan, J. S. (2004). Noninvasive in vivo demonstration of the connections of the human parahippocampal gyrus. *Neuroimage*, 22(2), 740-747.

Wagner, A. D., Schacter, D. L., Rotte, M., Koutstaal, W., Maril, A., Dale, A. M., ... & Buckner, R. L. (1998). Building memories: remembering and forgetting of verbal experiences as predicted by brain activity. *Science*, 281(5380), 1188-1191.

Chapter 5

Quantitative Convergence of Major-Minor Axes Cerebral Electric Field Potentials and Spectral Densities: Consideration of Similarities to the Schumann Resonance and Practical Implications

Published in Plos One

Co-Authors: David E. Vares, Michael A. Persinger

4.1 Introduction

One of the basic assumptions of modern Neuroscience is that ultimately all of the qualitative features of the ephemeral cognitive processes such as thinking and consciousness will be interpretable as quantitative configurations (Wackermann, 1999) of the complex temporal patterns of electromagnetic values that can be measured from the surface of the human cerebrum. The similarity of average duration of microstates and the duration of the human percept is an example of such transformation of perspective. The clever consideration (Lehmann et al, 1995; 1998) that four microstates (Koenig et al, 2002) could reflect functional cognitive units or “atoms of thought” that are the information within the stream of dynamic process within cerebral space, analogous to base nucleotide pairs for genetic information within DNA sequences, exemplifies the significance of this approach. The shift towards biophysical analyses (Johnson, 1980; Nunez, 1995; Balazsi and Kish, 2000; Park and Lee, 2007; Persinger and Lavallee, 2012) of complex cerebral functions once relegated to the domain of the philosopher and psychologist requires a verification of the physical parameters for these operations. Here we reiterate and report validation of quantitative phenomena that define the electric and

potentially magnetic features of our primary inferential measurement: quantitative electroencephalography (QEEG).

Our approach is that the human cerebrum is a functional, dynamic dipole whose voltage, or potential difference, is reflected as more or less steady-state potentials in the order of 10 to 30 mV (Rowland, 1967) and extremely low frequency time-varying components whose average intensities are about three orders of magnitudes less (μV range). Because the human cerebral volume is not a sphere but more typical of an ellipsoid there should be a slight difference in average μV intensity that reflects this ratio. The relatively fixed volume and surface area of the cerebrum and rostral-caudal bulk velocity of $\sim 4.5 \text{ m}\cdot\text{s}^{-1}$ should generate constant standing waves (Nunez, 1995; Persinger and Lavallee, 2012) with parameters much like the fundamental Schumann resonance of ~ 7.5 to 8 Hz (Campbell, 1967; Polk, 1982; Koenig et al, 1981; Schlegel and Fullekrug, 1999) which is the resonance solution for the velocity of light ($3\cdot 10^8 \text{ m}\cdot\text{s}^{-1}$) and the earth's fixed circumference ($4\cdot 10^7 \text{ m}$). The Schumann resonances were likely present during the origin of living systems (Persinger, 1974). The precision of the verification of measurement of QEEG data is important for developing models and extending physical interpretations of brain function.

4.2 Materials and Methods

Subjects

The subjects in this study were 184 individuals, measured singly, who had participated in various experiments within the laboratory between 2009 and 2013. Some subjects were measured more than once so that the total numbers of records were 238.

As part of the laboratory protocol, eyes-closed measurements were collected at the beginning of each experiment before testing. The majority of the individuals included in this study were university students between 19 and 25 years of age. The proportion of men and women were similar. Most measurements were completed within a commercial acoustic (echoic) chamber under dim light conditions.

Equipment and Recordings

Brain electrical activity was monitored using a Mitsar 201 amplifier equipped with a 19-channel Electro-Cap International. Measurements from 19 sites (Fp1, Fp2, F7, F3, Fz, F4, F8, T3, C3, Cz, C4, T4, T5, P3, Pz, P4, T6, O1, O2) consistent with the International Standard of Electrode Placement were obtained. Impedance for all measurements was maintained below 5 kOhms. The data recorded from the amplifier was delivered to a Dell laptop equipped with WinEEG v.2.8 that produced a digital copy of the recorded voltages. Sixteen-second epochs of eyes-closed data were extracted from each participant and exported into MATLAB software for further filtering and processing.

While most data collected with the amplifier were obtained using a sampling rate of 250 Hz, some measurements were collected with a sampling rate of 500 Hz. To insure homogeneity across subjects, data that were collected using a sampling rate of 500 Hz was re-sampled to 250 Hz using the resample function within the MATLAB platform. The data for each subject was then filtered between 1.5 and 40 Hz using the

eegfiltfft.m function within the freely available EEGLab toolbox (Delorme and Makeig, 2004). Once filtered, the data were submitted to spectral analysis, using the spectopo.m function, which computed spectral density within discrete frequencies for the Fp1 O2 T3 and T4 sensors.

These data was then imported into SPSS for further analysis for the computation of mean absolute potential difference along the rostral-caudal (Fp1-O2) axis as well as between the left-right temporal (T3 and T4) sensors. Absolute differences between rostral-caudal and left and right temporal sensors were also obtained by subtracting the absolute raw voltages (independent from spectral density) from the extracted EEG record for each 4-millesecond point interval over 16 seconds.

Random Sample of 10 Brain Measurements

To appreciate the difference between a sub-sample of the total population and the total population, 16 s of QEEG data (Fp1 O2, T3 T4) for 10 subjects were randomly selected using a random number generator. Z-scores for the $\mu V^2 \cdot Hz^{-1}$ values for the rostral-caudal, left-right measures were obtained first in order to minimize individual differences in absolute baseline values. Spectral analyses from SPSS 16 (a different algorithm from the one applied in the previous section) were then applied to each of the two measures for each of the 10 subjects. The frontal spectral density scores were then subtracted from the occipital spectral density scores for each subject. The z-scores for each of these new means were calculated so that there would be a standardized score for these differences to compare directly across individuals. The average values for the two orthogonal measures were calculated.

In order to examine the degree of individual differences of the spectral analyses each subject's results were assessed visually for the peak spectral density within the 10 Hz range. Because the Δf (increment of frequency) within this frequency range for 250 Hz samples is fractional (less than an integer, i.e., about .01 Hz), the bandwidth of the peak spectral density could be inferred. This was discerned by direct inspection of the quantitative values where the decline in z-scores on either side of the peak was conspicuous and greater than 2 standard deviations for the interval.

Discerning the Schumann Resonance Signature

Our approach is that the human cerebrum is a functional, dynamic dipole whose voltage, or potential difference, is reflected as more or less steady-state potentials in the order of 10 to 30 mV (Rowland, 1967) and extremely low frequency time-varying components whose average intensities are about three orders of magnitudes less (μV range). Because the human cerebral volume is not a sphere but more typical of an ellipsoid there should be a slight difference in average μV intensity that reflects this ratio. The relatively fixed volume and surface area of the cerebrum and rostral-caudal bulk velocity of $\sim 4.5 \text{ m}\cdot\text{s}^{-1}$ should generate constant standing waves (Nunez, 1995; Persinger and Lavallee, 2012) with parameters much like the fundamental Schumann resonance of ~ 7.5 to 8 Hz (Campbell, 1967; Polk, 1982; Koenig et al, 1981; Schlegel and Fullekrug, 1999) which is the resonance solution for the velocity of light ($3\cdot 10^8 \text{ m}\cdot\text{s}^{-1}$) and the earth's fixed circumference ($4\cdot 10^7 \text{ m}$). The Schumann resonances were likely present during the origin of living systems (Cole and Graf, 1974).

After re-sampling and re-filtering between 1.5 and 40 Hz for the 184 individuals by `eegfiltfft.m`, the anterior, middle, and caudal root mean square signals were derived from integrating frontal (Fp1,Fp2,F7,F3,Fz,F4,F8), middle (T3,C3,Cz,C4,T4) and caudal (T5,P3,Pz,P4,T6,O1,O2) sensors. These derived signals were spectral analyzed by `spectropo.m` with a window size equal to 2048 FFT points to maximize spectral resolution. Other researchers, e.g., Abeyuriya et al (2014), have recently employed the same approach to discern non-linear harmonics of sleep spindles in human electroencephalographic recordings.

Because of a connection between activity within the parahippocampus and naturally-occurring geomagnetic activity established in a previous publication (Saroka et al, 2013) and its prominent role as an integrator of experience before long-term memory processes within the hippocampus, inferences of left and right parahippocampal current source density ($\mu A \cdot mm^{-2}$) were computed in sLORETA (Pasqual-Marquis, 2002) within the classical frequency bands used in more conventional electroencephalographic studies [i.e. delta (1.5-4 Hz); theta (4-7 Hz); low-alpha (7-10 Hz); high-alpha (10-13 Hz); beta-1 (13-20 Hz); beta-2 (20-25 Hz); beta-3 (25-30 Hz); gamma (>30 Hz)].

The same epochs of electroencephalographic activity used in the sLORETA analyses were also imported into MapWin software (Koenig et al, 1999) for the computation of microstates and their related parameters (i.e. duration of microstate, occurrence of microstate class, etc.). During importation into MapWin, all epochs of QEEG observations were filtered digitally between 2-20 Hz, according to standard techniques. Average clusters of microstates were produced from 4x4-second epochs were produced for each individual. The resultant clusters (maximum=4) were then entered into a built-in cluster analysis that produced 4 topographical maps explaining

approximately 72% of the variance with topologies almost identical to those produced in the original publication by Koenig et al (2002). Finally, all data derived from the different softwares were integrated into an SPSS database for statistical analyses.

5.3 Results

Differential Potential Differences

The means for the μV^2 for global frequencies between the rostral-caudal (RC) axis and the left-right (LR) temporal lobe for the 177 records available for this study are shown in Figure 1. For this analysis, we only selected individuals whose z-score was within +/- one standard deviation from the mean. The amount of shared variance (r^2) was 67% (i.e., $r=0.82$). The square root of the two mean values was 3.89 μV and 3.05 μV , respectively, or a major (RC)-to-minor (LR) axis ratio of 1.27. According to Blenkov and Glazer (1968) the mean rostral-caudal length of the cerebrum is 172.5 mm (155-190 mm) while the RL length is 136 mm (131-141). The ratio is 1.27. Consequently the average disparity of potential difference between the two axes reflects the proportional distance between the sensors. The scattergram displaying the correlation between the discrete quantitative values for the RC and LR measurements is shown in Figure 2.

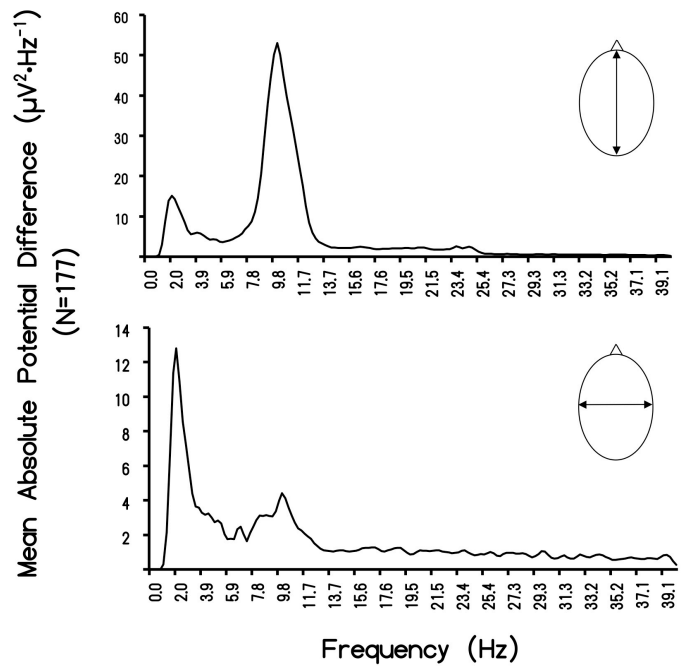


Figure 5.1 Absolute potential difference ($\Delta\mu\text{V}^2\cdot\text{Hz}^{-1}$) plotted as a function of frequency for the rostral-caudal and left-right measurements during QEEG for 177 subjects measured over a three year period

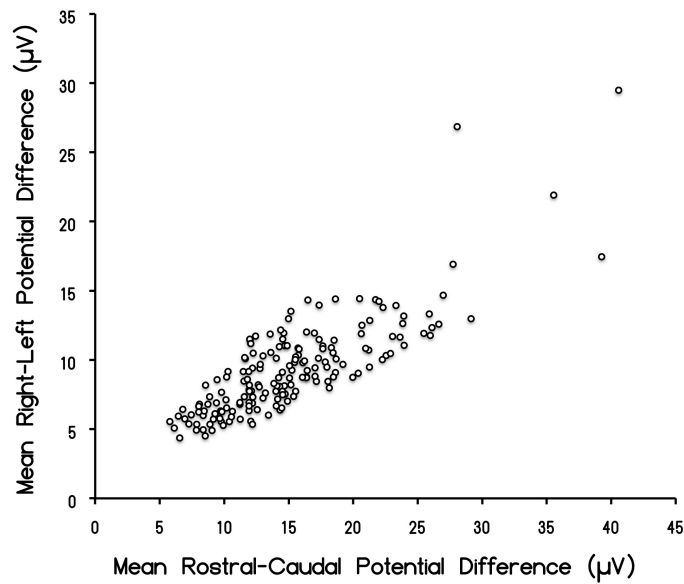


Figure 5.2 Scattergram of the correlation ($r=0.82$) between the discrete potential difference values for the caudal-rostral vs left-right potential differences.

Results of Random Sample (n=10) Analyses

The correlation of the voltage values between the RC and LR axes for the 10 subjects was $r=0.88$. Because the values were $\mu V^2 \cdot Hz^{-1}$, square root values were obtained for the FC value ($3.71 \pm 0.76 \mu V$) and RL ($2.88 \pm 0.47 \mu V$). The ratio was 1.29, compared to the ratio of 1.27 for the entire sample. The distributions of the spectral density profiles for the major and minor axes of the human cerebra in our sample are shown in Figure 3. The classic peak around 10 Hz, with the majority of the power within the area of the curve between ~ 7 Hz and 13 Hz, is evident. The mean for this population was 10.25 Hz. Although the later peak was evident for the minor (LR) axis, most of the power density for the LR axis was around 2 Hz (1.95 Hz) with a more leptokurtic boundary within the delta band. The primary beat (difference) frequency was 8.3 Hz.

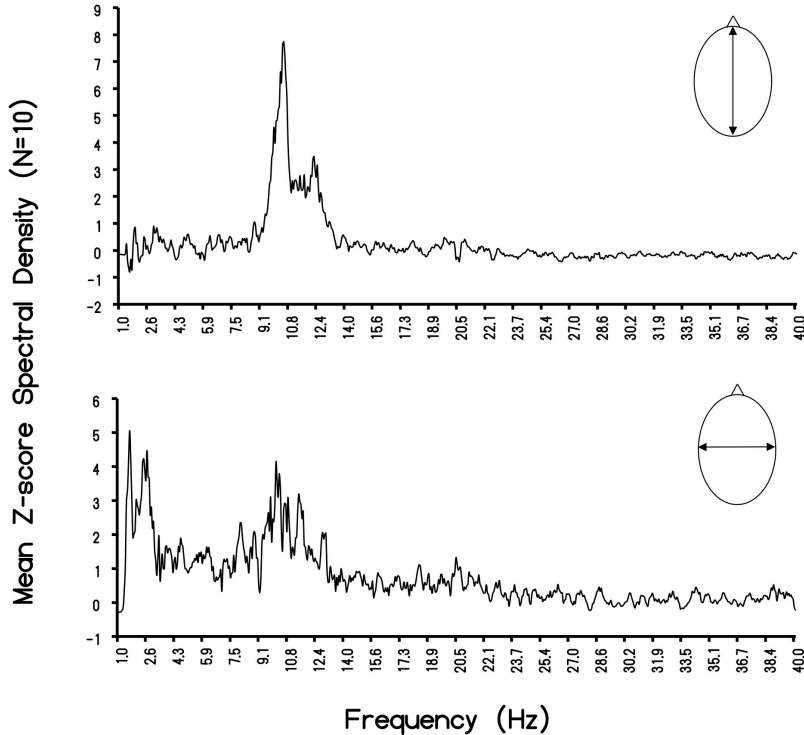


Figure 5.3 Means of the z-scores of the spectral density ($\mu V^2 \cdot Hz^{-1}$) of the measurements as a function of frequency for the rostral-caudal and left-right measurements.

More detailed examination of the power spectra for the 10 randomly sampled records employed to verify RC-LR differences in voltage revealed potentially relevant individual variability. Employing the peak z-range obtained from each of the increments of frequency from the spectral analyses, the mean peak was 10.12 Hz for the RC and 2.44 Hz for the LR axis. The primary beat (difference) was 7.7 Hz. The results of analyzing the “width” of the peak in spectral power densities are shown in Table 1 for each of the 10 subjects. The mean duration of the “peak band width” was 0.39 Hz.

Table 5-1 Range of the standardized (z-score) for the raw spectral density values for the peak band (in Hz) for the 10 randomly selected subjects. The “band width” for the peak band range is also shown.

Subject	Z-range	Peak Band (Hz)	Band Width (Hz)
1	12-14	11.43-11.68	0.25
2	10-14	10.18-10.75	0.57
3	8-14	10.31-10.50	0.19
4	10-11	12.18-14.43	0.25
5	3-6	10.51-11.31	0.80
6	9-19	10.31-10.68	0.37
7	15-18	10.43-10.68	0.25
8	2-4	11.00-11.37, 11.75-12.5	0.37, 0.75
9	6-19	9.75-10.18	0.43
10	9-15	11.93-12.31	0.38

The Schumann Resonance Signature

A spectral distribution comparable to the Schumann resonances recorded from the earth was observed with peak frequencies centering at approximately 7.5 Hz, 13.5 Hz and 20 Hz within the global QEEG power for 237 records. One outlier (with a $z > 10$) was removed. A 3-D plot showing the distribution of each individual's spectral profile for the caudal aspect is displayed in Figure 4.

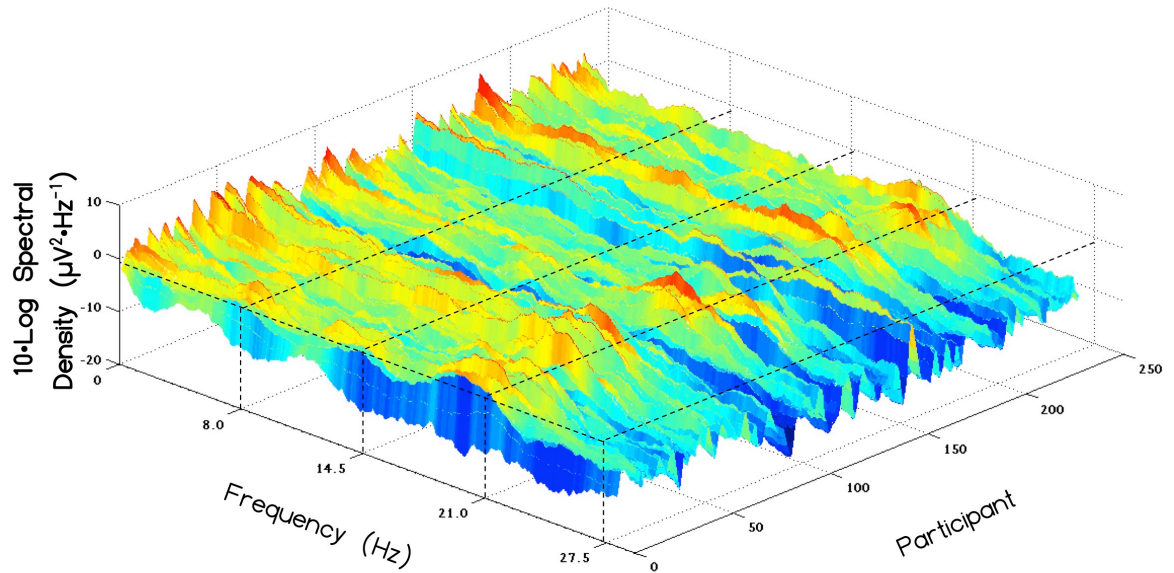


Figure 5.4 Log of spectral density of various frequencies reflecting the Schumann resonance for all 237 records.

We reasoned that if this resonance pattern within the human brain was normally distributed, certain individuals should show elevations in the spectral density of the Schumann resonance. Thus, we computed a measure of Schumann intensity by multiplying the spectral density of the mean of 7-8 Hz, 13-14 Hz and 19-20 Hz spectral densities. This value was then cube rooted for each signal (i.e. rostral, middle and caudal) separately. The average of the rostral, middle and caudal Schumann intensities was computed and then categorized into one of 3 groups based upon the between-subject z-scores. The groups were low ($z < -0.5$), medium ($-0.5 < z < 0.5$) and high ($z > 0.5$). This classification resulted in 19 individuals within the low group and 34 individuals within the high group; the rest of the individuals were within the medium group.

When the discrete spectral scores for each group were averaged (across individuals within a given group) and graphed, there were qualitative differences in the

definition of the spectral profiles. Whereas the low group could be described as "flat", the high group showed peaks and valleys more characteristic of standing waves of 7.18 Hz, 13.52 Hz and 20.29 Hz. The transformed difference for the high and low group was $\sim 1 \mu\text{V}$ and $0.3 \mu\text{V}$ per Hz, respectively. The peak to trough difference at the 20 Hz peak for the high spectral density group would be about $2 \mu\text{V}^2 \cdot \text{Hz}^{-1}$.

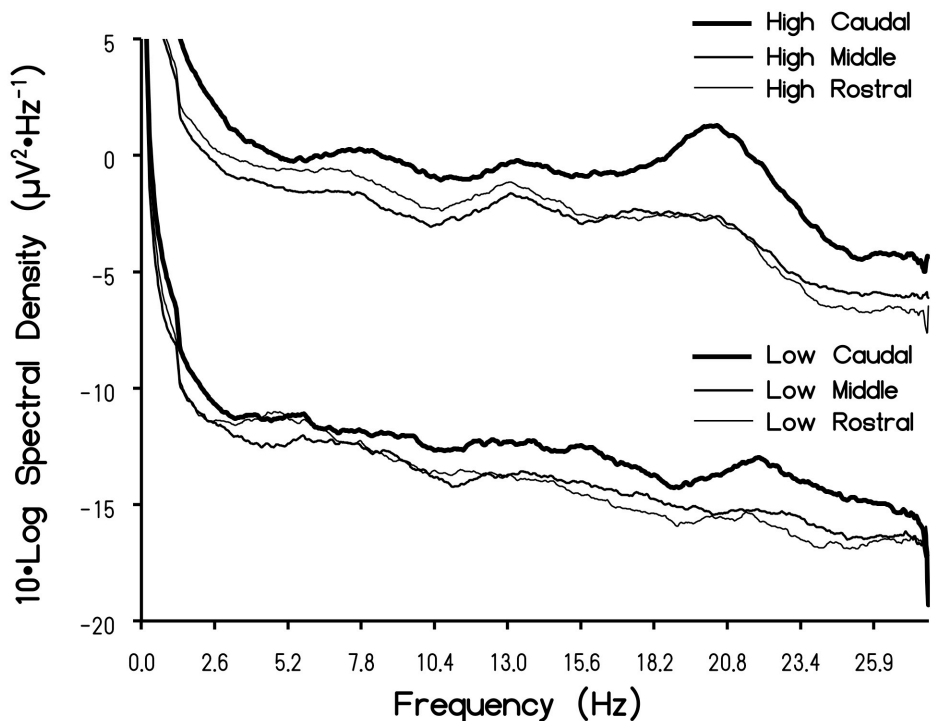


Figure 5.5 Mean Log value of the spectral density for high and low intensity subjects as a function of frequency for the rostral, middle, and caudal regions of the cerebrums. Note the peaks at the fundamental Schumann resonance (first harmonic) as well as the second (about 14 Hz) and third (about 20 Hz) harmonics.

When the rostral, caudal and middle signals for this group for the high and low intensity group were smoothed according to frequency (with a period of approximately 1Hz) and graphed, the spectral distributions were remarkably similar to those observed

from the earth, with particular enhancements within the caudal signal for the high-intensity group (Figure 5).

Selected Associations Between the Schumann Resonance Signature with Other Measures of Brain Activity

Given the remarkable rhythmic character of the subthreshold oscillation of ~8 Hz for stellate cells in Layer II of the entorhinal cortices (Alonso and Klink, 1993) and the importance of this region for receiving convergent inputs from the entire cortical manifold before their distribution to the hippocampal formation and amygdala, we specifically investigated the parahippocampal region by sLORETA. Separate one-way analyses of variance for the left and right parahippocampal current source densities within the pre-defined frequency bands with Schumann intensity (low, medium, high) as a between-subject factor indicated that there was significantly ($p < .001$) more current source density within the bilateral parahippocampus across most frequency bands for individuals who displayed high Schumann resonance intensities. The strongest effects were observed within the theta and gamma frequency ranges within the left hemisphere. The relationship appeared linear which suggested that as the endogenous Schumann Resonance intensity increased the activity in the left parahippocampus increased. These results are shown in Table 2.

Table 5-2 Means and Standard Errors of the Means (in parentheses) for current source density ($\mu\text{A}\cdot\text{mm}^{-2}$) of the parahippocampal gyrus within the classical frequency bands.

	Left					Right				
	Low	Medium	High	Significance	Effect Size	Low	Medium	High	Significance	Effect Size
Delta	737 (67)	1412 (81)	1999 (257)	<.01	0.06	678 (64)	1563 (112)	1856 (230)	0.02	0.04
Theta	122 (11)	341 (22)	866 (147)	<.01	0.19	115 (9)	408 (35)	897 (150)	<.01	0.12
Low-Alpha	188 (38)	1005 (90)	2710 (642)	<.01	0.12	149 (26)	1277 (116)	2888 (495)	<.01	0.13
High-Alpha	238 (54)	847 (71)	1435 (158)	<.01	0.09	279 (77)	951 (82)	1988 (272)	<.01	0.12
Beta-1	352 (50)	619 (40)	1134 (117)	<.01	0.12	345 (50)	667 (44)	1206 (142)	<.01	0.11
Beta-2	189 (49)	248 (26)	452 (62)	0.004	0.05	166 (32)	285 (37)	429 (45)	0.11	0.02
Beta-3	589 (224)	512 (93)	1188 (421)	0.050	0.03	471 (174)	499 (74)	918 (206)	0.08	0.02
Gamma	2649 (319)	5783 (280)	11356 (1088)	<.01	0.23	2419 (239)	6608 (350)	12004 (893)	<.01	0.20

We also decided to explore this categorization of Schumann intensities within the context of microstate topographies, which may be considered as geometric shapes of the electric field (and by association magnetic field) produced by constructive and destructive interference processes. A one-way analysis of variance indicated that the model described by Koenig and Lehmann of the four microstate clusters explained significantly more variance ($F_{2,234}=22.89$, $p<.001$, Ω^2 estimate=.16) in brain topographical patterns within individuals who displayed “strong” Schumann resonances. These results are shown in Figure 6.

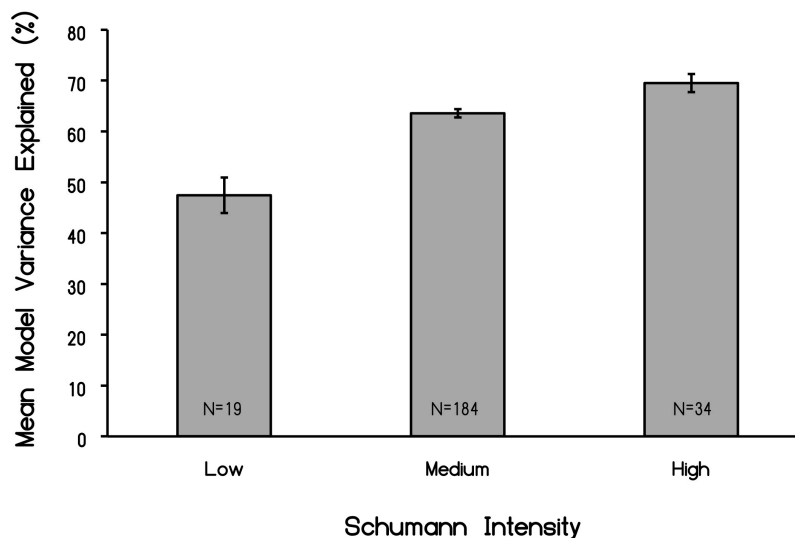


Figure 5.6 Variance explained of all classic microstates as a function of the intensity of the Schumann resonance (first three harmonics) within the EEG. N indicates numbers of records per post hoc group.

5.4 Discussion

Our results confirm and extend the results of relatively large samples of human brains from other researchers (e.g., Nunez, 1995). The absence of statistically significant differences between the strengths of the correlations of power between the RC and LR comparisons and their ratios of power for the total sample and the random sub-sample of 10 subjects indicates the robust nature of these relationships. The precision of the ratio of the physical differences in RC and LR distances of a population of adult cerebrums and the differences in the power densities of electrical activity support our disciplines assumption that the amplitude of QEEG activity is a physical reflection of potential difference (voltage).

Quantitative Inference of Cerebral Magnetic Field Strength

We reasoned that if the cerebral and earth-ionospheric resonances shared some characteristic that could allow potential interaction, some variant of “diffusivity” should be involved. Magnetic diffusivity, $\eta = (\mu_0 \sigma)^{-1}$, where μ_0 is magnetic susceptibility ($4\pi \cdot 10^{-7} \text{ N} \cdot \text{A}^{-2}$) and σ = electrical conductivity, is a concept relevant to geophysical (Ryskin, 2009) and neurophysical phenomena. Assuming the average resistivity of $2 \text{ } \Omega \cdot \text{m}$ ($\sigma \sim 0.5 \text{ S} \cdot \text{m}^{-1}$) for extracellular fluid, and the average potential difference of $3 \text{ } \mu\text{V}$, the resulting estimate for the magnetic field strength is $(3 \cdot 10^{-6} \text{ kg} \cdot \text{m}^2 \cdot \text{A}^{-1} \cdot \text{s}^{-3})$ divided by $1.58 \cdot 10^6 \text{ m}^2 \cdot \text{s}^{-1}$ or $\sim 1.9 \cdot 10^{-12} \text{ T}$, that is about 2 picoTeslas (pT). This is well within the range based upon direct measurement from of action potentials from isolated frog sciatic nerves at distance of 1 mm (Wikswow et al, 1980) as well as the typical intensities of Schumann resonances. The spatial domain is sufficiently large to have major influence upon the integrated cerebral field. This magnitude is within a factor of 10 of the transient magnetic oscillatory

response (Pantev et al, 1991) evoked in the human cerebrum, with a peak near 10 Hz and 30-40 Hz, when the measured values in $20 \text{ fT}\cdot\text{Hz}^{-1/2}$ are applied over the full frequency range of 100 Hz.

Although these intensities appear small, experimental application of pT, spatial and temporally-patterned magnetic fields have been reported to produce discernable improvement in some clinical disorders, such as Tourette's and multiple sclerosis (Sandyk, 1995; 1997) as well as some electrical foci associated with partial seizures (Anninos et al, 1991). Correlative responses associated with subjects' experiences have been associated with geomagnetic changes in the order of $\text{pT}\cdot\text{s}^{-1}$ (Booth et al, 2005). The latter occurred when ambient geomagnetic changes displayed progressive increases at this rate over an approximately 15 min interval.

Comparisons with the Fundamental Schumann Resonance and Interhemispheric Beats

It may be relevant that the recondite "beat" (the difference between the frequencies) between the rostral-caudal and left-right power peaks was between 7 Hz and 8 Hz, the range of the fundamental (first harmonic) of the Schumann resonance. This compliments the more global QEEG emergence of the first, second and third harmonics when a different method of analysis was employed. The intrinsic resonance frequency" mediated through the "external shell" of the cerebral cortices (Persinger and Lavalley, 2012) is also within this interval. Precise frequencies in this range can be important. For example Harmony (2013) found that 7.8 Hz power within the frontal lobes decreased in adults but increased in children during a task that emphasized short-term memory.

Resonances often arise in a cavity with sharp, homogeneous, and isotropic boundaries. The Schumann resonances, with a fundamental frequency around 7.8 Hz and harmonics around 14.1, 20.3, 26.4, and 32.5 Hz (Campbell, 1967), are generated within the approximately 100 km earth-ionospheric cavity. The higher modes (harmonics) are separated by ~ 6 Hz according to the general formula $f_n = f_1 [(n(n+1))]^{1/2}$ although some authors include geometric coefficients. Primary origins of the energy are attributed to global lightning activity (Persinger, 2012). The typical median value for the electric field is $\sim 1 \text{ mV m}^{-1}$ while the magnetic field strengths are in the order of 1 pT. At the lowest mode, around 8 Hz, the attenuation is ~ 1 db per 2000 km (Polk, 1982). The significance of these “weak amplitudes” become salient to neuroscience when one realizes that the potential differences involved with reconnection of flux lines within the geomagnetic field when solar wind energy is transferred into the magnetosphere is actually about $4 \mu\text{V}\cdot\text{cm}^{-1}$ (Phan et al, 2000), which is within cerebral parameters.

Although popular authors emphasize the exactness of the fundamental (first harmonic) frequency, empirical measurements indicate a range that would be significant from a QEEG perspective. For example injections of energies from protons (solar proton events) into the upper atmosphere are followed by systematic increases of between 0.04 to 0.14 Hz above the fundamental (7.5 Hz) and amplitude enhancements of between 0.11 and 0.42 pT relative to the 1 pT background (Schlegel and Fullekrug, 1999). In addition, splitting of Schumann resonances have been measured intermittently for decades (Fraser-Smith and Buxton, 1975). While pursuing the theoretical predictions of Madden et al (1965), Tanahashi (1976) noted doublet and triplet “split” peaks at 7.1, 7.85 and 8.5 Hz for the first mode and 12.4, 13.3, 14.0 and 14.8 Hz in the second mode. Fraser-Smith and Buxton (1975) showed that doublets (8 and 10 Hz) occurred for

several tens of minutes. The amplitudes of these discrete peaks were in the order of 1 or 2 pT·Hz^{-1/2}.

Analyses of global power of 16-second samples of QEEG data from almost 200 subjects over a three-year period indicated that spectral densities exhibited relatively wide-band peaks within the first three harmonics of the Schumann resonance. The origins of these fundamental and harmonic enhancements with the QEEG data cannot be identified at this time. One possibility is that the Schumann peaks may reflect some intrinsic feature of the cerebral space due to the average circumference and bulk velocity (Nunez, 1995; Persinger and Lavallee, 2012) or even a coupling between cerebral and ionospheric frequencies through mechanisms yet to be identified. If the latter condition is valid then intrinsic interactions, most likely intermittent, might occur and could be potentially quantified by near-future QEEG and source-location technology. Transience may define these phenomena within QEEG profiles. In our studies the harmonics were not obvious within single 16-s samples but were clear when aggregates from many subjects were averaged. Interestingly this process is also required to obtain spectral profiles (such as in Figure 5 for brain activity) even with direct environmental measurement of Schumann resonances (Nickolaenko and Hayakawa, 2014). It is also noteworthy that optimal filtering between 1.5-40 Hz was required in order to observe Schumann frequency peaks. When the low-cut frequency was set to below 1.5 Hz or above 3 Hz, the characteristic peaks were not observed. This may indicate that energies represented within the 1.5-3Hz frequency band are crucial in discerning the Schumann resonance within the brain.

Individual Differences

Although the statement that individual differences is the largest source of variance is well known to any first year psychology student, the relevance to electrophysiological measurements was obscured until QEEG became the general tool. If there is intercalation between exogenous sources of Schumann resonances and comparable global cerebral frequencies then quantifying and classifying these features may help explain sensitive populations. The individual differences were remarkable. In Table 1 the z-score for the peak band in the spectral densities for each person are shown. A representation of the 7.5 Hz Schumann line in brain activity would occur in only two of the 10 subjects. Line splitting of the Schumann resonance displays peaks with frequency spacing between ~ 0.2 to ~ 0.6 Hz. This overlaps with the bandwidth of the peak power frequency. That only about 10% to 13% of all brains showed enhancements in the intensity of the Schumann resonance may be useful for defining the characteristics of this subpopulation.

There were also individual differences (or more accurately group differences) for the amount of variance in the four classic microstates as a function of the intrinsic power of the first three harmonics of the Schumann frequencies within the cerebral volume. As the power for these bands increased the percentage of variance explaining the four microstates increased from about 48% to 68%. Or stated alternatively, less of the total variance for the classic microstates was explained for those brains that displayed the lowest Schumann spectral density. This could be interpreted as Schumann power functions like a “homogenizer” by removing “random” or “unique” sources of variation and enhancing the prevalence of the four basic microstates. Considering its global nature, a direct contribution of Schumann resonance-induced power to the proportional

predominance of the four major microstates if they are the building blocks of thought (Lehmann et al, 1998), could potentially affect large numbers of the human species for transient periods.

Potential Interactions Between Human Brain and Schumann Dynamics

Whether or not information from the cerebral volume could be represented within the Schumann volume (or visa versa) has significant philosophical and social implications that QEEG and neuroimaging could soon address. Even relatively complex mathematical solutions suggest that gravity waves would interface with the earth's second harmonic (14 Hz) Schumann resonance (Minakov et al, 1992). The energy associated with the loss or gain of a bit of information according to the Landauer Limit ($2 kT$ where k is the Boltzmann constant and T is temperature) is equivalent to about $2.97 \cdot 10^{-21}$ J, at brain temperature. In comparison, the energy upon a unit charge from the $\sim 2.6 (\pm 0.5)$ mV of stellate cells that occurs within the upper (Layer II) cortical neurons within the entorhinal cortices or parahippocampal region (Alonso and Klink, 1993), which is $4.16 \cdot 10^{-22}$ J would be precisely within this range because this energy is generated about 8 times per second (~ 8 Hz) by the persistent subthreshold oscillations. The stellate cells in the medial entorhinal cortices are involved with convergences of information from the entire cortices and are a primary origin of the perforant path fibers to the dentate gyrus of the hippocampal formation.

Our results indicated that the average current source density within the parahippocampal regions was greatest within the theta and gamma bands for individuals who displayed elevated amplitudes for the three first harmonics of the Schumann

resonance. This may be relevant not only because the “gamma” or “40 Hz” ripples are superimposed upon hippocampal theta oscillations (Buzsaki, 2002). The interconnectedness between hippocampal theta and cerebral cortical gamma activity has been considered an important electrophysiological correlate for the intercalation between neurocognitive processes such as consciousness and memory (Whitman et al, 2013). Theta phase can modify the synchrony or coherence between gamma oscillations originating in multiple regions. It may also be relevant that the hippocampal formation and the parahippocampal regions, particularly within the right hemisphere appear, to be particularly responsive to small changes in geomagnetic activity and experimentally applied fields within the pT range (Booth et al, 2005; Mulligan et al, 2010; Sandyk, 1995; 1997).

One of the basic assumptions of modern Neuroscience is that ultimately all of the qualitative features of the ephemeral cognitive processes such as thinking and consciousness will be interpretable as quantitative configurations (Wackermann, 1999) of the complex temporal patterns of electromagnetic values that can be measured from the surface of the human cerebrum. The similarity of average duration of microstates and the duration of the human percept is an example of such transformation of perspective. The clever consideration (Lehmann et al, 1995; 1998) that four microstates (Koenig et al, 2002) could reflect functional cognitive units or “atoms of thought” that are the information within the stream of dynamic process within cerebral space, analogous to base nucleotide pairs for genetic information within DNA sequences, exemplifies the significance of this approach. The shift towards biophysical analyses (Johnson, 1980; Nunez, 1995; Balazsi and Kish, 2000; Park and Lee, 2007; Persinger and Lavallee, 2012) of complex cerebral functions once relegated to the domain of the philosopher and

psychologist requires a verification of the physical parameters for these operations. Here we reiterate and report validation of quantitative phenomena that define the electric and potentially magnetic features of our primary inferential measurement: quantitative electroencephalography (QEEG) and how their characteristics are shared by a unique pervasive property of the earth-ionosphere cavity.

5.5 References

Alonso A and Klink R (1993) Differential electroresponsiveness of stellate and pyramidal-like cells of medial entorhinal cortex Layer II. *J Neurophysiol* 70:128-143.

Anninos PA, Tsagas N, Sandyk R and Derpapas K (1991) Magnetic stimulation in the treatment of partial seizures. *Int J Neurosci* 60:141-171.

Balazsi G, Kish LB (2000) From stochastic resonance to brain waves. *Phys Lett A* 265:304-316.

Blinkov SM and Glezer II (1968) *The human brain in figures and tables: a quantitative handbook*. Basic Books: N.Y.

Booth JN, Koren SA and Persinger MA (2005) Increased feelings of the sensed presence and increased geomagnetic activity at the time of the experience during exposures to transcerebral weak complex magnetic fields. *Int J Neurosci* 115:1053-1079.

Buzaski G (2002) Theta oscillations in the hippocampus. *Neuron* 33:325-340.

- Campbell WH (1967) Geomagnetic pulsations. In: Physics of Geomagnetic phenomena, Matshushita A and Campbell WA (eds). Academic Press: N.Y., pp 821-909.
- Delorme A and Makeig S (2004) EEGLAB: an open source toolbox for analysis of single-trial EEG dynamics including independent component analysis. *J Neurosci Methods* 134:9-21.
- Fraser-Smith AC and Buxton JL (1975) Superconducting magnetometer measurements of geomagnetic activity in the 0.1- to-14 Hz frequency range. *J Geophys Res* 80:3141-3147.
- Harmony T (2013) The functional significance of delta oscillations in cognitive processing. *Front Integrat Neurosci* 7:Article 83.
- Johnson LC (1980) Measurement, quantification, and analysis of cortical activity. In Martin, I. and Venables, P. H. (eds). *Techniques in Psychophysiology*. John Wiley: N.Y, pp 329-429.
- Koenig T, Lehmann D, Merlo MCG, Kochi K, Hell D, Koukkou M (1999) A Deviant EEG Brain Microstate in Acute, Neuroleptic-Naïve Schizophrenics at Rest. *European Eur Arch Psychiatry and Clin Neurosci* 249:205-211.
- Koenig T, Prichep L, Lehmann D, Sosa DV, Braker E, Kleinlogel H, Ishehart R and John ER (2002) Millisecond by millisecond, year by year: normative EEG microstates and developmental stages. *NeuroImage* 16:41-48.
- Konig HL, Krueger AP, Lang S and Sonnik W (1981) *Biologic effects of environmental electromagnetism*. Springer-Verlag: N.Y.

Lehmann D, Grass P and Meier B (1995) Spontaneous conscious covert cognition states and brain electric spectral states in canonical correlations. *Int J Psychophysiol* 19:41-52.

Lehmann D, Strik WK, Henggeler B, Koenig T and Koukkou M (1998) Brain electric microstates and momentary conscious mind states as building blocks of spontaneous thinking: visual imagery and abstract thoughts. *Int J Psychophysiol* 29:1-11.

Madden T and Thompson W (1965) Low-frequency electromagnetic oscillations of the earth-ionosphere cavity. *Rev Geophys* 3:211-254.

Minakov AA, Nikolaenko AP and Rabinovich LM (1992) Gravitational-to-electromagnetic wave conversion in electrostatic field of earth-ionosphere resonator. *Radiofizika* 35:488-497.

Mulligan BP, Hunter MD and Persinger MA (2010) Effects of geomagnetic activity and atmospheric power variations on quantitative measures of brain activity: replication of the Azerbaijani studies. *Adv Space Res* 45:940-948.

Nikolaenko A and Hayakawa M (2014) *Schumann Resonance for Tyros*. Springer: Tokyo.

Nunez PL (1995). *Towards a physics of neocortex*. In: Nunez PL (ed) *Neocortical dynamics and human EEG rhythms*. Oxford University: N.Y., pp 68-130.

- Pantev C, Makeig S, Hoke M, Galambos R, Hampson S, Gallen C (1991) Human auditory evoked gamma-band magnetic fields. *Proc Natl Acad Sci USA* 88:8996-9000.
- Park TS and Lee YL (2007) Effects of neuronal magnetic fields on MRI: numerical analysis with axon and dendritic models. *NeuroImage* 35:531-538.
- Pasqual-Marquis RD (2002) Standardized low resolution brain electromagnetic tomography (sLORETA): technical details. *Methods Find Exp Pharmacol* 24:D5-D12.
- Persinger MA (1974) ELF and VLF electromagnetic field effects. Plenum Press: N.Y.
- Persinger MA (2012) Brain electromagnetic activity and lightning: potentially congruent scale-invariant quantitative properties. *Front Integrat Neurosci* 6:Article 19.
- Persinger MA and Lavallee C (2012) The Sum of N=N concept and the quantitative support for the cerebral-holographic and electromagnetic configurations of consciousness. *J Conscious Stud* 19:128-153.
- Phan TD, Kistler LM, Klecker B, Haerendel G, Paschmann G, et al. (2000) Extended magnetic reconnection at the earth's magnetopause from detection of bi-directional jets. *Nature* 404:848-850.
- Polk C (1982) Schumann resonances. In: Volland H (ed) *CRC Handbook of atmospheric*. CRC Press: Boca Raton (Fla), pp 111-178.

Rowland V, Bradley H, School P (1967) Cortical steady-potential shifts in conditioning.
Cond Reflex 2:3-22.

Ryskin G (2009) Secular variation of the earth's magnetic field: induced by ocean flow?
New J Physics 11:1-23, 063015.

Sandyk R (1995) Improvement of right hemispheric function in a child with Gilles de la
Tourette's syndrome by weak electromagnetic fields. Int J Neurosci 81:199-213.

Sandyk R (1997) Therapeutic effects of alternating current pulsed electromagnetic fields
in multiple sclerosis. J Alt Compar Med 3:365-386.

Saroka KS, Caswell JC, Lapointe A, Persinger MA (2013) Greater
electroencephalographic coherence between left and right temporal lobe
structures during increased geomagnetic activity. Neurosci Lett 560:126-130.

Schlegel K and Fullekrug M (1999) Schumann resonance parameter changes during
high-energy particle participation. J Geophys Res 104:10111-10118.

Tanahashi S (1976) Detection of line splitting of Schumann resonances from ordinary
data. J Atmosph Terr Phys 38:135-142.

Wackermann J (1999) Towards a quantitative characterization of functional states of the
brain: from the non-linear methodology to the global linear description. Int J
Psychophysiol 34:65-80.

Whitman JC, Ward LM and Woodward TS (2013) Patterns of cortical oscillations organize neural activity into whole-brain functional networks evident in the fMRI bold signal. *Front Human Neurosci* 7:Article 80.

Wikswo JP, Barach JP, Freeman JA (1980) Magnetic field of a nerve impulse: first measurements. *Science* 208:53-55.

Chapter 6

Quantitative Evidence for Direct Effects Between Earth-Ionosphere Schumann Resonances and Human Cerebral Cortical Activity

Published in International Letters of Chemistry, Physics and Astronomy

Co-Author: Michael A. Persinger

6.1 Introduction

When two systems share remarkably similar physical characteristics such as dynamic amplitudes and intrinsic frequencies the possibility for direct interaction emerges. This assumes impedances and reluctances match or shared resonance occurs between the electromagnetic energies. The thin shell between the ionosphere and earth generates continuous harmonics of frequencies from a fundamental of about 7 to 8 Hz that is caused by global lightning which occurs between 40 to 100 times per second (40 to 100 Hz). These frequencies are the Schumann resonances.

The bulk velocity of neuronal activity around the human cerebral cortices caused by discharge of action potentials within this thin shell of tissue generates a resonance with a fundamental between 7 to 8 Hz. On the bases of the average durations of the travelling waves over the cerebral cortices the repetition rate and phase velocities are in the order of 40 to 80 times per second (40 to 80 Hz). The current density around the annulus of an axon associated with a single action potential is equivalent to about 10^5 $\text{A}\cdot\text{m}^{-1}$ or the value associated with a single lightning discharge [1].

For both cerebral and earth-ionosphere phenomena the average potential difference for these time-varying processes is in the range of $0.5 \text{ mV}\cdot\text{m}^{-1}$. The magnetic field component is the order of 2 pT (10^{-12} T). The ratio of this voltage gradient to the magnetic field intensity is effectively the velocity of light, $\sim 3\cdot 10^8 \text{ m}\cdot\text{s}^{-1}$. These general similarities suggest that more detailed congruence could occur. Here we present quantitative evidence that the electric and magnetic fields of the Schumann resonances and those equivalent frequencies generated by the human cerebral cortices can interact and may be in a persistent state of equilibrium.

6.1.1 Basic Features of the Schumann Resonance

A recent discussion [2] of the Schumann Resonance characteristics summarizes the information found within Nickolaenko and Hayakawa [3], König et al [4] and Cherry [5]. Briefly, the harmonics or modes of the Schumann resonances peak around 7.8 Hz, 14.1 Hz, 20.3 Hz, 26.4 Hz, and 32.5 Hz. This serial shift of about 6 Hz is consistent with the relation of:

$$[\sqrt{n(n+1)}] \cdot [(v\cdot(2\pi r))^{-1}]$$

where n are serial integers ≥ 1 , v is the velocity of light in the medium (which is effectively c) and r is the radius of the earth. The first component of the relation when “ n ” is substituted as a quantum number is also employed to calculate the magnitude of the orbital angular momentum [6]. When magnetic moments are expressed as Bohr magnetons the electron state is associated with a magnetic moment equal to $\sqrt{n(n+1)}$. Changes in electron states or different shells are associated with emissions of photons.

The peak values are not precise and can vary by ± 0.2 Hz depending upon ionospheric-earth conditions, time of day, season, influx of protons from solar events, pre-earthquake conditions, and yet to be identified sources. According to Nickolaenko and Hayakawa [3] monthly variations in the first mode (7.8 Hz) range between 7.8 and 8.0 Hz. The diurnal variation in frequency shift has been attributed to drifts in global lightning or alterations in ionospheric height. Peak frequencies and amplitudes occur in May whereas minima occur in October-November. The peak to peak modulations are about $\pm 25\%$ of the median value.

The optimal metaphor is that every lightning strike of the approximately 40 to 100 per second between the ionosphere and ground is an expanding wave that moves until it ultimately interfaces with itself on the earth's spherical surface. The resulting interface elicits a return wave that arrives at the original source within about 125 ms after the initiation. The approximate equivalent frequency is 8 Hz. The attenuation is minimal over megameters.

Resonance amplitudes are remarkably similar even when recorded simultaneously at observatories separated by large distances and reflect the variations in global thunderstorm activity. The maximum intensities, displayed by the first and second harmonic, are ~ 3 pT which diminish to ~ 1 pT around 20.3 Hz and less than 0.5 pT for the higher harmonics. The vertical electric (E) field strengths display ranges in the order of 0.3 to 1.0 $\text{mV}\cdot\text{m}^{-1}$. The coherence of the E field strength for the first harmonic is about 0.8 to 0.9 over thousands of km.

To discern the Schumann spectral densities continuous measurements between 10 and 100 s are required. This is similar to the optimal sampling for clear resolution for

spectral densities of human cerebral activity. With 10 s and 100 s samples the spectral resolutions are between 0.1 Hz and 0.01 Hz, respectively. For discerning the relationship between phase shift and frequency at various stations record lengths are about 10 min.

The first or fundamental resonance “splits” into three subfrequencies because of the different phase velocities and attenuation rates corresponding to standing waves and those moving in either an east-west or west-east direction. Because the peak width of the fundamental or base frequency is 2 Hz (7 to 9 Hz) and separation is in the order of a few 0.1 Hz, discrimination has been a technical challenge. A frequency shift between 7 Hz and 9 Hz with 8 Hz as the reference involves a phase shift between -20° and $+20^\circ$.

The Schumann resonances are subject to modification by imminent seismological and thermal energies. Different amplitudes of the fourth harmonic, concurrent with a shift as much as 1 Hz, can appear approximately one week before an earthquake. The modification remains for days and can still be present during aftershocks [3]. For every 1 deg C increase in tropical temperature the magnetic field measured increases by about $3 \mu\text{A}\cdot\text{m}^{-1}$ or 3.8 pT. Recently Streltsov et al [7] experimentally doubled the amplitude of the 8 Hz E field of the Schumann resonance by focusing packets of energy into the cavity that matched the second to third gyroharmonic electromagnetic wave (MHz range) values of electrons.

The spherical cavity of the earth-ionosphere that “traps the Schumann resonances” exhibits Eigen values that can be characterized by the first three equivalents of the quantum numbers: p, n, and m. P indicates how many half-wavelengths can fit the ionospheric height which reflect the Eigen-values or resonance

frequencies. N (zonal number) describes how many wavelengths fit around the circumference of the earth. M, the azimuthal number, reflects the numbers of wavelengths along the equator moving from east to west or west to east [3].

These descriptors are similar to the four quantum numbers that have been employed to describe the primary dynamic features of the atom that is the electron. These are mentioned from the perspective of integrating physics, chemistry and astronomy within the interdisciplinary framework. The similarity may also support the traditional philosophical concept that microcosm reflects macrocosm.

6.1.2 Basic Features of the Dynamic Human Brain

The human cerebrum (1.35 kg) is an ellipsoid aggregate of matter that occupies about $1.3 \cdot 10^{-3} \text{ m}^3$. The three-dimensional metrics [8] are: length (155-190 mm), width (131-141 mm), depth (108-117 mm). The cerebral cortices are approximately 1 to 4 mm thick but occupy almost 40% of the cerebral volume with an average value of 490 cc [9]. The surface area of the human brain is not smooth but exhibits convexities (gyri) and concavities (sulci).

Two-thirds of the surface is buried within the sulci. Mathematical modeling indicates that this topological surface is similar to that of a flat surface “wrinkled” into the third dimension. Secondary extrusions with widths of about 1 mm emerge intermittently along the trough of the sulci and the apex of the gyri [10].

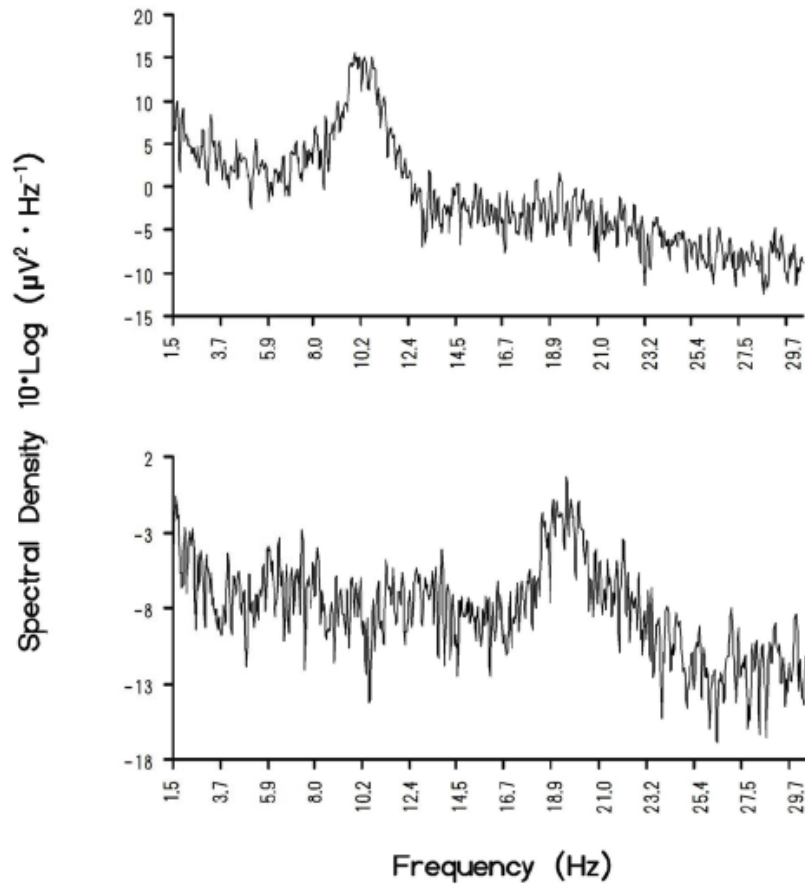


Figure 6.1 (Above) Sample power spectra of a classical quantitative EEG of an average person and (Below) Schumann resonance profile associated with the same segment of quantitative electroencephalographic activity.

The primary source of the electromagnetic activity measured from the scalp emerges from the cerebral cortices because of the parallel arrangement of the dendrite-soma-axon orientations perpendicular to the surface for most of the approximately 20 billion neurons. The resulting steady state potential between the cerebral surface and a relative reference such as the lateral ventricle ranges between 10 and 20 mV. There is almost a linear correlation between ontogeny, the emergence of neuronal processes, and the magnitude of that potential.

Superimposed upon the steady potential are fluctuating voltages that define the electroencephalogram (EEG). Most of the discernable frequencies occur within the ELF (extremely low frequency) range or 1 and 100 Hz. However, fast frequencies up to 300 to 400 Hz, approaching the absolute refractory period of an axon, have been measured in epileptic brains [11]. An example of a traditional spectral density from an average adult human brain is shown in Figure 6.1.

The amplitudes of the scalp EEG range between 10 and 100 μV . In comparison corticographic discharges exhibit amplitudes between 0.5 and 1.5 mV [12]. The most prominent dynamic pattern is the alpha rhythm (8 to 13 Hz) which during wakefulness is more evident over the posterior cerebral space with amplitudes in most (68%) of the population between 20 and 60 μV .

The average frequency increases from about 4 Hz in the 4 month old to 10 Hz by 10 years of age. The mean frequency in adults is 10.2 ± 0.9 Hz. Within the adult human alpha frequency slows between 0.3 and 1 Hz after ovulation. Amplitude asymmetry favors the right hemisphere in normal people [12].

Theta rhythms (4-8 Hz) have been considered “intermediate waves” that are significantly involved with processes associated with infancy and childhood as well as drowsiness and specific stages of sleep. The power of theta activity is evident even within the third decade (25 to 30 years of age) when the EEG parameters asymptote. This inflection is sometimes considered an index of cerebral maturation.

A transient 6 Hz to 7 Hz rhythm, which disappears by adolescence, is common over the frontal midline and is enhanced by mental tasks related to memory function. Theta activity is the prominent frequency band within which most of the power within the

hippocampus, the critical structure for consolidation of “memory”, is displayed. The power or proportion of voltage within the theta range is associated with hypnagogic (dreamy or “apparitional” transitions) states particularly in late infancy and childhood.

For adults drowsiness is associated with the disappearance of the alpha rhythm and the emergence of low voltage 2 to 7 Hz activity intermixed with 15 to 25 Hz bursts. The hall mark of deep drowsiness is the appearance of vertex waves over the posterior portion of the supplementary motor area of the frontal lobe along the interhemispheric fissure. These transients are analogous to Q-bursts recorded from the Schumann cavity [3]. They are transient events of natural radio pulses with durations between 0.3 and 1.5 s detected globally due to exclusively powerful lightning discharges. The amplitude of Q-bursts, like vertex waves, can exceed the background by a factor of 10 and emerge as elevations in the Schumann harmonics in spectral analyses.

The theta-alpha range occurs within the band of the fundamental Schumann harmonic. The second harmonic, 14 Hz, also has an equivalent within the EEG that emerges during light sleep (Stage 2). Sleep spindles or sigma waves are trains or envelopes of synchronous activity between 12.5 and 15.5 Hz with a peak around 14 Hz. As alpha rhythms dominate the posterior region of the cerebrum, spindles emerge primarily over the frontal and frontal midline.

The other classical “frequency” bands associated with the human EEG are delta (1- 4 Hz), which are the highest amplitude time-variations associated with Stage IV sleep, beta (13-30 Hz) and gamma (30 to 50 Hz) patterns. The ranges are effectively arbitrary and related to EEG features associated with particular behaviors or power densities.

Large areas of the cerebral cortices demonstrate integrated spatial and temporal characteristics. Two that are relevant to Schumann interfaces involve the rostral-caudal “travelling waves” that are recursively (recreated) every 20 to 25 ms with an implicit frequency of about 40 Hz [13]. The bulk velocity is about $4.5 \text{ m}\cdot\text{s}^{-1}$ [14]. Assuming an average cerebral circumference of 0.6 m the resonance frequency is 7.5 Hz, or within range of the fundamental harmonic of the Schumann Resonance. Llinas and Pare [15] also showed that there is a phase modulation of the 40 Hz recursive wave that was equivalent to 80 Hz or about 12.5 ms.

The second major organization of human brain activity involves microstates which are defined by specific configurations of dipoles with isopotential lines over the entire cerebral cortices [16]. Most of the variance can be accommodated by four microstates whose patterns are similar across the human population and over ontogeny. According to convention these A, B, C and D states are characterized by polarity from the right frontal to left occipital region, left frontal to right occipital region, equally distributed between the frontal and occipital region, and a dorsal central to caudal arrangement, respectively.

Together each state explains about three-quarters of the variance in EEG voltage variations. Each microstate’s duration exists for between 80 and 120 ms. These primarily four discrete and spatially-temporally bounded organizations could correspond to the “building blocks” for cognition and may be the basis for the unit “percept” of experience. This is equivalent to 8.3 to 12.5 Hz, the inclusive band of the alpha range. Assuming these microstates are the “basic units” for thinking in a manner similar to the digital units (base pairs) for DNA [17] there would be 4^{10} or about 10^6 possible different combinations or “serial patterns” per second.

The magnetic field component of human cerebral function is the same order of magnitude as the Schumann resonances. Although $\sim 10^{-12}$ T divided into $\sim 10^{-3}$ V·m⁻¹ results in a velocity term that, with the appropriate coefficients, is the velocity of light (c), intrinsic magnetic properties of space can produce this value through spatial diffusion.

Magnetic diffusivity is:

$$\dot{\eta} = (\mu_0 \sigma)^{-1} \quad (2),$$

where μ_0 is magnetic susceptibility ($4\pi \cdot 10^{-7}$ N·A⁻²) and σ =electrical conductivity [18]. Assuming the average resistivity of 2 Ω ·m ($\sigma \sim 0.5$ S·m⁻¹) for extracellular fluid, and the average potential difference of 3 μ V, the resulting estimate for the magnetic field strength is ($3 \cdot 10^{-6}$ kg·m²·A⁻¹·s⁻³) divided by $1.58 \cdot 10^6$ m²·s⁻¹ or $\sim 1.9 \cdot 10^{-12}$ T (about 2 picoTeslas, pT). This is well within the range based upon direct measurement from of action potentials from isolated frog sciatic nerves at distance of 1 mm [19]. The spatial domain is sufficiently large to have major influence upon the integrated cerebral field. This magnitude is within a factor of 10 of the transient magnetic oscillatory response Pantev et al [20] evoked in the human cerebrum (with a peak near 10 Hz and 30-40 Hz) when their measured values for 20 fT·Hz^{-1/2} are applied over the full frequency range of 100 Hz.

Although these intensities appear small, experimental application of pT-intensity, spatial and temporally-patterned magnetic fields have been reported to produce discernable improvement in some clinical disorders, such as Tourette's and multiple sclerosis [21] as well as some electrical foci associated with partial complex seizures [22]. As shown by Booth et al [23] correlative responses associated with subjects' experiences that suggest more input from the right temporal lobe into the left temporal

lobe (the sense of a presence) have been associated with geomagnetic changes in the order of $\text{pT}\cdot\text{s}^{-1}$. The latter occurred when ambient geomagnetic changes displayed progressive increases at this rate over an approximately 15 min interval.

6.2 Construction and Characterization of an Induction Coil Magnetometer

In order to compare directly the properties and interactions between human electroencephalographic activity and Schumann resonances, sensitive equipment is required. For the brain activity the standard 10-20 sensor array directly connect to a Mistar 201 Amplifier System. The standard configuration is all sensors are referenced the ears, i.e., “monopolar” recording.

The induction coil employed to detect the Schumann frequencies was modeled after a designed outlined by Hans Michlmayr (<http://www.vlf.it/inductor/inductor.htm>). The length of the coil was designed to be 80 cm with copper wire wrapped around a 5 cm pipe. Approximately 15 kg of 0.3 mm (AWG 28) copper magnet wire were wound onto the PVC pipe with an electric power drill as suggested by Michlmayr. Our “Herbert” (after H. L. König) induction coil magnetometer is shown in Figure 6.2. The copper wire wrapping procedure is shown in Figure 6.3.

Assuming the weight associated with one turn of the pipe was 144 mg, division by the total weight indicates there were between 96,000 and 97,000 turns. The total resistance of the coil measured after winding was 3.97 k Ω . The induction was 1000

Henry's once 182 cm insulated welding steel sheets were placed inside of the coil's frame. The finished coil was then housed in a larger PVC pipe for protection.

The preamplifier circuit was modeled after the ICS101 magnetometer designed by Renato Romero who operates an open-source website for the monitoring of VLF frequencies. The circuit can be found at <http://www.vlf.it/romero3/ics101.html>. For our preamplifier we omitted the 0-30 Hz low-pass filter. When the magnetometer was connected the pre-amplifier operated with a gain of 40 db.

The signal was sent to a USB soundcard, recorded and spectral analyzed automatically by SpectrumLab software designed by Wolfgang Buscher. The free source is located at: <http://www.qsl.net/dl4yhf/spectra1.html>. The software contains filters (set between 0 and 55 Hz) and a 60 Hz notch filter that removed power-line frequencies before it was encoded into a Microsoft WAVE file with the sampling rate set at 204 Hz. For calibration purposes as well as for real-time coherence measurements between human electroencephalographic activity and the Schumann resonance, the output from the preamplifier was directed to the ECG input of a Mitsar-201 amplifier.

With the Mistar interface, we calculated the gain ratio of the signal after amplification through the preamplifier was $3.85 \cdot 10^1$. Using this gain ratio we calculated the approximate magnetic field intensity by integrating Faraday's Law of induction or

$$V = -n \cdot [\Delta(BA) \Delta t^{-1}]$$

where V is the voltage generated, n is the number of turns of the coil, A is the area of the coil and $\Delta B / \Delta t$ is the changing magnetic field intensity in Teslas per second. Substituting the appropriate values for n (96,000 turns) and A (0.125 m^2) we obtained a constant by

which B could be solved based upon the raw voltages from the Mistar interface at one of our station locations (Laurentian University soccer field). When the signal's time series was spectral analyzed the approximate magnetic field intensity at 7.94 Hz was $1.21 \text{ pT}^2 \cdot \text{Hz}^{-1}$ or 3.09 pT which is with range (Figure 6.4) reported by others [3,24].



Figure 6.2 Cylinder containing the induction magnetometer “Herbert” by which local Schumann resonances were measured.



Figure 6.3 The magnetometer during stages of wrapping the copper wire. There were between 96,000 to 97,000 turns.

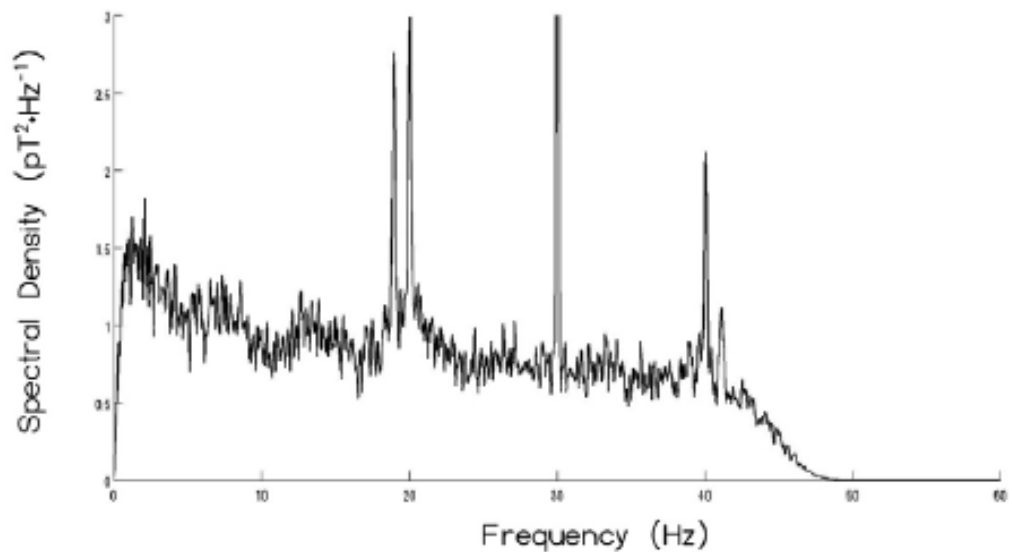


Figure 6.4 Calibration of the “Herbert” induction coil magnetometer demonstrating that the peak intensities at the harmonics were consistent with the measures of other stations. The mean peak values around 8 Hz is approximately 2 pT, within the range of other measurements.

During fair weather conditions, the power density of the Schumann frequencies near our laboratory was similar to that reported from other researchers in the U.S.A., Italy, Russia and Japan.

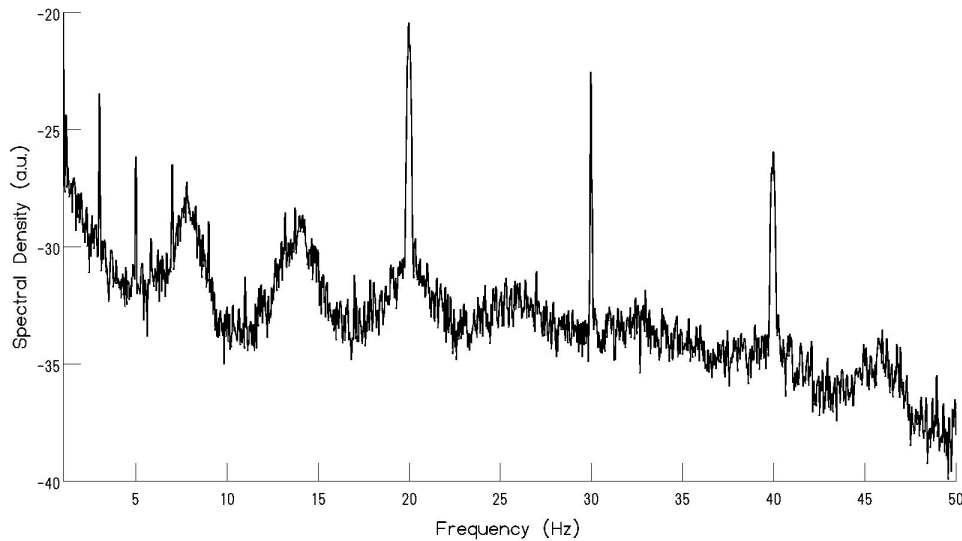


Figure 6.5 Log of spectral power density for Schumann resonances as a function of frequency from our local station recorded using a USB soundcard. The relative harmonic peaks in arbitrary units (au) are veridical.

An example of the spectral density of the magnetic field component in relative units and frequency is shown in Figure 6.5. The peaks are clearly evident at the fundamental and expand to the 7th harmonic. However, by far the most conspicuous enhancement occurred for the first four harmonics.

The spectral analyses of the QEEG for our subjects have shown the presence of the Schumann resonances within cerebral cortices for potentials recorded between the left frontal and right occipital regions. In general the Schumann resonances are most prominent over the caudal portion of the cerebral measurements that include the occipito-parieto-temporal interface. As shown in Figure 6.6, the representations of the Schumann frequencies which are often recondite within the “noise” of the QEEG data

become evident when filtering occurs. An example of a single participant's 'Schumann Resonance Signature' is shown in Figure 1.

The primary frequencies that appear within the caudal region were between 7-8 Hz, 13-14 Hz, and 19-20 Hz. Of the approximately 200 subjects measured under standardized conditions over the last three years only about 25% show the representation of the Schumann resonances within their EEG records. Because all subjects (records) were treated similarly the likelihood of artifact for this representation of the Schumann resonances from sampling, filtering, or instrumental anomalies is minimal.

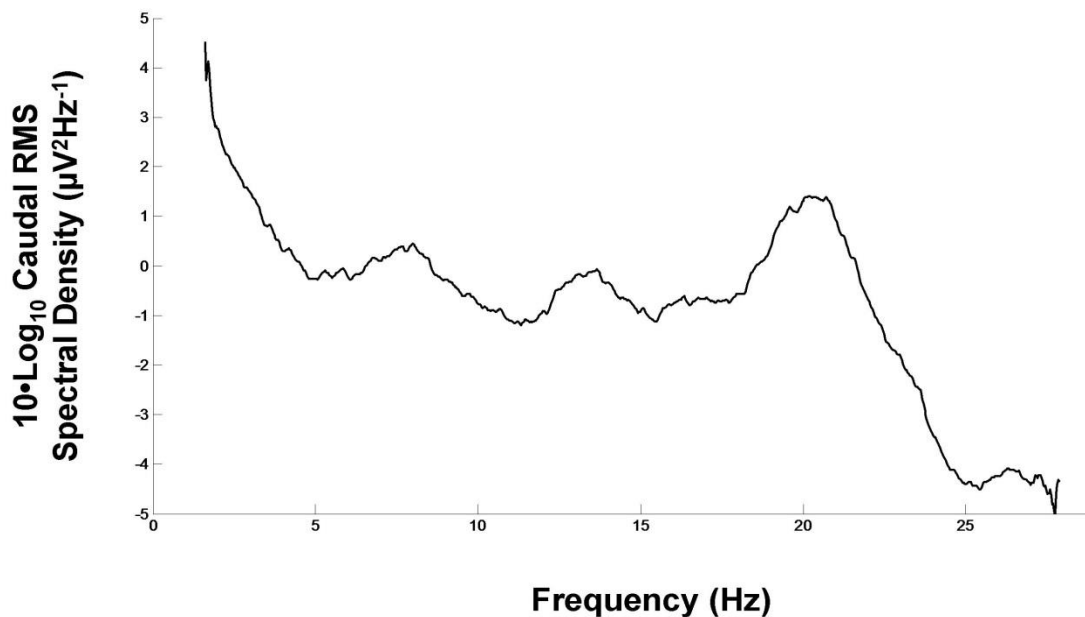


Figure 6.6 Spectral density over the caudal region (temporal-T5 T6, occipital O1 O2 and parietal, P3, P4, Pz) of 34 subjects whose brain activity was measured while sitting in a quiet Faraday chamber.

6.3 Potential Fugal Patterns in the Schumann Resonance Signal

The potential information contained within the Schumann frequencies has not been frequently or systematically pursued. Even a cursory inspection of actual raw data

from direct Schumann resonances suggests that if it were a musical score, it may display the features of a “fugue”. A fugue is a form of music in which a subject melody (usually only about 5 to 10 notes) is repeated but in combination with different harmonics over time.

To discern if there are “higher order” arrangements of Schumann patterns, the a 300 second signal recorded through the Schumann coil was directed to the USB soundcard and imported into MATLAB where the signal was decomposed into harmonic signals by filtering the original signal within frequency bands characteristic of Schumann eigenfrequencies with bandwidths of +/- .5Hz around center frequencies of 7.8, 13.8, 20.2, 33, 39 and 45Hz . The most conspicuous result was the detection of spindle-like occurrences primarily within the 14 Hz range, but also apparent in other frequency bands, which was apparent from preliminary testing with data collection through the Mitsar amplifier. This is the same range (13-15 Hz) as Stage II spindles measured over the human brain (particularly over the frontal regions) that has defined the interface between waking and light sleep [11]. The similarity between the Schumann spindles and the human cerebral spindles that define Stage 2 sleep was discovered and articulated many times by one of Schumann’s students H. L. König [4]. An example is shown in Figure 6.7 which shows spindle-like activity among various harmonics of the Schumann resonance.

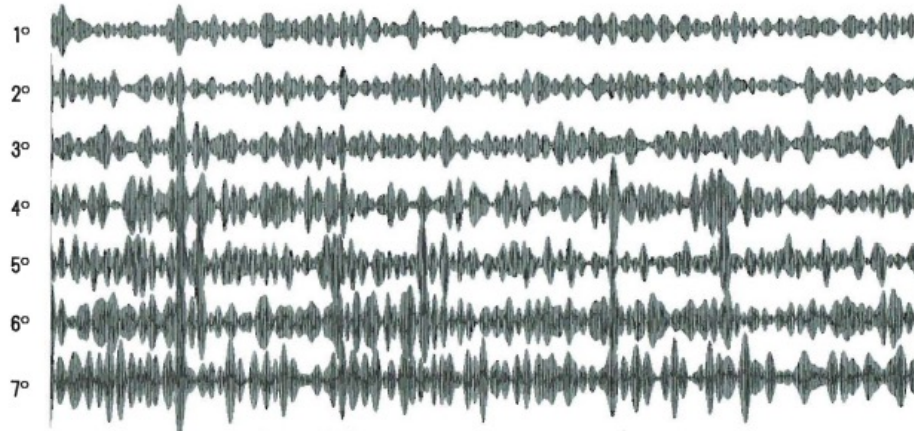


Figure 6.7 Pattern of spindle-like activity recorded locally by a Schumann unit after filtration within each of the Schumann resonance modes. Each line represents a harmonic of the Schumann resonance starting with the fundamental 7.8Hz (top line) and ending with the 7th harmonic 45Hz (bottom line).

Next a Hilbert Transform was applied to discern the envelopes (“spindle amplitudes”) for each of the signals. The results are shown in Figure 6.8. The resultant signal, from a recording that was approximately 2 hours in duration, was then re-filtered between 0 and 2 Hz to focus primarily on the changes within the envelope over time. These data were entered into coherence analysis to discern if any “fugal” coupling occurred between each resonance.

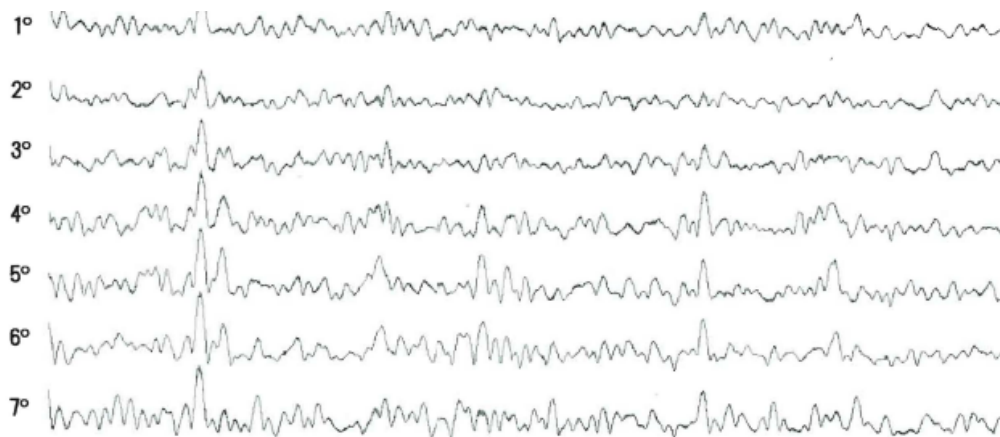


Figure 6.8 Frequency pattern within each envelope or spindle from Figure 6 after Hilbert transformation.

The results, in Figure 6.9, reveal a clear coupling between harmonics of the Schumann resonance, in this instance between 7 and 45 Hz. This couplet of frequencies, 7 and 45 Hz, is within the range of the coupling of activity found in the most fundamental activity of the hippocampus [25]. This brain structure is essential for the formation of the representation of particularly the spatial features of experiences that define semantic, episodic and autobiographical memory. The “pacemaker” cells for the two frequencies displayed by the hippocampus have been attributed to the midline structure between the two lateral ventricles, the septum.

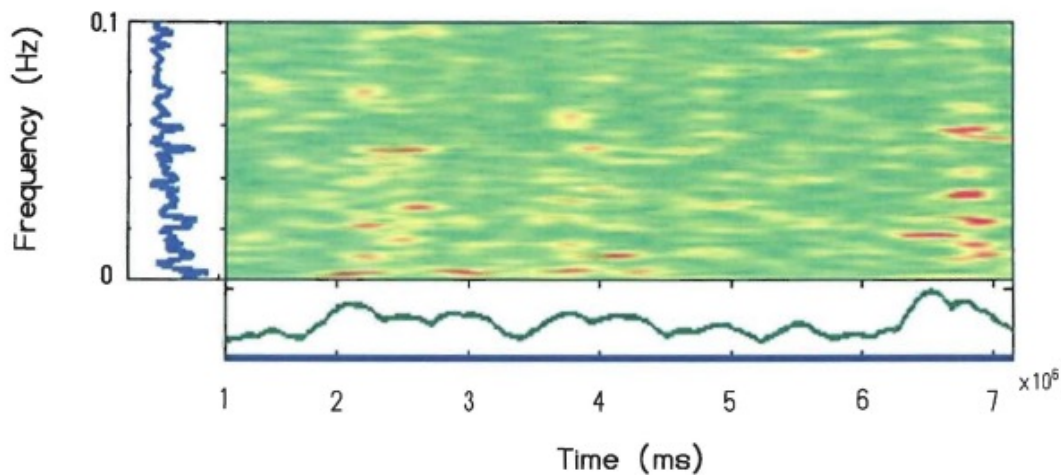


Figure 6.9 Demonstration of a type of fugal coupling between the various harmonics of the Schumann values. This example depicts coupling specifically between the first and seventh Schumann harmonics. Red and yellow areas indicate cross-frequency coherence intervals.

The intrinsic high amplitude population voltage of ~ 7 Hz (theta range) within this mesiobasal structure within the ventral portion of the temporal lobe effectively defines the dynamic properties of the structure. Superimposed upon this fundamental frequency are much smaller amplitudes or “ripples” that range between 40 to 45 Hz. Several researchers [26] have proposed that the 45 Hz ripples superimposed upon the theta

activity within the hippocampus allows the interaction between “memory” and “consciousness”.

The structure of the hippocampal formation, the technical definition of the hippocampus proper and the dentate gyrus [27], is important because they are effectively a small spherical condenser wrapped and partially interdigitated by a larger spherical condenser. This C-shaped structure is similar to a toroid with a gap which allows a discrete leakage of magnetic flux. According to classic electromagnetic theory geometries exhibiting this configuration are strongly affected by polarization or phase vector [28].

The numbers of neurons within the human hippocampal formation are in the order of 1 to $3 \cdot 10^7$. Burke and Persinger [29] have shown quantitatively at least, that this number of neurons contains the potential to converge with parameters of fundamental constants such as Planck’s mass and the hydrogen line.

The emergence of a similar temporal coupling between 7 Hz and 45 Hz patterns in the Schumann and cerebral domains suggests that occasionally resonance might occur between the two sources. Because the magnetic field strengths of the first Schumann harmonic and the human brain are in the order of 2 pT shared energy occurs. The magnetic energy within the human cerebral volume estimated by:

$$E=B^2 \cdot (2\mu)^{-1} m^3 \quad (4),$$

where B is the strength of the field, μ is the magnetic permeability and m^3 is volume, results in $2.1 \cdot 10^{-21}$ J.

The energy lost when 1 bit of information is removed into entropy (or gained if accessed from this source) according to Landauer is $\ln 2 kT$, where k is the Boltzmann constant ($1.38 \cdot 10^{-23} \text{ J} \cdot \text{T}^{-1}$) and T is the temperature in degrees K for brain temperature is $\sim 4.3 \cdot 10^{-21} \text{ J}$. This convergence suggests that the energy shared by both the magnetic field strength of the first harmonic of the Schumann resonance and the human cerebrum are equivalent to the threshold where bits of information are dissipated into or acquired from entropy. At this threshold intercalation of energy sources may not be restricted necessarily by conventional limits of impedance, masking by thermal agitation, the “weak” strength, or distance.

If the volume of both left and right hemispheric hippocampal formations (6 cc) were substituted for the total cerebral volume the energy equivalence would be $\sim 9.6 \text{ J} \cdot 10^{-24} \text{ J}$. However the power ($\text{J} \cdot \text{s}^{-1}$) required to approach the Landauer threshold would require a frequency equivalent to the duration between 1 and 3 ms, the approximate duration of an action potential. This value is the shortest interval for inter-hemispheric communication and is the duration for the expansions of electrons and protons by one Planck’s length [29]. Thus from a simplistic resonance approach, the loss or gain of bits of information between the Schumann sources and the human brain, would require this weak intensity magnetic field and the fluctuating range of perturbations that are routinely generated by the human brain.

Although 1 bit per second could be considered minimal, within 24 hrs the information would be within the tens of kilobytes. Within a 15 min period, the time required for the growth of a new dendritic spine in the hippocampus and cerebral cortices and the spatial representation of a “memory”, the potential shared information would be in the order of 1 kbit. This would be sufficient to affect the occurrence or non-

occurrence of information during the ephemeral period (about 15 minutes) of memory consolidation which can be quickly “erased” by excessive electrical stimulation. When the research by Li, Poo and Dan [31] is considered that experimentally demonstrated that the activity of only **one** neuron can affect the state of the entire cerebral cortices, such small values are not trivial.

Additional analyses indicated in Figure 6.9 indicate that incidence rate at which the couplings occurred between the 7 and 45 Hz Schumann sources. The vertical axis displays the frequency at which the couplings occur while the horizontal axis reveals the numbers of times they occur. The value was about 2 to 2.5 times per 1000 s or approximately once every 7 seconds. Hence even if the estimates for direct addition or removal of information is diluted by a factor or about 10, there would be sufficient intercalation to affect neuronal processes at the synaptic level.

Figure 6.9 suggests that these complex analyses of direct measurements of local Schumann features reveal temporal clusters. If the envelopes of spindles are considered analogous to “subject melodies” then the frequencies “harmonize” with each other over time. The second and third order derivatives or “harmonies” could have the potential to interact with similar changes within the human brain volume. In other words the mode of interaction between the ionosphere-earth cavity and the cerebral cortices would be mediated through the fugal patterns rather than the single frequency resonances.

6.4 Correlation between Real Schumann and Cerebral Coherence Values

One of the most common comments concerning the “impossibility” of the potential interaction between or representations of Schumann resonances within human brain activity as defined by QEEG is the very weak magnitudes of the vertical electric field (about 0.1 to 1 mV·m⁻²) and the horizontal magnetic field (~2 pT) for both sources. Yet most physical perspectives one smaller volume (the human cerebrum) immersed within a much larger volume (the earth-ionospheric shell) should share quantitative values for primary parameters. This would be expected for organic systems that have been organized, evolved and maintained this system since abiogenesis [32].

Empirical support for this expected interaction should be apparent considering the sensitivity of modern QEEG and Schumann technology. There are several processes that could facilitate interactions. If they occurred and equilibrium ($B+E=k$) occurred between the Schumann (E) and brain (B) sources, negative correlations would be expected between the magnetic field and electric field strengths for the harmonics for the Schumann modes and corresponding power or distribution of “energy” within specific frequency intervals or “bands” within the quantitative electroencephalographic activity for the human brain.

If an immersion model were valid it might be tested by the effect of the more expansive source (the transglobal Schumann field strengths) upon the coherence of the more localized source (the human brain). Coherence can be defined as the proportion of congruence between power spectra of one source with that of another. It is typically

expressed as a correlation coefficient or its squared value which is an indicator of shared temporal variance. Hence coherence values range from 0 to 1.

Coherence is functionally a juxtaposition of two or more or “identical” complex temporal patterns that are usually displaced in time with respect to each other. One common description is “phase-shifted”. If two sources with “identical” complex oscillations are phase shifted completely by 90 degrees, the average would be a form of cancellation that would emerge as “random” noise. However if the two patterns from the two sources were shifted to overlap precisely within each other at the same “time”, then the coherence would be maximum and the average strength of the coherence would be maximum.

Coherence from shifting phases requires, usually, minimal energy because the larger proportion of energy that constructs the complex patterns is not changed. What is changed is the energy of the dynamic process that produces the rate of change which will determine when the patterns will occur in real time within each locus as well as the transposition of axes. In this situation each locus is each cerebral hemisphere. This is often reflected as a first or second derivative and is implicitly associated with symmetry of a process moving in a circle.

The immersion model predicts that as the intensity of the primary field (the Schumann sources) increases, the intercalation between disparate but coupled asymmetrical processes in a more or less equal volume should increase. For the human brain the two volumes refer to the left and right hemisphere. On average the volumes of the cortices of the two hemispheres (right larger) differ by about 10 cc. The effect should

be most evident between the maximum widths of two hemi-ellipsoids which would occur approximately at the level of the temporal lobes.

The dynamic asymmetry of the human brain has been attributed to the approximately 10% greater white-to-grey matter ratios and blood flow in the right hemisphere which is slightly larger and heavier than the left. The structural component for most interactions between the two hemispheres, primarily the corpus callosum and anterior commissure, is composed of numbers of axons that are less than 1% of the numbers of neurons within the cerebral cortices of either hemisphere. Hence there should be specific latencies for quantities of information to be transmitted between the two loci.

Effectively the human cerebrum is two boundaries or loci within which processes associated with more than 90% of the neurons in each locus remain and do not interact directly with the homologous area in the other hemisphere. The differences in morphological structure between the two cerebral hemispheres have been underestimated. As shown by Van Essen and Drury [10], only four of the shapes and lengths of the approximately 176 sulci and gyri that comprise both human cerebral hemispheres are very similar. If structure dictates function then the two hemispheres should have qualitatively different functions whose integration or interface is limited by the fidelity and accuracy of interhemispheric communication.

“Awareness” or “consciousness” in the classic “awake” sense involves a dynamic dominance of more left hemispheric activity information. During this state the temporal patterns (information) from right hemisphere must be represented within left hemispheric

space. The representation, because of the function of the left hemisphere, would be primarily the images associated with verbal or symbolic labels.

The congruence or accuracy between stimuli preferentially affecting the right hemisphere and the experience should be determined not only by the pattern of reinforcement history of the individual (in large part determined by culture) but by the proportion of coherence between the activities of the two hemispheres within millisecond time. Direct measurements indicate that the shortest interhemispheric time for action potential propagation from one area to another is in the order of 2 to 3 ms [33].

For the present experiment, the coherence strength between the left (T3) and right (T4) temporal lobes from routine QEEG measurements from human volunteers were calculated for those days in which the electric field strength data were also available. The electric field waveform data for this study were accessed through the Northern California Earthquake Data Center (NCEDC). The instrument (BQ2) was an electric field dipole situated at Jasper Ridge Station (JRSC) in Stanford California USA, which recorded the electric field intensity (V/m) 40 times per second. Only data between August 2009 and August 2010 was used for this study because the Schumann resonance 8 and 14Hz peaks were readily visible after spectral analyses for these data.

As can be seen in 6.10, there were moderate strength correlations between the proportion of coherence strength between the left (T3) and right (T4) temporal lobes around 11.6 Hz and the average Schumann electric field strength (in $\text{mV} \cdot \text{m}^{-2}$) for its first harmonic ($r=0.43$, $\rho=0.53$) and second harmonic ($r=0.45$, $\rho=0.51$). This pattern is conspicuous even by visual inspection. The fact that the brain activity was measured in

Sudbury, Ontario, Canada and the electric field measurements of the Schumann data were recorded in Italy supports the concept of the global nature of the effect.

Within the 95% confidence band for the linear regression, the minimum to maximum change in interhemispheric coherence involved an increase of $0.2 \text{ mV}\cdot\text{m}^{-1}$ in the global field strength. The slope was 0.32 and 0.41 respectively indicating that for every $0.1 \text{ mV}\cdot\text{m}^{-1}$ increase in the Schumann E field, coherence increased by 0.32 and 0.41 within the potential range of 0 to 1.

If a similar field strength was induced within the human cerebral cortices, the potential difference would be $2\cdot 10^{-4} \text{ V}\cdot\text{m}^{-1}$ over the cerebral length of 10^{-1} m or $2\cdot 10^{-5} \text{ V}$. Assuming the classic resistivity of extracellular fluid within the brain of $2 \Omega\cdot\text{m}$, the current would be $10^{-5} \text{ A}\cdot\text{m}^{-1}$ or, over the averaged length of the cerebrum, 10^{-6} A .

This current value when divided by $1.6\cdot 10^{-19} (\text{A}\cdot\text{s}) \cdot \text{q}^{-1}$ (unit charge), indicates that the change would be equivalent to $0.6\cdot 10^{13} \text{ q}\cdot\text{s}^{-1}$. Because approximately 10^6 unit charges are associated with the membrane potential [34], $\sim 0.6\cdot 10^7$ neurons could be involved. The estimated numbers of soma whose axons compose the corpus callosum and that intercalate the functions of the left and right hemispheres are about $2 \cdot 10^8$.

On the other hand if only the fibers within the dorsal hippocampal commissure were considered [35], approximately 0.5 to $0.7\cdot 10^7$ neurons would be involved. This is remarkably similar to the numbers of neurons within the hippocampal formation. Because the dynamic changes within the parahippocampal gyrus are strongly affected by the hippocampal input and this gyrus can influence the entire cortical manifold, this small number of neurons could affect hemispheric coherence.

Thus, a first order estimate indicates that the proportion of neurons affected by a Schumann-matched voltage shift would be ~1%. This small percentage is within the range required to produce the slight shift in discharge frequencies that would allow the population convergence of activity between the left and right hemispheres. That our results were largest for the temporal lobes (or a region strongly coupled to it) indicates that this region could be a preferential locus for the influence from the ambient Schumann intensities or a region strongly coupled to it.

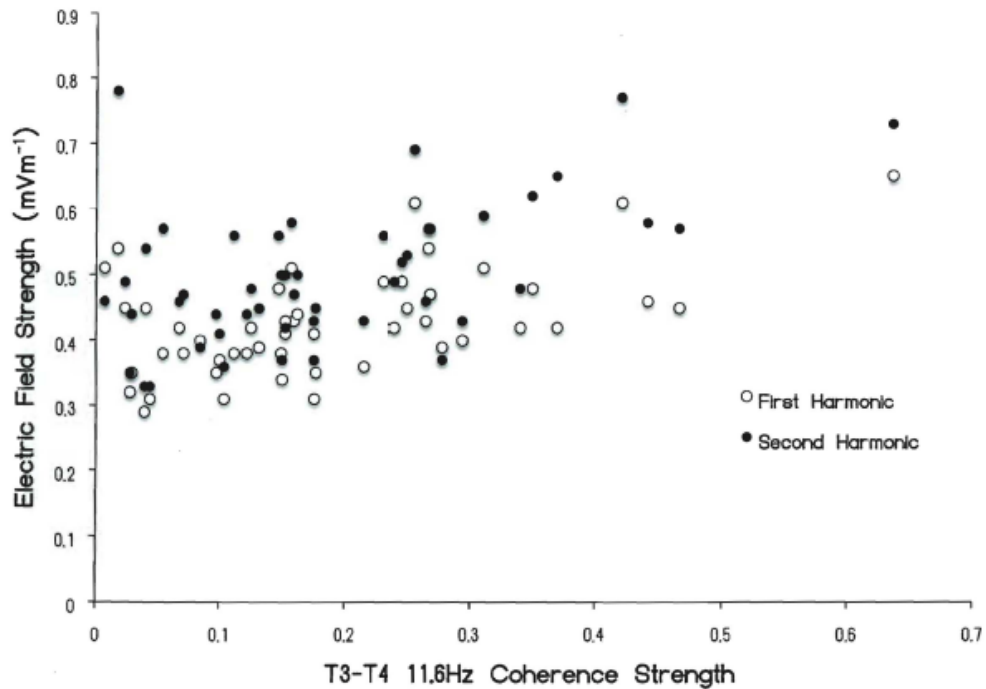


Figure 6.10 Correlation between the coherence strength between the left (T3) and right (T4) temporal lobes for subjects whose QEEGs were measured in Sudbury, Ontario and the electric field strength of the first two Schumann harmonics in California

The strongest correlation between the increased electric field of the first two Schumann harmonics and the 11.6 Hz bin for coherence between the left and right temporal lobes could suggest the emergence of a “beat” frequency from the first two

harmonics within brain space. If the first and second harmonic of the Schumann sources were 7.8 Hz and 14.1 Hz, the beat would be approximately 11 Hz, assuming equal biases for the intensities. The “11.6” Hz bin is within the normal variation of the classic peak alpha power in human EEG profiles. The width of most power curves before attenuation into background variations is between ~7 to 14 Hz.

6.5 The Parahippocampal Region as a Locus of Interaction

The maximum correlation between Schumann electric field shifts and the coherence between the left and right temporal lobes compared to other regions should reflect a structural or dynamic difference compared to other regions of the brain. The ventral portions of the temporal lobe are unique in that interhemispheric intercalation is primarily determined through the anterior commissure rather than the corpus callosum only. The hippocampal formation, the gateway to the representation of experiences (memory), is connected interhemispherically through the dorsal hippocampal commissure. It occupies the anterior one third of the splenium of the caudal corpus callosum.

In addition the middle and particularly the inferior temporal gyri are strongly influenced by the parahippocampal gyrus. This area of the human brain may be essential for the transduction and transformation of Schumann frequency changes for several reasons. First, neurons within the two upper layers of the entorhinal cortices that form a significant portion of the parahippocampal region (and the uncus) display an intrinsic (subthreshold) oscillation with a peak around 8 Hz. The prominent sub-threshold

oscillations ranged between 5.5 Hz and 14.5 Hz [36] which would include the first and second Schumann harmonics.

This region is unique structurally. Layer II, or the layer of star cells (stratum stellare of Stephan) exhibits large, dark staining stellar-shaped neurons with spine-covered dendrites radiating into all three planes of space. The neurons in Layer II are clustered in “islands” or “bands” which define the characteristics of the entorhinal cortices. These protrusions on the cortical surface (“verrucae gyri hippocampi”) are visible macroscopically. Fibers originating from these cells terminate in the dentate gyrus before the information is propagated to the hippocampus proper [37].

The mean amplitude of these subthreshold oscillations averaged 2.6 mV. This periodic increment of potential difference upon a unit charge is equivalent to $4.2 \cdot 10^{-21}$ J of energy which is within the Landauer limit for the loss or gain of one bit of information into or from entropy. The access to energy contained within the “random” processes that defines entropy may reflect a component of the Zero Point Vacuum Fluctuations [38].

These phenomena, especially when Casimir forces are considered, are interconnected with the transformation of virtual particles into real particles and could alter the limit for interaction between and information of the “weak” electric and magnetic fields shared by the Schumann and brain sources. As stated by Bordag et al [39] the creation of particles from a vacuum requires energy transference from the external field to the virtual particles or vacuum oscillations. However the boundary conditions must be dynamic or dependent upon time.

Secondly, neurons within the parahippocampal gyrus, particularly the upper two layers of the entorhinal cortices, are the major pathway to and from the

hippocampal formation. Third, through a cascade of corticocortical projections the entire manifold of the cerebral cortices converges within the second and third layers of the entorhinal cortices. This allows all of the activity of the cerebral cortices to be affected by and to affect the entorhinal area. A specific coupling or resonance between the Schumann fields and this portion of the human brain could affect the entire cerebral cortical manifold for protracted durations. These durations are juxtaposed and could certainly exceed the time required to form new synapses and patterns of neuronal connections that define and determine “memory”. From some perspectives a person is defined by his or her memories.

The parahippocampal region preferentially relays more spatial information, an essential component for most memories. It contains dominating reciprocal connections with the prefrontal cortices, especially the dorsolateral aspect. Consequently changes within the parahippocampal region could alter the major cerebral region associated with reasoning, self-monitoring and decision-making. The second major input, from the cingulate, would add the component of emotion of the type commonly associated with bonding to another human being.

Fourth, the parahippocampal region is an intermodality integrator where “line codes” from different sensory modalities such as vision and hearing are transformed to equivalent and potentially interactive frequencies. E. R. John [40] had shown experimentally several decades ago that learning through different modalities was transferable in a single trial if the frequency patterns of the pulses from different modalities were identical. Interactions of input from different modalities information could be synthesized into experiences.

The intensities of the Schumann resonance E-field 30 min before to 30 min after the time of 16-s resting eyes-closed QEEG records for 49 subjects measured from August 2009 to August 2010 were used for this analysis. The e-field data waveform data was accessed from the NCDEC as previously described. Derivations of the absolute difference in voltages between the right and left parahippocampal region from 1 to 35 Hz and the amplitude of the mean activity between 7.8 to 8 Hz were correlated.

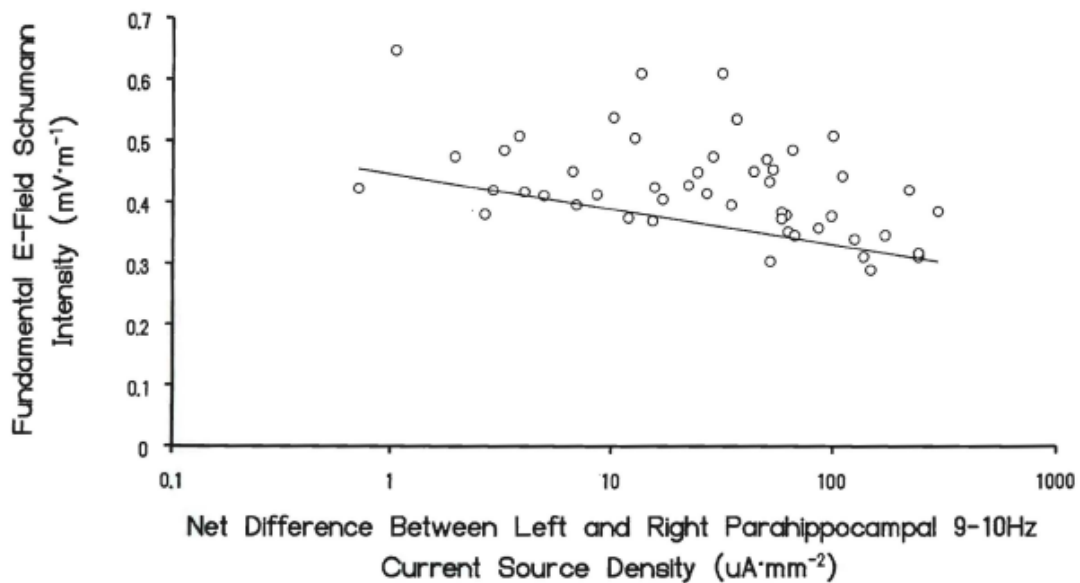


Figure 6.11 Correlation between the intensity of the contemporary fundamental electric field of the Schumann resonance in California and the net difference in current density as measured by sLORETA for the 9 to 10 Hz band between the left and right parahippocampal regions for 49 subjects whose QEEGs were measured between 2009 and 2010.

Preliminary analyses indicated that there was a conspicuous increase in correlation strength between the first Schumann harmonic and 9-10Hz activity within the parahippocampal region. The strength of the Pearson and Spearman correlations were -.50 and -.49, respectively. In other words as shown in Figure 6.11, as the intensity of the fundamental 7.8 to 8 Hz Schumann frequency increased the absolute discrepancy

between the right and left parahippocampal regions decreased. This would be consistent with an increased coherence between the two hemispheres as observed between the left and right temporal lobes.

It is also evident that an absolute shift in current density ratios between the right and left parahippocampal region of more than 100 units (1 to $100 \mu\text{A}\cdot\text{mm}^{-2}$) was associated with a range change of only about 0.2 mV in the electric field component of the fundamental Schumann frequency. Approximately $10 \mu\text{A}$ within a cross-sectional area occupied by the parahippocampal region convergences with the activity of the numbers of neurons likely to be involved with intercalation of left and right temporal lobes. This occurred with an increase of only $0.1 \text{ mV}\cdot\text{m}^{-1}$ of the Schumann electric field.

If the amplitude of the fundamental Schumann frequency was in the lower range, the current density would be 100 times larger. This would indicate the right hemisphere was more active than the left. Even when general metabolic activity or peak-to-peak voltages of alpha rhythms are considered the “default” condition is for more energetic utilization or potential difference within the right hemisphere compared to the left.

If the interaction between the Schumann and cerebral cortical voltages were in the right hemisphere, then the resonance would facilitate a reduction in current density. The diminished current density in the right parahippocampal region might be dissipated extracerebrally, that is, in the direction of the ionospheric-earth resonance cavity.

We have not correlated the relationship between simultaneous electric or magnetic field components of the Schumann resonance and cerebral power or coherence during REM (rapid eye movement) or dreaming conditions. These periods occur once every approximately 90 to 120 min for about 5 to 10 minutes during the first

episode to 10 to 20 minutes towards the termination of the sleeping period. During REM there is a marked increase in cerebral blood flow and general cerebral metabolic activity, including the protein synthesis associated with memory consolidation, as well as cardiac arrhythmia.

An equilibrium model would predict that during this period there should be an increase in current density within the right parahippocampal region as the Schumann amplitudes decrease. That would suggest the direction of this metaphoric “Poynting vector” would be towards the intracerebral locus. The direction of the equilibrium would be from the ubiquitous Schumann sources into the right hemisphere. Thus over the diurnal period there would be an oscillation or vectorial property with respect to the direction of the brain-Schumann interaction.

6.6 Extended Correlations

Considering the caudal position of the splenium and the dorsal hippocampal commissure, one would expect a more likely representation of Schumann frequencies within the caudal portions of the human cerebrum. This predominance has been supported directly by our QEEG measurements. To discern the relationship in greater detail a data set consisting of spectral densities (N=18) from the caudal root-mean-square of the posterior channels (T5,P3,Pz,T6,O1, O2) as well as the spectral densities for the electric field measured in Italy were combined and compared. The electric field data was provided courtesy of Mr. Renato Romero who continuously monitors very-low frequency electric field perturbations with a Marconi-T antenna.

Canonical correlations between the various frequencies from this cerebral composite and the spectral densities of the E-field data from the Schumann frequencies indicated that 14.65 Hz or the presence of the second Schumann harmonic within brain activity was a strong predictor. Both parametric and non-parametric correlations showed consistent negative correlations. The effect sizes, the square of the correlation coefficient, when graphed as a function of frequency displayed peaks that were very similar to Schumann resonances with the strongest effects for the first three harmonics.

Figure 6.12 shows this association. The effect size was about 0.4, indicating that 40% of the variance was shared between the route-mean-square of the posterior brain activity and the range of the Schumann electric field. The overlap is particularly prevalent for the second and third harmonic. The second harmonic has been shown mathematically to be a possible interface between gravitational waves and the earth's ionospheric-earth cavity [41].

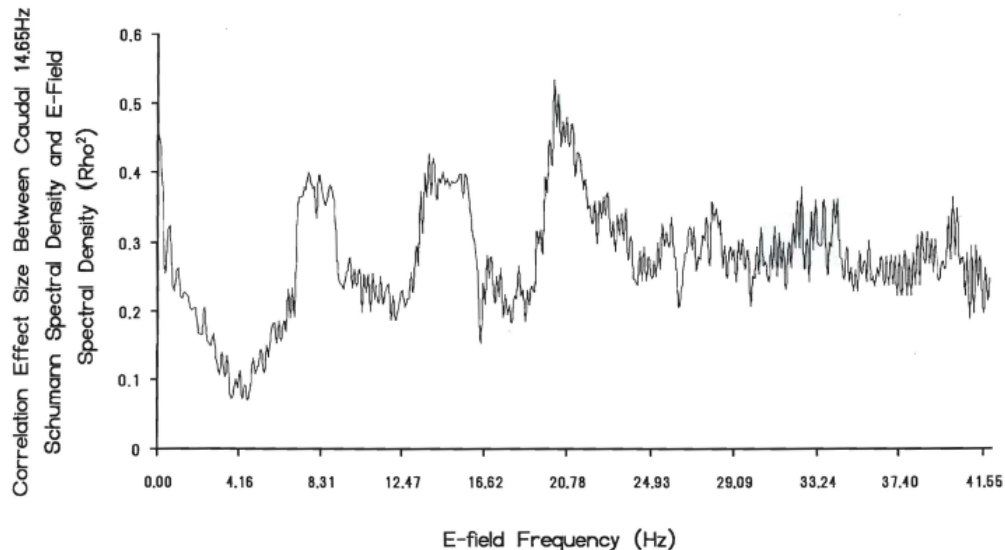


Figure 6.12 The effect size (correlation coefficient squared) for the association between the caudal 14.7 Hz QEEG activity in Sudbury and Schumann E field spectral density in Italy and the frequency band of the E field. Note the strongest correlation for the first three harmonics of the Schumann resonance.

The increased coherence between left and right temporal lobes by an increase of only $0.1 \text{ mV}\cdot\text{m}^{-1}$ may be critical for cosmological interface. A comparable change in potential over the cerebral cortices, assuming a length of 10^{-1} m , is $1\cdot 10^{-5} \text{ V}$. The effect on a unit charge of $1.6\cdot 10^{-19} \text{ A}\cdot\text{s}$ would be $1.6\cdot 10^{-24} \text{ J}$. The quantum frequency, obtained by dividing by Planck's constant ($6.626\cdot 10^{-34} \text{ J}\cdot\text{s}$) is $2.4\cdot 10^9 \text{ Hz}$ which is very proximal to the neutral hydrogen line that permeates the universe.

When the correlations between cerebral spectral density and the Schumann E fields were lagged and lead, the associations were still statistically significant within a three day window. Additional lag/lead analyses indicated that the relationship was no longer statistically significant for two weeks. This suggests that the temporal interval for direct coupling between the cerebral and terrestrial sources could be limited. Interesting 10 days was the first peak in power density for spectral analyses of Schumann intensities that were not related to solar effects according to Nicolaenko and Hayakawa [3].

If "gravity" waves share a similar source of variance to Zero Point Vacuum Potentials [37], then the "coincidental" similarities of the threshold Landauer value for information dissipation into entropy or its emergence from it and the amplitude fluctuations of the $\sim 8 \text{ Hz}$ subthreshold variations could reflect one intercept between human brain activity, the Schumann frequencies and "gravitational" phenomena.

Although gravitational phenomena are often considered too weak to be of significance for biological matter, there is quantitative evidence that the energies are within the range of those relevant to cell membranes [42] and interactions with cerebral-electromagnetic interactions [43]. The alternative explanation for gravitational

phenomena and dark matter developed by Borowski [44] suggests there are relationships yet to be discerned.

Applications of the calculations by Ahmed et al [45] to bulk cerebral cortical velocities of $4.5 \text{ m}\cdot\text{s}^{-1}$ indicated that the effects of gravity as inferred by weightlessness upon the human EEG would be about ~ 3 to 4 parts per 10 million. When divided by the common frequency in the universe, 1.42 GHz, the emergent duration would be 20 and 30 ms or the recursive cerebral waves associated with consciousness. This interesting solution suggests that the subtle effects of gravity or its intrinsic variations [46] could interface with the phase-modulations of cerebral activity.

Phase-modulation has often been considered the most effective means to propagate the most information over great distances. One solution is:

$$t/(v^2 \cdot c^2) \quad (5),$$

where, t is the reference time, v is the velocity and c is the velocity of light. Because the median frequency of the electromagnetic fields associated with lightning, the sources of the Schumann resonance, is between 10 kHz and 100 kHz, the $\Delta c \cdot c^{-1}$ is 0.05 according to Tu et al [47]. This indicates that the means of the phase shifts for every second would be $\sim (0.9897)^{-1}$ or in the order of 15 to 20 ms. This value is congruent with the phase comparisons of approximately 10 to 20 ms associated with the ~ 40 Hz integrated waves that spread over the entire cerebral cortical mantle. Quantitatively, the conditions are set for resonance interactions and exchange of information between the cerebrum, the ionospheric-earth cavity, gravitational waves, and potentially astronomical sources.

6.7 Implications of Schumann Amplitude Facilitation of Interhemispheric Coherence in the Human Brain

Our calculations indicate that only a 0.1 mV per m increase in the electric field of the global Schumann fundamental frequency is sufficient to increase the coherence from the lower one-third to the upper one-third of the potential range between the left and right temporal lobes of the human brain. If this can be generalized then the involvement of $0.6 \cdot 10^7$ neurons with implicit or active shifts in potential of $\sim 10^{-20}$ J per s associated with a given action potential would be $0.6 \cdot 10^{-13}$ J.

Over the cross-sectional area of the cerebral cortices ($\sim 10^{-2}$ m²) the $0.6 \cdot 10^{-13}$ J·s⁻¹ would be equivalent to a flux density of $\sim 0.6 \cdot 10^{-11}$ W·m⁻². This value is within range of fluctuation of measurement error for the increases in photons that emerge from the right hemisphere when people sitting in hyper-dark chambers engage in imagination of white light compared to more mundane thoughts [48]. This convergence could suggest that the processes involved with this light emission from the human brain is coupled to the degree of coherence and dynamic intercalation between the two hemispheres rather than more direct metabolic activity of cerebral cortical activity.

In the sample population of approximately 200 brains that were measured by QEEG within more or less the same conditions (in a quiet, Faraday room, darkened and subject instructed to close eyes and relax), only 34 subjects exhibited strong Schumann resonances intensities in the spectral densities of their 10-20 sensor array. Such individual differences would be expected if this phenomenon were like any other

natural phenomenon. If the data are representative of the human population than about 25% of the population would exhibit electroencephalographic power densities that reflect the Schumann harmonics.

The most conspicuous appearance of the Schumann resonances within the brain power densities occurred for the caudal regions of the cerebrum. This would be consistent with a particular sensitivity of this region. We suggest that the source of this sensitivity may be to the influence from the parahippocampal region because the actual locus for the dorsal hippocampal commissure is located within the anterior one-third of the splenium of the corpus callosum. The splenium is the primary source of interhemispheric fibers that intercalate visual, auditory-visual, and visual-spatial information between the left and right hemispheres.

If the primary means by which the effects of the Schumann-related intensities and information are mediated between the “dreaming” and “unconscious” right hemisphere and the left hemisphere (associated with awareness and consciousness) is the dorsal hippocampal commissure within the anterior one-third of the corpus callosum, then “memory” would be one of the primary areas of influence for the Schumann-cerebrum interaction. It is relevant that electrical lability or (limbic) epileptic events involving this pathway produce a single, powerful effect: amnesia [35].

A less extreme condition where mass depolarization would not occur but rather the normal flow of information between the hippocampal structures would only be modulated by Schumann-sourced electromagnetic fields could modify the memory consolidation. The retrieval and experience of “a memory” that is different from a fantasy, a dream, or an actual representation of experience involve the integrity and integrative

activity of the right prefrontal region. The modified “consolidations of experiences” could be experienced as actual memories.

6.8 Real-time Coherence Between Brain Activity and Schumann Frequencies

Although the moderate correlations between the averaged values per day for the measures of $\text{mV}\cdot\text{m}^{-1}$ (vertical) from the Schumann measurements at a distance and QEEG activity completed in our laboratory strongly supports effects from distal sources, a real time-coupled demonstration was ultimately required. For this measurement a volunteer lay in supine position approximately 1 m away from and parallel with the Schumann (Herbert) system shown in Figure 6.2. The subject wore the 10-20 sensor cap (Electro-Cap International; 19 AgCl sensors). Thirty (30) minutes of simultaneous data were collected.

The input from the sensory (EEG) cap and the input from the induction coil magnetometer were directed to the Mitsar 201 amplifier (input range $\pm 500 \mu\text{V}$, 16 bit analogue-digital conversion) system so the raw voltage fluctuations in real time could be visualized. An example of the results is shown in Figure 6.13.

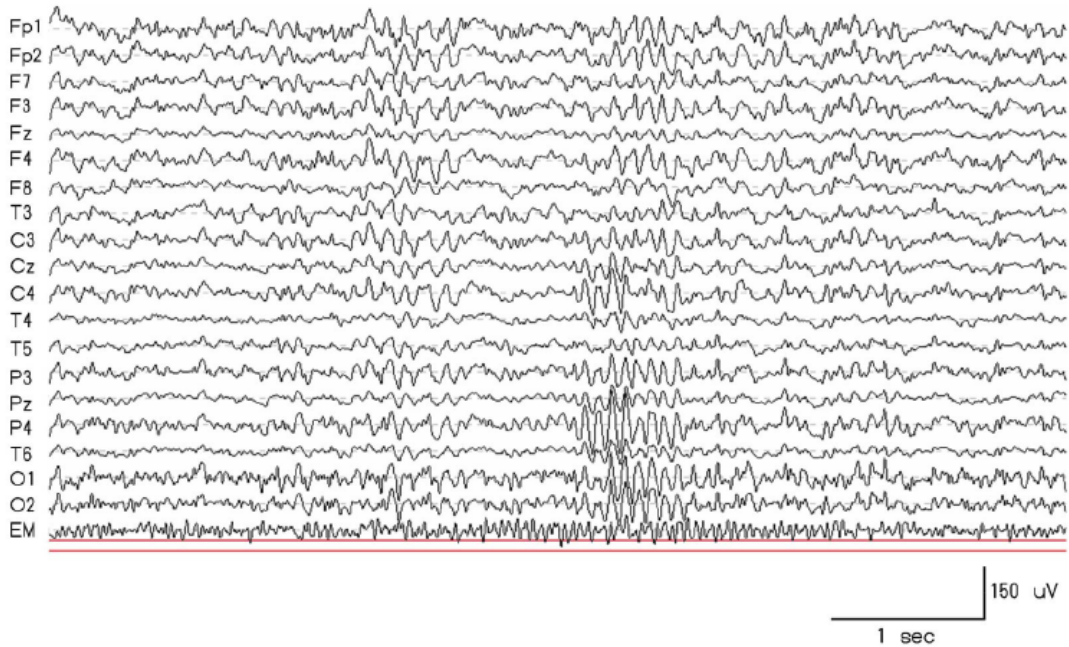


Figure 6.13 Sample (about 5 s) electroencephalographic voltage pattern from the different sensor sites over the skull (indicated by traditional identifiers) and the voltage fluctuations associated with the simultaneous recording of the Schumann.

A sixty (60)-second segment of EEG/EM data for which the Schumann resonance was readily apparent within the EM signal during initial spectral screening within WinEEG was exported. Once imported into MATLAB the EEG data were filtered between 1.5 and 40 Hz and caudal root mean-squared signals were obtained by averaging the square of posterior sensors (T5,P3,Pz,P4,O1,O2) in accordance with our usual methods. The caudal RMS as well as the signals from the magnetometer were then consolidated and z-scored. These data were then entered into Delorme and Makeig's [49] EEGLab for the computation of channel cross coherence.

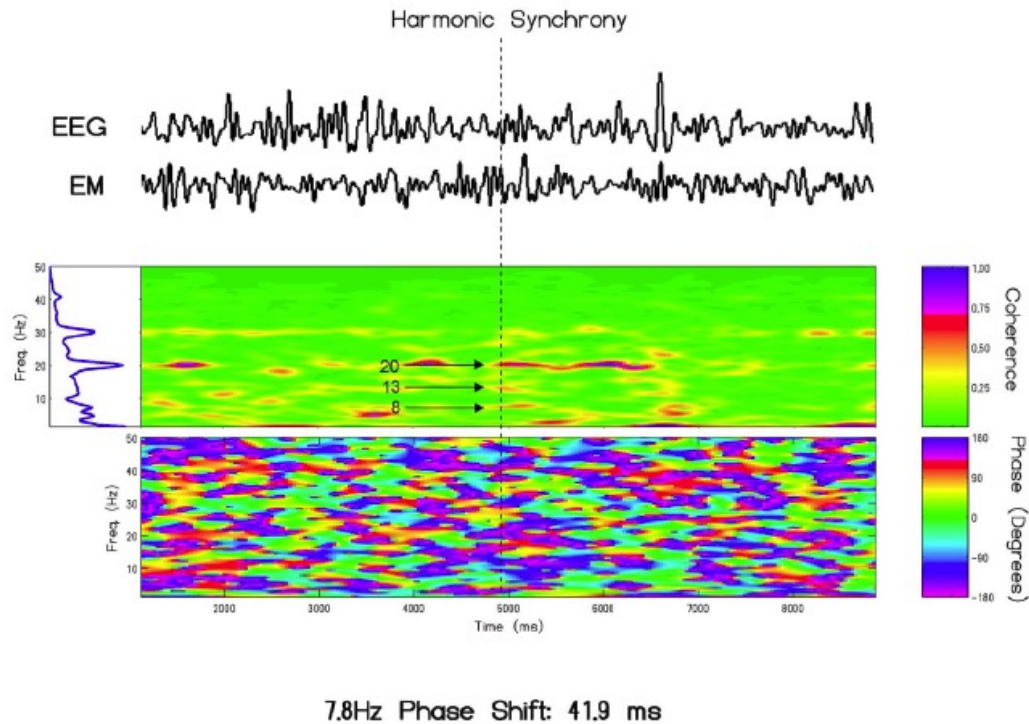


Figure 6.14 Sample record (about 10 s) of the composite EEG from the caudal portions of the subject’s cerebrum (EEG) and the Schumann resonance (EM) measured 1 m away. The horizontal axis is real time in ms while the vertical axis is frequency. The first, second and third harmonic of the Schumann resonance measured with the magnetometer were coherent with the 8, 13, and 20Hz activity occurring within the integrated caudal root-mean-square signal. The yellow indicates weak (0.30 coherence while the red indicates stronger (0.5 to 0.7) coherence. In the first panel (below the raw data) the coherence durations in the indicated frequencies occurred primarily as brief periods between 0.3 s to about 2 s. The phase shift is noted in the lower panel. The phase shift for this event at 7.8 Hz with cerebral activity was equivalent to about 41.9 ms. “Harmonic synchrony” or simultaneous coherence across two or more harmonics (possibly 4 or 5 with different magnitudes of coherence) is indicated by the vertical dotted line.

The results of the coherence analyses are shown in Figure 6.14. “Harmonic synchrony” coherence between two or more frequencies at the same time involved four and perhaps 5 bands (if weaker coherence values are included). This synchrony is indicated by the vertical dotted line. The analyses revealed moderately strong coherence (0.7) between the 8, 13 and 20Hz Schumann frequencies measured from the magnetometer and the power within the person’s electroencephalographic activity at 8, 13, and 20 Hz respectively. The durations of the coherence were transient but

consistent and extended between 0.3 s to about 2 s (red). The weaker coherences (yellow) were more protracted. Less frequent episodes of very brief strong coherence was evident in the 30 Hz range.

The phase shift (in degrees) of the coherence is shown in the multicolored bottom panel for this “Harmonic” event. The green indicates no phase shift, that is, a coupling between the 7.8 Hz Schumann fundamental and the various spectral power bands of the EEG. Qualitatively the periods of no phase shift suggested as irregular vertical patterns across most frequencies are interspersed with more irregular distributions over scattered frequencies at the $\pm 180^\circ$ shift. The mean phase shift for this subject was about 42 ms or -118° which indicated that, for example, the 7.8Hz activity occurring within the earth-ionosphere lead the 7.8 Hz activity occurring in the caudal regions of the cerebrum.

To our knowledge this is the first demonstration of a functional and time-coupled relationship between the areas of the human brain associated with the representation of Schumann resonances and the actual real-time occurrence of these resonances. The moderate strength coherence value was similar to what was found for the brain activity of our larger population and Schumann E field values from Italy and California, based upon daily values. The present measurement involved effectively continuous 2 ms to 2 ms (500 Hz sampling for both the Schumann and brain activity) sequences and revealed similar strength concordance.

The fact that the periods of coherence between Schumann resonance and brain activity within frequencies that matched the Schumann harmonics were brief, ranging from about 0.25 s to about 2 s and irregular temporally is more typical of nature

phenomena than of artifact. If they were related to a shared artifact the coherence would be have been continuous which it was not.

Although perhaps spurious we think it is interesting that the range of the strength of the coherence between the Schumann eigenfrequencies and the harmonics within the cerebral cortical activity of this subject would be consistent with the standard deviations of the magnetic component for the 7.8 Hz fundamental, about 2 to 3 pT, and the calculated and inferred strength of the global cerebral cortical of 2 to 3 pT. From this perspective the inclusion of diffusivity term (Equation 2) for the calculation of the 2 to 3 pT we derived from the μV variations for the cerebral magnetic field is directly relevant.

If the human cerebral and the Schumann resonances are coupled then a mechanism implicitly connected to diffusivity through a magnetic medium would be expected if not required [50]. The involvement of the magnetic diffusivity term in deriving pT fields which when divided into the range of potential differences generated by Schumann resonances and cerebral cortical activity ($10^{-3} \text{ V} \cdot \text{m}^{-1}$) approaches a velocity term for photons in a vacuum might help relate the chemistry, physics and astronomical variables shared by these “micro” and “macro” spherical wave conductors.

The representation of Schumann resonances within the human EEG profile in context of the normal power peak of $\sim 10\text{-}11$ Hz or between the first and second harmonic of the Schumann series could have had adaptive value. If the cerebral power profile was bimodal or 8 Hz and 14 Hz, the probability of more continuous congruence with the information contained within the Schumann carriers or wave guide would have increased.

If our inferences are even partially valid concerning the coupling or equilibrium of the magnetic field and electric field intensities between the Schumann and human cerebral cortical sources, then near-continuous earth-ionosphere-brain interaction could dominate brain activity. It may be relevant that two major populations of human beings sometimes display a “splitting” power spectrum that drifts upwards toward 14 Hz and downwards towards 7 Hz. The first is a subpopulation of human beings often diagnosed with terms such as schizophrenia. The second is the geriatric population, particularly when the cerebral histological changes emerge that are most frequently correlated with senile dementia.

The physical properties, complexity, and temporal congruence between real-time Schumann and brain values in our laboratory indicate that these considerations may have significant implications for the recondite influence of this planetary biofrequency source.

6.7 The Importance of Human Density For Potential Convergence Between Global Schumann Frequencies and Aggregates of Human Brains

The phenomena of consciousness are often attributed to a relatively wide band of electrical fluctuations in the order of about $2 \mu\text{V}\cdot\text{Hz}^{-1}$ within the 40 Hz range. This is equivalent to about 25 ms which is within the range of the recursive, coherent waves of electroencephalographic potentials that move in a rostral to caudal direction over the

cerebral hemispheres during the waking and rapid eye movement (REM) or dream states [15].

Assuming the average of $2 \cdot 10^{-6}$ V for this activity through the cerebral cortical tissue for which the intracellular resistivity is $\sim 2 \Omega \cdot \text{m}$, the current would be $10^{-6} \text{ A} \cdot \text{m}^{-1}$ and when applied across the averaged linear distance of the cerebrum ($\sim 10^{-1}$ m), would be 10^{-7} A per human brain. For the present population of $\sim 7 \cdot 10^9$ human brains, the summed current is $7 \cdot 10^2$ A and when spread over the surface of the earth ($5 \cdot 10^{14} \text{ m}^2$) is about $1.4 \cdot 10^{-12} \text{ A} \cdot \text{m}^{-2}$. For comparison the mean of the air-earth current over land is about $2.0 \pm 0.3 \cdot 10^{-12} \text{ A} \cdot \text{m}^{-2}$ [51].

There are several independent indicators to discern this current density. According to Hill [52] a typical columnar resistance of $6 \cdot 10^{16} \Omega \cdot \text{m}^2$ is evident up to 6 km; the total columnar resistance is $\sim 8 \cdot 10^{16} \Omega \cdot \text{m}^2$. The fair weather field at an altitude of 6 km is $2.2 \cdot 10^5$ V with a slight increase to $2.8 \cdot 10^5$ V within the domain of the electrosphere. Distributed over the surface of the earth, the current might be as high as $3.5 \cdot 10^{-12} \text{ A} \cdot \text{m}^{-2}$.

One increment of magnetic field intensity associated with QEEG activity within the human cerebrum has been shown to be $\sim 2 \cdot 10^{-12}$ T. The product of magnetic flux density ($\text{kg} \cdot \text{A}^{-1} \cdot \text{s}^{-2}$), current density ($\text{A} \cdot \text{m}^{-2}$) and magnetic diffusivity ($\text{m}^2 \cdot \text{s}^{-1}$), one potential process by which brain that share the earth's magnetic field or common current density might be associated, is $\text{kg} \cdot \text{s}^{-3}$ or $\text{W} \cdot \text{m}^{-2}$. Assuming the value of 10^{-12} T for either the functional magnetic field intensity of human cerebral activity or the first harmonic of the Schumann Resonance, $10^{-12} \text{ A} \cdot \text{m}^{-2}$ current density for either the earth-air value or the average for all of the brains of the human population, and $10^6 \text{ m}^2 \cdot \text{s}^{-1}$ (from $(\mu \cdot \rho)^{-1}$ where

μ is magnetic permeability ($4\pi \cdot 10^{-7} \text{ N}\cdot\text{A}^{-2}$) and ρ =the inverse of $2\cdot\Omega\cdot\text{m}$ or 0.5 S , the radiant flux density would be $\sim 10^{-18} \text{ W}\cdot\text{m}^{-2}$.

The significance of this relatively small flux density becomes apparent when it is applied over the cross-sectional area of human cerebrum (cortex), about 10^{-2} m^2 . The resulting value is 10^{-20} W or $\text{J}\cdot\text{s}^{-1}$. This is the unit energy for a single action potential. Energy is the square root of the product of voltage-squared, the band width, and Coulombs ($\text{A}\cdot\text{s}$)². For the typical voltage ($2\mu\text{V}$) of the QEEG across a band width of 100 Hz (where actual cerebral activity can range over 500 Hz) and unit charge is $1.6\cdot 10^{-19} \text{ A}\cdot\text{s}$, the square root of the E^2 of $1\cdot 10^{-40} \text{ J}^2$ is about $1\cdot 10^{-20} \text{ J}$ [53]. This relates the single energy associated with the action potential with the unit reflective of the operation of the whole cortices.

In addition the sharing of the solution for a velocity term that approaches c for the fundamental electric and magnetic fields for both the human brain and the earth-ionosphere cavity introduces the potential for quantum process coupled with photons emission and absorption. The time required for a photon with a velocity of c to traverse the plasma cell membrane (10^{-8} m) of a neuron is about 10^{-16} s which is sufficient to converge with a single orbit of an electron thus allowing information from outside of the brain to influence brain matter and for brain matter to affect the photons emitted into space.

6.8 Conclusions

The quantitative mathematical solutions and data presented here strongly support previous and pioneering research that there is a direct connection between electromagnetic properties of the earth-ionosphere cavity and human cerebral activity. Generally speaking, the correlations observed between human quantitative encephalograms measured within our laboratory and the Schumann resonance measured here, in California and Italy suggests that the earth-ionosphere-brain connection is not bounded by local perturbations but exists across the entirety of the planet. The cerebral representations appear to be mediated through structures located within the caudal aspect of the brain, especially the temporal lobe.

While we have not systematically assessed structures outside of this general locus, previous experiments involving correlation and simulated geomagnetic activity suggest a strong involvement. The simultaneous recording of the Schumann resonances within an induction magnetometer and brain activity with a QEEG indicates that there are discrete temporal increments in which the Schumann resonances harmonize with the brain with phase shifts approaching 40 milliseconds.

6.9 References

- [1] M. A. Persinger, *Frontiers in Neuroscience* 6 (2012), article 19.
- [2] M. A. Persinger, *International Letters of Chemistry, Physics and Astronomy* 11 (2014) 24-32.

- [3] A. Nickolaeno, M. Hayakawa, Schumann Resonances for Tyros. Springer, Tokyo, 2014.
- [4] H. L. König, A. P. Krueger, S. Lang, W. Sonning, Biologic Effects of Environmental Electromagnetism. Springer-Verlag, New York, 1981.
- [5] N. Cherry, Natural Hazards 26 (2002) 279-331.
- [6] W. Hume-Rothery, Electrons, Atoms, Metals and Alloys 1963 Dover, N.Y.
- [7] A. V. Streltsov, T. Guido, B. Tulegenov, J. Labenski, C.-L. Chang, Journal of Atmospheric and Solar-Terrestrial Physics 119 (2104) 110-115.
- [8] S. M. Blinkov, I. I. Glezer, The Human Brain in Figures and Tables: A Quantitative Handbook. Plenum Press, New York, 1968.
- [9] B. Pakkenberg, J. G. Gundersen, The Journal of Comparative Neurology 384 (1997) 312-320.
- [10] D. C. Van Essen, H. A. Drury, The Journal of Neuroscience 17 (1997) 7079-7102.
- [11] A. Bragin, C. L. Wilson, R J. Staba, M. Reddick, I. Fried, J. Engel, Annals of Neurology 52 (2002) 407-415.
- [12] E. Niedermeyer, F. Lopes Da Silva, Electroencephalography: Basic Principles, Clinical Applications and Related Fields. Urban and Schwartzenbert, Baltimore, 1987.
- [13] D. Kahn, H. F. Pace-Schott, J. A. Hobson, Neuroscience 78 (1997) 13-38.

- [14] P. L. Nunez, *Neocortical Dynamics and Human EEG Rhythms*. Oxford University Press, New York, 1995.
- [15] R. R. Llinas, D. Pare, *Neuroscience* 44 (1991) 521-535.
- [16] T. Koenig, L. Prichep, L. Lehmann, D. V. Sosa, E. Braker, H. Kleinlogel, R. Ishehart, E. R. John, *NeuroImage* 16 (2002) 41-48.
- [17] D. Lehmann, W. K. Strik, B. Henggeler, T. Koenig, M. Koukkou, *International Journal of Psychophysiology* 29 (1998) 1-11.
- [18] G. Ryskin, *New Journal of Physics* 11 (1995) 0603015.
- [19] J. P. Wilswo, J. P. Barach, J. A. Freeman, *Science* 208 (1980) 53-55.
- [20] C. Pantev, S. Makeig, M. Joke, R. Galambos, S. Hampson, C. Gallen, *Proceedings for the National Academy of Sciences U.S.A.* 88 (1991) 8996-9000.
- [21] R. Sandyk, *Journal of Alternative and Complimentary Medicine* 3 (1997) 365-386.
- [22] P. A. Anninos, N. Tsagas, R. Sandyk, K. Derpapas, *International Journal of Neuroscience* 60 (1991) 141-171.
- [23] J. C. Booth, S. A. Koren, M. A. Persinger, *International Journal of Neuroscience* 115 (2005) 1039-1065.
- [24] D.D. Sentman, in *Handbook of Atmospheric Electrodynamics Vol I*, H. Volland (Editor). CRC Press, Boca Raton, 1995.
- [25] G. Buzaski, *Neuron* 33 (2002) 325-340.

- [26] M. F. Bear, Proceedings of the National Academy of Sciences, U.S.A. 93 (1996) 13453-13459.
- [27] D. G. Amaral, R. Insausti, in G. Paxinos (Ed) The Human Nervous System, Academic Press, New York, 1990, pp. 711-754.
- [28] D. R. Corson, D. Lorrain, Introduction to Electromagnetism and Waves. W. H. Freeman, San Francisco, 1962.
- [29] R. C. Burke, M. A. Persinger, NeuroQuantology 11 (2013) 1-7.
- [30] M. A. Persinger, S. A. Koren, International Journal of Neuroscience 117 (2007) 157-175.
- [31] C-Y. T. Li, M-m. Poo, Y. Dan, Science 324(2009) 643-645.
- [32] Graf, Cole in M. A. Persinger (ed) ELF and VLF Electromagnetic Field Effects, Plenum Press, N.Y., 1974.
- [33] F. Aboitz, A. B. Scheibel, R. S. Fisher, E. Zaidel, Brain Research 2 (1992) 143-153.
- [34] M. A. Persinger, Current Medicinal Chemistry 17 (2010) 3094-3098.
- [35] P. Gloor, V. Salanova, A. Olivier, L. F. Quesney, Brain 116(1993) 1249-1273.
- [36] A. Alonso, R. Klink, Journal of Neurophysiology 70 (1993) 128-143.
- [37] P. Gloor, The Temporal Lobe and Limbic System. Oxford, N.Y., 1997.
- [38] H. E. Puthoff, Physical Review A General Physics 39 (1989) 2333-2342.
- [39] M. Bordag, U. Mohideen, V. M. Mostepanenko, Physics Reports 353 (2001) 1-205.

- [40] E. R. John, *Mechanisms of Memory*. New York: Academic Press, 1967.
- [41] A. A. Minakov, A. P. Nikolaenko, L. M. Rabinovich, *Radiofizika* 35 (1992) 488-497.
- [42] M. A. Persinger, *International Letters of Chemistry, Physics and Astronomy* 2 (2014) 15-21.
- [43] M. A. Persinger, *International Letters of Chemistry, Physics and Astronomy* 19 (2014) 181-190.
- [44] T. Borowski, *International Letters of Chemistry, Physics and Astronomy* 11 (2013) 44-53.
- [45] S. N. Ahmed, S. A. Kamal, K. A. Siddiqui, S. A. Husain, M. Naeem, *Kar University Journal of Science* 5 (1997) 19024.
- [46] M. A. Persinger, L. S. St-Pierre, *International Journal of Geosciences* 5 (2014) 450-452.
- [47] L. C. Tu, J. Luo, G. T. Gilles, *Reports on Progress in Physics* 68 (2005) 1-110.
- [48] B. T. Dotta, K. S. Saroka, M. A. Persinger, *Neuroscience Letters* 513 (2012) 72-80.
- [49] A. Delorme, S. MaKeig, *Journal of Neuroscience Methods* 134 (2004) 9-21.
- [50] M. A. Persinger, *The Open Biology Journal* 6 (2013) 8-13.
- [51] H. Volland, *Handbook of Atmospheric Volume I*, CRC Press, Boca Baton (Fla), 1982, pp. 66
- [52] R. Hill, *Pure and Applied Geophysics* 84 (1971) 67-74.

[53] M. A. Persinger, C. F. Lavalley, *Journal of Consciousness Studies* 19 (2012) 128-153.

Chapter 7

Occurrence of Harmonic Synchrony Between Human Brain Activity and the Earth-Ionosphere Schumann Resonance Measured Locally and Non-locally

7.1 Introduction

That a possible temporal relationship between electrical components of the time-varying potentials produced by the brain may occasionally overlap and become synchronous with activity occurring within the earth-ionosphere was originally observed by Konig and his colleague Angermuller (1960). In their publication they noted qualitative congruencies between the waveforms of electroencephalographic activity recorded from the scalps of human subjects and patterns of naturally occurring electromagnetic activity (Type I and II signals). This observation is now supported by additional quantifications showing that the space-time parameters of signals derived from both the earth-ionosphere and brain electrical activity are complimentary. In particular the Schumann resonances, which are traditionally defined by spectral peaks at approximately 8, 14, 20, 26, and 33 Hz (Balsler and Wagner, 1960), show remarkable consistency with electroencephalographic activity in terms of frequency and intensity; both exhibit average magnetic field intensities of about 1-2 picoTeslas and when the average cortical thickness of about 3 mm is accommodated both exhibit electric field intensities approaching .1 to 1 mV/m.

The apparent relationship between the Schumann resonance and brain activity has been assessed theoretically. Nunez modeled the skull-brain cavity after the earth-ionospheric cavity and predicted mathematically that the dominant resonant frequency of the brain would be about 10 Hz (Nunez, 1995); this peak frequency decreased as a function of increasing skull size of the individual (Nunez, 1978). Persinger, applying the concepts of scale-invariance, showed that the current densities of action potentials propagating along an axon were similar to those of lightning strikes suggesting that a fractal relationship between processes occurring within the brain were reflective of processes occurring over the entire planet (Persinger, 2012).

Many research groups have quantitatively assessed coupling of activities occurring globally and electrically within the human brain. Replicating observations made by Azerbaijini, Mulligan and Persinger (2010) described that theta (4-7 Hz) activity within the right prefrontal sensor was positively correlated with terrestrial atmospheric power, an indicator of the strength of the DC magnetic field of the earth. Later, Saroka et al. (2013) showed that both bi-temporal coherence and parahippocampal activity was positively correlated with the strength of geomagnetic displacement, the k-index. More detailed analyses indicated that the strength of the relationship between posterior left-right temporal lobe coherence and geomagnetic activity was strongest for coherences at 7.81 and approximately 20Hz, or stated alternatively the first and third harmonic of the Schumann resonance.

Recently Saroka and Persinger (2015) found that the Schumann resonances could be discerned within human brain electroencephalographic activity when averages of spectral analyses were computed over a large population. While the spectral peaks at ~8, 13 and 20 Hz were apparent over most averaged sensor sites it was most evident

over the caudal portions encompassing the posterior temporal lobes to the traditional occipital sensors, regions of the brain that classically display higher densities of 8-13 Hz alpha activity when the eyes are closed. Schumann-like frequencies were also reported by Cosic who showed that the spinal cord exhibits its own selective response profile when stimulated electrically (2006).

To test direct synchrony between magnetic processes occurring in the earth-ionosphere cavity and the human brain, Saroka and Persinger (2014) measured simultaneously the Schumann resonance and brain electrical activity of a single individual that was sitting quietly outside with eyes-closed. Results of the analysis indicated the presence of transient periods of 'harmonic synchrony' that appeared when cross-channel coherence was computed between the caudal root-mean-square signal derived from the brain and the extremely-low frequency (ELF) magnetic activity occurring in the proximal environment. These periods of harmonic synchrony lasted approximately 200-300 msec and consisted of simultaneous coherence within the 7-8, 13-14 and 19-20Hz bands.

The purpose of the following analyses was to 1) replicate earlier findings of harmonic synchrony between the Schumann resonance and brain electrical activity, 2) to explore potential biophysical relationships that might be predictive of the probability for this coherence using measures of skull size and 3) to assess the degree to which current models of human thought, defined by quantitative electroencephalography and implementation of microstate analysis, are possibly influenced by signals generated within the earth-ionosphere.

7.2 Materials and Methods

Data Acquisition

Experiment 1

To replicate previous findings indicating a synchrony between signals measured from the earth-ionospheric cavity and electroencephalographic activity two participants (1 male and 1 female) were recruited to participate. Both individuals were outfitted with a 19-channel QEEG cap (Electro-Cap International) which was connected to a Mitsar-201 amplifier while laying in a supine position outside the Laurentian University Arboretum, which was distant enough from sources of electrical interference (i.e. power and telephone lines) to allow for relatively noise-free recordings. All sensor impedances were maintained below 5 kOhms and were sampled at 500 Hz within WinEEG 2.8 software. A lead from a custom-constructed induction coil magnetometer system was fed into the ECG input of the amplifier in order to allow simultaneous recordings of brain electrical activity and electromagnetic perturbations occurring within the local earth-ionosphere.

The exact specifications and methodology of the experiment and equipment were identical to a protocol previously described (Saroka and Persinger, 2014). For brevity, the coil was composed of 28 gauge copper wire (approximately 14 kg) wound around a 5-cm diameter PVC pipe and was connected into a pre-amplifier with a gain of 40 dB. Calibration with the Mitsar box demonstrated that the magnetometer was sensitive to changes on the order of a picoTesla and on clear and cloudy days with minimal wind

Schumann resonances were readily observable in the averaged spectrum after 1-2 minutes of continuous sampling.

Experiment 2

Seventy-two males and females were recruited from Introduction to Psychology (N=43) and Brain and Behaviour (N=29) courses taught locally at Laurentian University to participate in this study. After informed consent was obtained each participant was invited to sit in a comfortable chair located inside of a sound-proof chamber. Once seated, the 19-channel QEEG used in the previous experiment was applied with the same specifications; however the sampling rate in this instance was 250 Hz. The source of the ELF electromagnetic signal was obtained from Mr. Renato Romero's live feed of a Marconi antenna located in Cumiana, Italy which measured the electric-field perturbations (<http://78.46.38.217/vlf15.m3u>). This audio stream was directed from a separate computer into the ECG input of the Mitsar amplifier.

Each participant was tested singly in the darkened acoustic chamber. Before any brain electrical measurements were initiated, various indicators of skull size (circumference, nasion-inion distance and ear-ear distance) were obtained in accordance with methods developed by Nunez. Approximately 5-minutes of eyes-open and 5-minutes of eyes closed measurements were collected from each individual along with the e-field occurring simultaneously in Italy.

Signal Processing and Analysis

All data from both experiments was processed and analyzed with the same techniques. Sixty seconds of the 20 channels sampled during the baseline collections

were exported into an ASCII text file and imported into MATLAB software. The 20 channels (19 QEEG + 1 ELF) collected for each participant were then further segmented into 12x5-second segments, filtered between 1.5 and 40Hz using the `eegfiltfft.m` function found inside the EEGLab toolbox (Delorme and Makeig, 2002), and a measure of caudal root-mean-square (cRMS) was computed. This derivation has been shown to produce spectral profiles very similar to the Schumann resonance in a separate population () and is defined as the squared mean of the integrated posterior channels (T5,P3,Pz,P4,T6,O1,O2). The 2-channel data that was composed of the cRMS and the ELF activity of either station, were then merged and entered into EEGLab (Delorme and Makeig, 2002) where cross-channel coherence was computed to display time-frequency decompositions of maximal coherence in 10-second bins using sinusoidal wavelet transforms, 3 cycles in length.

The cRMS derivation was entered into a coherence analysis with the ELF occurring either in Italy; the script for this computation can be found at <http://sccn.ucsd.edu/pipermail/eeglablist/2005/001056.html>. This data was then saved for further statistical analysis with other variables, including head size defined as the cube root of the product of head circumference, rostral-caudal length, and ear-to-ear length.

Identification of Occurrence, Duration and Topographies Associated with Harmonic Synchrony

Based upon the same analysis presented to find harmonic synchronies, cross-channel coherence between cRMS-ELF was completed for 41 participants in 30-second time bins. Selection criteria for 'harmonic synchrony' included simultaneous coherence across the 7.8-8 Hz, 13.7-14.3 Hz and 19-20 Hz frequency bands. Any occurrences that did not meet the criteria were not extracted. The onset and offset times, as indicated by the cross-channel spectrograms, of each of the occurrences was then recorded and extraction of only these time-periods was performed and mean occurrence and duration were calculated.

For each occurrence, 4 topographical maps were produced based upon the 19 channels of time-varying voltages associated with the 200 milliseconds before and after onset of harmonic synchrony separately using a k-means clustering algorithm within SPSS. The resultant 4 topographical maps for each baseline and onset conditions were then saved and entered into a secondary clustering procedure (N=228 per condition) for each condition separately, again using the k-means clustering algorithm. The resultant cluster centers were then saved and interpolated onto 2-D scalp maps based upon the locations of the channel using the `topoplot.m` function within EEGLab software.

To compare directly differences between average topographies associated with baseline and 'harmonic synchrony' occurrences, within-topography z-scores for each of the 8 clusters that characterized baseline (4) and harmonic synchronies (4). Because of the high degree of similarity between the two cluster sets, similar topographies from both conditions were simply subtracted from each other.

Microstate Analysis

Microstates can be described as transient organizations of the brain's intrinsic electric field. Koenig and Lehmann (2002) reported that approximately 4 classes of microstates could explain approximately 80 percent of the variance in electric field topography. Interestingly it has been reported that schizophrenic and closed head injury populations display shortened durations of some of these microstates lending to the hypothesis that the sequence of these 4 topographies may define the information component of consciousness (Corradini and Persinger, 2014). To assess the degree to which 'normal' consciousness is influenced by coupling with naturally-occurring ELF activity, a microstate analysis (Koenig et al., 1999) was performed on the raw EEG data collected during Experiment 2. In brief, the 12x5 second samples of each participant were entered into MapWin where electric field maps were created without normalization and averaged for each participant. The resultant maps were then clustered using the "Combine Microstate" function within the software. The clustering algorithm produced 4 topographies which were subsequently rearranged according to the norms published by Koenig and Lehmann (2002); the shapes of the topographies were almost identical to those originally described and explained approximately 64% of the variance in brain electrical topographic categorization. The mean microstate parameters of each participant (coverage, occurrence, duration, etc.) were then saved for further statistical analysis within the SPSS platform.

7.3 Results

The results of the cross-channel coherence analysis indicated periods of harmonic synchrony between the cRMS and ELF recorded in both Canada and Italy. These periods of synchronization were ubiquitous across most subjects and were on average about 300 msec in duration and occurred approximately 1-2 times per 60 seconds. Maximal synchronization was commonly observed simultaneously within the 7-8 Hz, 13-14Hz and 19-20Hz frequency bands. Figures 7.1 and 7.2 display exemplary cases of harmonic synchrony both locally and non-locally between 2 males and 2 females.

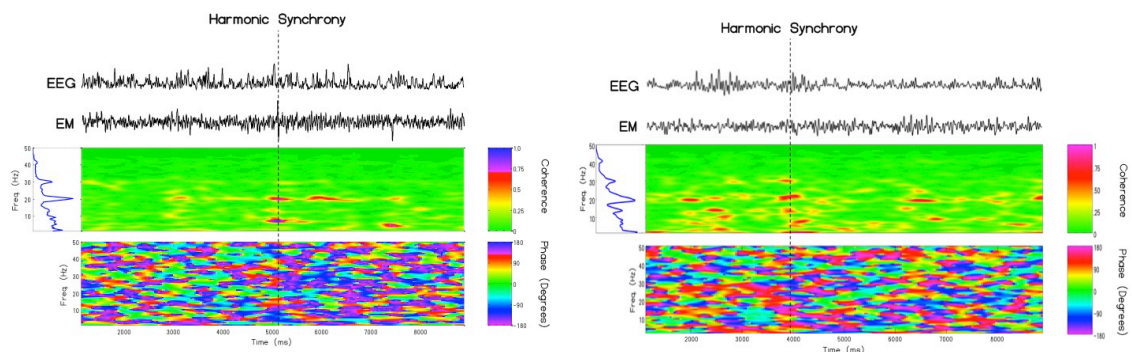


Figure 7.1 Examples of harmonic synchrony observed between a male and female participant during simultaneous measurements of their EEG and ELF activity measured with a magnetometer locally in Sudbury, Canada.

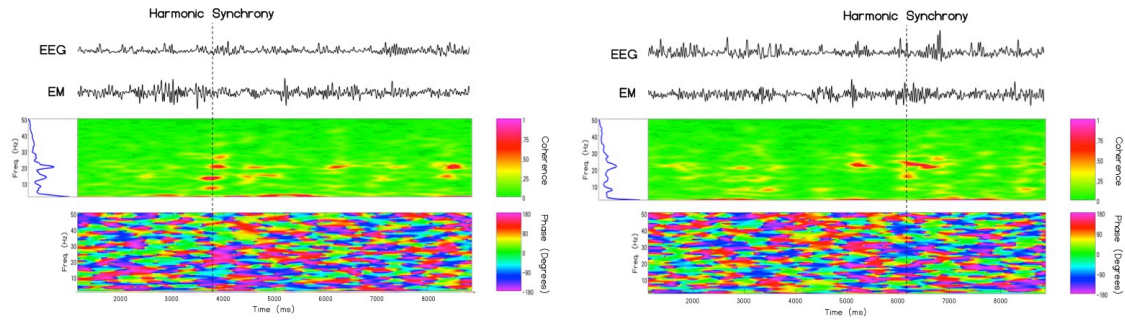


Figure 7.2 Examples of harmonic synchrony observed between a male and female participant during simultaneous measurements of their EEG and ELF activity measured with a magnetometer non-locally in Cumiana, Italy.

In order to discern patterns of coherence between the EEGs of the participants located in Sudbury and ELF activity occurring in Italy, the coherence values between the two measures were averaged across all participants from Experiment 2. When a moving average, with a period equal to 0.98Hz, was applied over the averaged data, a spectrum very similar to the Schumann resonance was apparent, with peaks at approximately 8, 14.5, 20, 25.5 and 33 (Figure 7.3). This result recapitulated findings observed from at least 2 independent analyses with a different population providing further assurance that previous analyses were not simply artifacts of signal processing techniques (Saroka and Persinger, 2014).

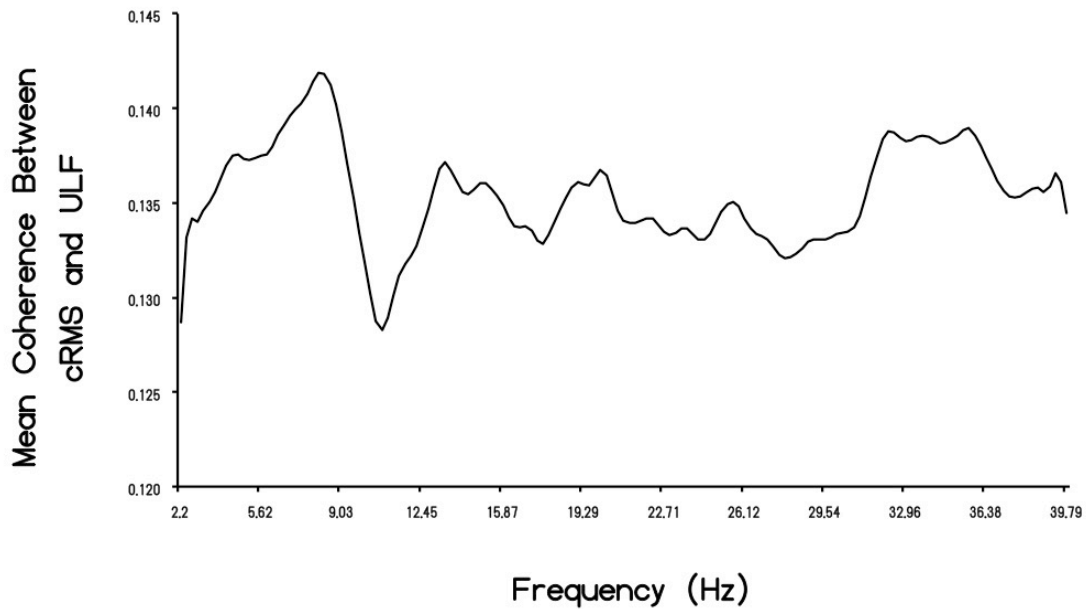


Figure 7.3 Averaged coherence between the caudal root-mean-square and ELF activity recorded in Italy plotted as a function of frequency.

Characterization of Harmonic Synchrony

Of the 41 cases analyzed, 33 (80%) displayed at least one occurrence of a harmonic synchronous event within a 60-second interval. The average occurrence and duration of these events was 1.72 occurrences/minute (SD=.97) and 349 milliseconds (SD=75).

Clustering analysis revealed four topographies consistent between the two baseline and harmonic synchrony conditions (Figure 7.4A). They are characterized as 1) bilateral prefrontal, 2) inferior temporo-posterior, 3) bilateral caudal and 4) rostral-caudal (Figure 3A). Evident is the appearance of a polarity shift for cluster 3. Oneway analyses analysis of variance for both cluster sets (baseline and event) on the averaged channel voltage across 19-channels indicated that the cluster models explained 63 and

65 percent of the variance in classification. To ascertain that the clusters were consistent between conditions (baseline versus harmonic synchrony), Spearman rank-order correlations were completed between the arrays of cluster channel mean centers. The results indicated significant relationships for each cluster between conditions with respective correlation coefficients of 1) $Rho=.59$, $p<.05$, 2) $-.85$ ($p<.05$), 3) $Rho=.54$ ($p<.05$) and 4) $Rho=.77$ ($p<.05$).

To directly compare differences in topographical orientations between baseline conditions (200 milliseconds before the event) and during the occurrence of harmonic synchrony, each map was z-scored separately. The z-scores of topographies were then simply subtracted from each other. The results (Figure 7.4B) indicated that only the second cluster, characterized by the right inferior temporo-parietal focus, displayed z-score differences greater than 3, likely attributed to the polarity shift observed between conditions. Here, positive z-scores (red) indicate that the standardized voltage for the synchronous event is greater than baseline while negative z-scores (blue) indicate the opposite.

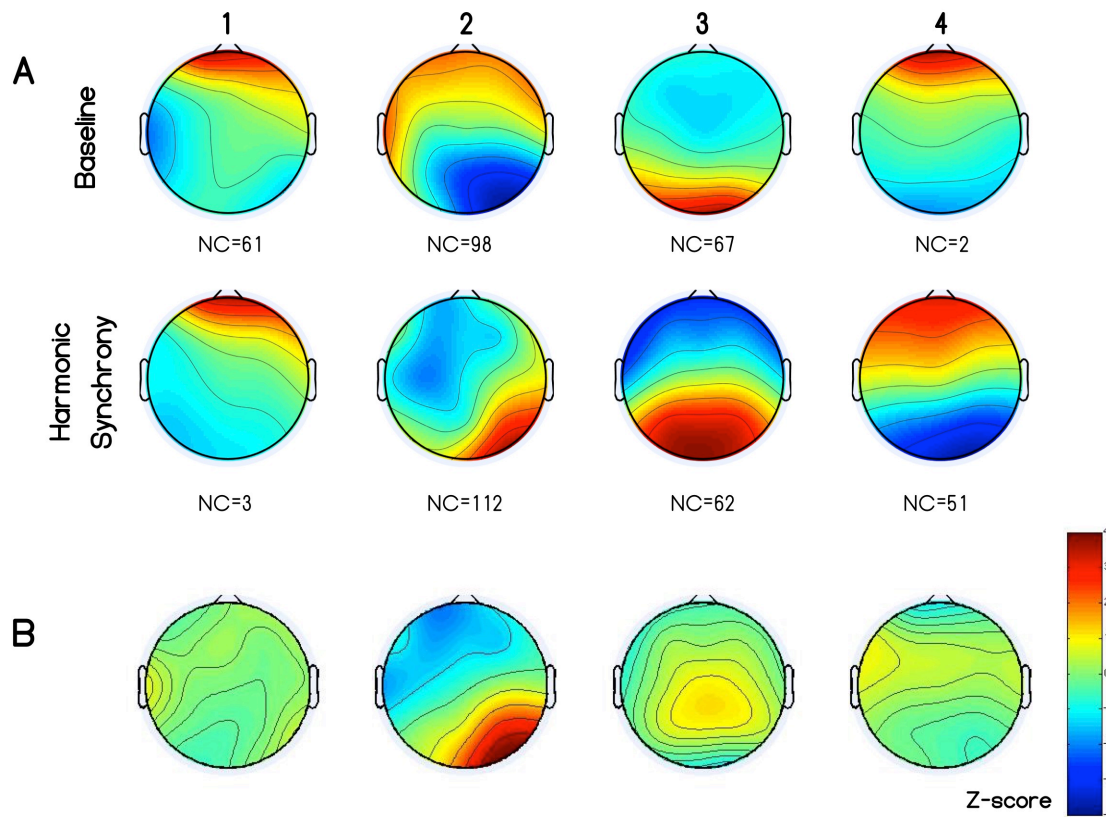


Figure 7.4 (A) Topographical maps of clusters before (top line) and during (middle line) the onset of harmonic synchronous events. NC refers to the number of clusters contributing to the grand mean cluster. (B) Standardized differences between the two conditions (bottom line). Colour bar indicates z-score.

A stepwise linear multiple regression (maxsteps=2) was performed in order to discern whether skull size of the individual could be predicted based upon the 0.3 Hz bins of coherence between cRMS and ELF. The analysis indicated that skull size was inversely related to cRMS-ELF coherence within the 20.46 (Beta=-.32) and 10.5 Hz (Beta=-.31) frequency bands (Multiple R=.40, $p < .001$). The resultant regression equation was

$$\text{Skull size} = -13.15(\text{cRMS-ELF } 22.46\text{Hz}) - 12.71(\text{cRMS-ELF } 10.5) + 42.59 \text{ (Eq. 1)}$$

To determine whether the traditional 4-class model of microstate topographies was influenced by coherence between the brain-ELF, a stepwise linear multiple regression (maxsteps=2) was performed. The analysis revealed a significant relationship (Multiple R=.54, $p<.05$) whereby the 4-class model effect size was influenced by 4.39 (Beta=.46) and 23.44 (Beta=-.38) Hz cRMS-ELF coherence. The results are summarized in Equation 2 and indicated that maximal model-fitness was associated with an increase in 4.4Hz cRMS-ELF coherence and decrease in 23.44 cRMS-ELF coherence.

$$\text{ModelFit}=137.78*(\text{cRMS-ELF } 4.39\text{Hz}) -122.78(\text{cRMS-ELF } 23.44\text{Hz}) + 48 \text{ (Eq. 2)}$$

7.4 Discussion

The results reported here replicate findings that periods of harmonic synchrony exist between the earth-ionosphere and human cortical activity within frequencies characteristic of the Schumann resonance. These transient synchronicities were equally robust when natural electromagnetic signals recorded approximately 6000 km away are substituted for proximal measurements. This finding is not surprising given that the coherence of the Schumann resonance when measured by distant observatories approaches 0.8 (Sentman, 1995).

The average duration of these synchronicities was about 350 milliseconds and occurred on average about 1-2 times per minute. If the average duration, about 100 msec, of a microstate were considered there would be approximately 2-4 microstates that would have been coherent with activity occurring

within the earth-ionosphere. Flashes of 'insight', which are more probable during periods of frontal alpha-synchronization, have been reported historically for years by many individuals and often occur 'out of nowhere', such as in the case of the Kekule (benzene) ring; however whether or not these 'spontaneous' insights occur more frequently during EEG-ELF coherence cannot be discerned at this time.

We considered the possibility of time-lags between the live feed originating in Cumiana, Italy and measured average ping times to assess the duration of these latencies. Measurements of ping times indicated 4-60 msec delays indicating that the synchronicities occurring in the experiments would not have been sufficient to produce false time-frequency representations because the duration of the delay was a factor of 2 smaller than the average occurrence of the duration of a synchronicity.

Averaged data indicated that maximal coherence between EEG-ELF occurred at the classic Schumann frequencies. The coherence values for these peaks ranged between .1 and .16. These results support previous findings demonstrating that 14Hz cRMS activity occurring in Sudbury was associated with maximal coherence in Schumann frequency bands recorded in Italy when broad non-time-locked averages were employed. Although they may be considered minimal, these values reflect an average of 60 seconds of data. Our observations indicated that periods of harmonic synchrony rarely occurred more than 2 times per second. Taking into consideration the average duration and frequency of these synchronicities, low coherence values within Schumann resonance frequencies would be expected.

The topographical mapping analysis revealed that the cluster characterized by a right inferior temporoparietal focus was most sensitive to the occurrence of a harmonic

synchronous event. This topography corresponds to the class B microstate typically observed in microstate analyses and is shortened in patients who are clinically labeled as 'schizophrenic'. Recently Persinger et al (2015) showed that an individual whose cognitive abilities were within average range but heard voices not attributed to the environment, showed elevated beta-band activity within the right temporal region and the right parahippocampal gyrus inferred by source localization. She also displayed an increased sensitivity to an applied magnetic field modeled after amygdaloid burst activity with an associated spectral peak at around 8-12 Hz. If the analyses presented here are relevant it is possible that the voices, attributed to non-local sources, could have occurred during these transient synchronies along the earth-ionosphere-brain axis.

The shift in polarity could be a revealing characteristic of these events with respect to mechanism. It is well known that a static magnet accelerating into or out of a coil induces a voltage with a respective polarity. Moving the magnet out of the coil induces negative voltage across the coil terminals while moving in produces a positive voltage. If this principle is applicable to the observed topographical orientations and a reflective process is assumed, the data would suggest that 200 milliseconds prior to brain-atmosphere synchrony the direction of the magnetic flux is from the head to the atmosphere, while 200 milliseconds during the event the direction is from the atmosphere to the head. In information technology, this would be classified as a 'ping'.

Mathematically the magnetic field strengths associated with the change in frequency would be consistent with this model. If the ping reached the lower D-layer of the atmosphere and was reflected back towards the human brain, the total distance travelled would be about 200 km. If the ping time was 400 milliseconds to complete one full cycle, the quantum of information would be travelling at a velocity of 5×10^5 m/s. The

absolute potential difference between the two conditions within the right inferior temporoparietal focus was about 10 microVolts. Dividing 1×10^{-5} volts by 5×10^5 m/s results in 20 picoTesla-metres. In radio science, bursts of megahertz frequencies are sent into the ionosphere and reflect back to a sensor in order to infer ionospheric density. For the D layer, frequencies which reflect back to the earth are between 1 and 5 megaHertz. If the ping associated with harmonic synchrony were a megahertz burst superimposed upon the Schumann waveguide, the wavelength would be about 10 meters. Dividing 20 picoTesla-metres by 10 metres reveals a magnetic field magnitude of 2 pT which is the operating intensity of the magnetic field of the brain and the approximate intensity of the Schumann resonance.

We found that skull size was negatively related to EEG-ELF coherence within around the 10.5 and 22.5Hz frequency bands. The most consistent finding of quantitative EEG in general is that the dominant frequency displayed by the adult human brain is on average 10 Hz. We have previously demonstrated that when rostral-caudal differences in spectral density are calculated, there was a conspicuous peak at 10 Hz. This finding is also consistent with Nunez and colleagues (1978) original work who showed that peak alpha frequency was inversely correlated with skull size. In light of recent analyses demonstrating the existence of harmonic relationships between 10 and 20Hz cerebral activity (Abey Suriya et al., 2014) we contend that these harmonic connections between ELF and EEG exist along a continuum of strengths that are strongly influenced by biophysical resonant features of the human brain.

Microstate analysis coupled with regression indicated that the fitness of the 4-class model was moderately influenced by the degree of EEG-ELF coherence within the 4 and 23 Hz frequency bands, the latter of which is correlated with the action of 'creative

thinking'. According to the microstate analysis, the occurrence of a given microstate was between 3.5 and 4 times per second. While it was not formally assessed here, this convergence in frequency suggests the possibility of a 'pacemaker' microstate by which the brain becomes synchronized with electromagnetic signals generated within the earth-ionosphere and would be consistent Wever's (1974) original work demonstrating that occlusion of the Schumann resonance was associated with shifts in human circadian rhythms. This would mean that the sequence of microstates that are correlated with patterns of human thought are synchronized by the activity occurring within the earth-ionosphere cavity.

Such synchronization may be a potential quantitative method of assessing Carl Jung's theory of archetypes within a biophysical context (Jung, 1964); here patterns of behaviour 'inherited' by the individual would be a function of the physical features of their brain and electrophysiology and could be modulated by the patterns of intermittent harmonic synchronies with the Schumann resonance. It is not uncommon for individuals who have sustained mild closed head injuries to report shifts in personality that are often sources of tremendous stress for themselves and those within their social group. Such shifts, while largely associated with the integrity and reinforcement of the neuronal networks that define the "self", could produce shifts in the synchrony of assemblages of neurons that change the individual's connection with the Schumann resonance by modulation of alpha spectral density. Therefore stimulation of the brain by means of weak-intensity magnetic fields for re-synchronization with previous 'selves' might be a potential treatment for these populations in the future.

7.5 Conclusion

The data and analyses presented here support further the observations originally made by Konig and Angermuller (1960) and replicate earlier findings. In particular, the results indicate transient periods of harmonic synchrony between human brain electrical activity and earth-ionosphere electromagnetic activity within Schumann frequencies that are equally strong irrespective of location on the planet. Coupling of the two phenomena was strongly related to the physical dimensions of the skull and by extension the human brain and are predictable by simple biophysical principles of resonance and standing waves. Finally the 'fitness' of the model that governs the classical arrangement of microstate topographies was strongly related to EEG-ELF coherence within the 4 Hz frequency band.

7.6 References

- Abeyasuriya, R.G., Rennie, C.J., Robinsin, P.A., Kim, J.W. (2014). Experimental observation of a theoretically predicted nonlinear sleep spindle harmonic in human EEG. *Clinical Neurophysiology* 125(10), 2016-2023.
- Balser, M., & Wagner, C. A. (1960). Observations of Earth-ionosphere cavity resonances. *Nature*, 188(4751), 638-641.
- Ćosić, I., Cvetković, D., Fang, Q., & Lazoura, H. (2006). Human electrophysiological signal responses to ELF Schumann resonance and artificial electromagnetic fields. *FME Transactions*, 34(2), 93-103.

Jung, C.G. (1964). *Man and his symbols*. Dell U.S.

Koenig, T., Lehmann, D., Merlo, M. C., Kochi, K., Hell, D., & Koukkou, M. (1999). A deviant EEG brain microstate in acute, neuroleptic-naive schizophrenics at rest. *European archives of psychiatry and clinical neuroscience*, 249(4), 205-211.

Koenig, T., Prichep, L., Lehmann, D., Sosa, P. V., Braeker, E., Kleinlogel, H., ... & John, E. R. (2002). Millisecond by millisecond, year by year: normative EEG microstates and developmental stages. *Neuroimage*, 16(1), 41-48.

König, H. L. and Angermüller, F. 1960, Einfluß niederfrequenter elektrischer Vorgänge in der Atmosphäre. *Die Naturwissenschaft*, 47, 485-490

Mulligan, B. P., Hunter, M. D., & Persinger, M. A. (2010). Effects of geomagnetic activity and atmospheric power variations on quantitative measures of brain activity: replication of the Azerbaijani studies. *Advances in Space Research*, 45(7), 940-948.

Nunez, P. L. (1995). *Neocortical dynamics and human EEG rhythms*. Oxford University Press, USA.

Nunez, P.L., Reid, L. and Bickford, R.G. (1978). The relationship of head size to alpha frequency with implications to a brain wave model. *Electroencephalography and Clinical Neurophysiology*, 44: 344-362.

Persinger, M. A. (2012). Brain electromagnetic activity and lightning: potentially congruent scale-invariant quantitative properties. *Frontiers in integrative neuroscience*, 6.

- Pobachenko SV, Kolesnik AG, Borodin AS, Kalyuzhin VV. The contingency of parameters of human encephalograms and schumann resonance electromagnetic fields revealed in monitoring studies. *Complex Syst Biophys.* 2006;51(3):480–3
- Saroka, K. S., Caswell, J. M., Lapointe, A., & Persinger, M. A. (2014). Greater electroencephalographic coherence between left and right temporal lobe structures during increased geomagnetic activity. *Neuroscience letters*, 560, 126-130.
- Saroka, K.S. and Persinger, M.A. (2015). Quantitative convergence of major-minor axes cerebral electric field potentials and spectral densities: Consideration of similarities to the Schumann resonance and practical implications. Submitted to *Naturwissenschaften*.
- Saroka, K.S. and Persinger M.A. (2014). Quantitative evidence for direct effects between earth-ionosphere Schumann resonances and human cerebral cortical activity. *International Letters of Chemistry, Physics and Astronomy*, 20(2): 166-194.
- Sentman, D. D. (1995). Schumann resonances: In Volland, H. (Ed.). (1995). *Handbook of atmospheric electrodynamics* (Vol. 1). CRC Press.
- Wever, R. (1974). ELF-effects on human circadian rhythms. In Persinger (Ed) *ELF and VLF electromagnetic field effects* (pp. 101-144). Springer US.

Chapter 8

Synthesis, Implications and Conclusion

The fugue is by definition a song with a repeating pattern consisting of multiple probabilities of convergence and divergence of a central melody all within an overarching harmonic context. The recapitulated 'subject', here proposed as the convergences of earth-ionosphere-brain electromagnetic activity, has taken its form in the collection of analyses presented here. According to Diane Ackermann's insight into the nature of the relationship between human beings and patterns,

"Once is an instance. Twice may be an accident. But three times or more makes a pattern." (Ackerman, 1994).

Whether observed pattern is an artifact of perception and observation of the subject rather than an indication of some element of 'truth' cannot readily be discerned. Indeed this question has occupied considerable attention from many lines of philosophical and cosmological inquiry and its effect is evidenced in the apparent duplicity of the behaviour of particles when in the presence of an observer. However, within the constraints of the analyses presented here the data seems to indicate that the relationship between the human brain and the earth's geomagnetic field, a concept previously described by many theologians scientists and artists, is more robust than may have been expected, given its occurrence in the multitude of analytic approaches on the micro (human) and macro (earth) scale.

Synthesis

The first convergence is the synonymous correlation between left and right temporal lobe coherence and indices of geomagnetic disturbance (Chapter 2) within frequencies related to the Schumann resonance (~8 and 20Hz) that was recapitulated in a separate analysis which demonstrated that the electric field strength (measured in California) at the first and second harmonics of the Schumann resonance were positively correlated with coherence within the T3-T4 sensors at frequencies approximating the alpha frequency (Chapter 6). The third restatement of this finding was found on a 'macroscopic' scale with increases in coherence at approximate 'T5-T6' sensors of the earth when electroencephalographic analytic techniques were applied to magnetometer data collected around the world; the same analysis indicated the presence of similar patterns of electromagnetic field topographies observed within the human brain (Chapter 3).

Left and right temporal lobe coherence has been shown to be a potential correlate of the experience of the 'sensed presence' (Saroka and Persinger, 2013). In this case, electromagnetic fields, approximating microTesla intensity and similar to background static geomagnetic field, applied in a pattern that imitates signals derived from nature elevated this left-right interaction for individuals who reported the experience of the sensed presence. On average, the coherence doubled from 0.2 (4 % of the variance) to .4 (16 % of variance). The magnitudes observed in this collection of correlational analyses reported here were similar and may re-affirm a fundamental 'fractal' electromagnetic relationship between the two spheres as predicted by Persinger (2012).

The Class A microstate (Figure 3.6), explaining the most variance within the 4-class model, of the earth is similar in topography to the Class C microstate measured from human cerebrums (Figure 1.11) and is evident even in raw strip-chart recordings when the eyes are closed with preponderances of alpha activity observed over the caudal hemisphere. According to Koenig and colleagues' (2002) normative data this microstate remains the most preponderant (30-40% of the time) of the 4 microstates starting in early adulthood. If the relationship were valid, this representation of the topography in the human brain might represent an interface that allows the interaction with the earth's geomagnetic field to occur for alignment and disturbance during solar proton events. This relationship may be valid when the data indicating changes in the migration behaviour of birds (Thalau et al, 2005), or increases in aggression in populations male rats (St-Pierre et al., 1998), during the time of geomagnetic disturbance is considered.

The second and most instructive convergence observed during the analysis of the data presented in this dissertation were the almost ubiquitous and numerous correlations between brain activity and electromagnetic activity within the ultra-low frequency range, and more specifically the frequencies that define the Schumann resonance. The data presented in Chapter 4 indicated that the brain becomes resonant with background AC magnetic field measurements specifically at frequencies that approximate 8, and 40 Hz even though the instrumentation was sensitive to only nanoTesla rather than the expected picoTesla fluctuations. This pattern was observed two additional times when the Schumann resonances were found to be an intrinsic signature within the averaged brain activity of a large population (Chapter 5) and when the greatest effect sizes between the relationship of the 8-Hz electric field activity

measured in Italy and 14 Hz caudal activity within the cerebrums of individuals located in Sudbury occurred at frequencies characteristic of the Schumann resonance, specifically at frequencies of 8, 14, 20, 26 and 33 Hz (Chapter 6).

The validity of these correlations was internally verified through the simultaneous measurement of brain and the earth-ionosphere where intermittent periods of coherence, lasting on average about 300 millisecond once every minute, were observed over the caudal hemisphere within frequencies of the Schumann resonance when 'atmospheric noise' was measured locally in Sudbury, Canada and over 6000 kilometers away in Italy (Chapters 6 and 7). The term 'harmonic synchrony' was employed in order to illustrate that the caudal electrical activity becomes synchronous with this noise at precisely harmonics of the Schumann resonance. In more detailed analyses, these events were shown to have considerable overlap in terms of localization when compared against previous data. For instance, the right caudal hemisphere was shown to be mostly affected during the times of synchronous events.

Implications

Dr. Carl Gustav Jung proposed the concept of 'synchronicity' as an unconscious process where symbols in dreams and lucid thoughts manifest physical representation in 'reality' (Jung, 1964). These occurrences are taken by many as personal 'totems' that validate their decision-making process while others view these occurrences as mere 'coincidence' that would have been bound to happen by chance due to their infrequency.

The findings reported here may add quantitatively to the hypotheses offered by Jung; the seemingly irregular interface between the electrical activity of the cerebrums of individuals may approximate the temporal durations associated with insight, a likely correlate of synchronicity. While measuring the electroencephalograms of individuals engaging in compound-remote-associates problem-solving in which one word can form a compound-word with three supplied words, those instances where the individuals 'felt' the solution (the word connecting the three) rather than logically derived it were associated with gamma (>30 Hz) and alpha (~7-13 Hz) bursts localized over the right caudal hemisphere 300 milliseconds prior to overt verbal indications of their methodology for problem-solving (Kounios et al, 2009).

In addition to the data presented in Chapter 7 (localization of harmonic synchrony) and Chapter 4 (correlations with the proximal electromagnetic environment precisely within these two frequency bands), this region was also activated in a unique individual during times when he interpreted the personal histories of individuals sitting in close proximity (Persinger and Saroka, 2012). If these earth-ionosphere interactions are viewed as 'rewards' in a classical behaviourist context, their occurrences should follow the principles of learning and would be associated with subtle elevations in dopaminergic activity, particularly mediated from the ventral tegmental area to medial prefrontal regions, including the anterior cingulate and a primary correlate of bonding between human beings. It may be relevant that this neurochemical compound is also elevated during experiences of the 'musical chill' phenomenon frequently reported within the normal population and described phenomenologically as a pleasurable 'shiver down the spine' (Blood et al., 2001). Experience of this chill can be encouraged through

appropriate stimulation of the medial frontal regions with an electromagnetic field pattern modeled after burst-firing dopaminergic neurons (Saroka and Persinger, 2013).

The recruitment of neuronal assemblages within a locus of the right caudal hemisphere that predicts activity within the parahippocampal gyrus, a region highly associated with the integration of multiple streams of information into memory unconsciously, may also be supportive of the work of Dr. Jung. This region displays a negative voltage of about 10 microvolts prior to a 'harmonic synchrony' event followed by a positive voltage of the same magnitude and may be akin to simultaneous sending and receiving of packets of information or 'bouncing', if the model of a static magnet moving into and out of a coil is apt. If so, this model might predict a 'pay-it-forward' mechanism whereby individuals experience synchronicity, and while perceived as an isolated (between two people) incident, is actually occurring globally in a chain of reactions or simultaneously. In summary the ideas of 'synchronicity', 'collective unconscious', and 'archetype' (which may be recognized in modern times as the patterns of interaction between the earth-ionosphere), may now have a metric by which it can be explored quantitatively.

As has been demonstrated numerous within the context of psychology, the boundaries of working memory are 7 ± 2 items. However, if one applied the concept of the fractal arrangements, it may be argued that this is true at several temporal scales; for example, the amount of personally significant events within one day, one month, one year, or one lifetime may approach the same figure. If this is true then consciousness as experienced by the human being may exist on alternative temporal and spatial levels, as would have been predicted by many Eastern philosophies. Persinger's (2010) calculations indicate that the energy equivalent of all human memory from every human

being that has ever existed could potentially be stored within the earth's geomagnetic field. Accordingly, the transient interactions that occur along the earth-ionosphere-brain axis approximately once every minute may be indicative of levels of consciousness that, by definition, can only be perceived on their respective time scale and would potentially be evidenced by the repeated but independent re-visiting of concepts and ideas that permeated throughout the course of history, such as the interdisciplinarity that was once central to the major creative achievements of the Renaissance period as well as during the times of Ancient Greece. If this is true, Jung's 'collective unconscious' may have more relevance than suspected.

Conclusion

The fugal, scale-invariant, or fractal coupling between human cortical activity and earth-ionospheric electromagnetic parameters has been thoroughly explored. In all analyses similar shapes, intensities, frequencies, activations and energies have been observed from the perspective of a multitude of different analytic approaches. The three major findings are that 1) the spatial and temporal properties of natural electromagnetic fields are similar at microscopic and macroscopic scales, 2) as predicted by König (1960) and Persinger (2012) the interface between the two systems converges at the nano-to-picotesla range intensity at frequencies characteristic of the Schumann resonance, and 3) this interface is a regular occurrence within all human beings, within cerebral loci that are traditionally associated with memory and for durations (300 msec) that approximate insight and creativity.

References

- Ackerman, D. (2011). *A Natural History of Love: Author of the National Bestseller A Natural History of the Senses*. Vintage.
- Blood, A. J., & Zatorre, R. J. (2001). Intensely pleasurable responses to music correlate with activity in brain regions implicated in reward and emotion. *Proceedings of the National Academy of Sciences*, *98*(20), 11818-11823.
- Koenig, T., Prichep, L., Lehmann, D., Sosa, P. V., Braeker, E., Kleinlogel, H., ... & John, E. R. (2002). Millisecond by millisecond, year by year: normative EEG microstates and developmental stages. *Neuroimage*, *16*(1), 41-48.
- König, H. L. and Angermüller, F. 1960, Einfluß niederfrequenter elektrischer Vorgänge in der Atmosphäre. *Die Naturwissenschaft*, *47*, 485-490
- Kounios, J., & Beeman, M. (2009). The Aha! Moment the cognitive neuroscience of insight. *Current directions in psychological science*, *18*(4), 210-216.
- Jung, C.G. (1964). *Man and his symbols*. Dell U.S.
- Persinger, M. A. (2012). Brain electromagnetic activity and lightning: potentially congruent scale-invariant quantitative properties. *Frontiers in integrative neuroscience*, *6*.
- Persinger, M. A., & Saroka, K. S. (2012). Protracted parahippocampal activity associated with Sean Harribance. *International journal of yoga*, *5*(2), 140.

- St-Pierre, L. S., Persinger, M. A., & Koren, S. A. (1998). Experimental induction of intermale aggressive behavior in limbic epileptic rats by weak, complex magnetic fields: Implications for geomagnetic activity and the modern habitat?. *International journal of neuroscience*, *96*(3-4), 149-159.
- Saroka, K. S., & Persinger, M. A. (2013). Potential production of Hughlings Jackson's "parasitic consciousness" by physiologically-patterned weak transcerebral magnetic fields: QEEG and source localization. *Epilepsy & Behavior*, *28*(3), 395-407.
- Thalau, P., Ritz, T., Stapput, K., Wiltshko, R., & Wiltshko, W. (2005). Magnetic compass orientation of migratory birds in the presence of a 1.315 MHz oscillating field. *Naturwissenschaften*, *92*(2), 86-90.